Naval Oceanographic Office
Stennis Space Center
MS 39522-5001

Technical Report
TR 308
July 1993

TR 308

A UNIFIED APPROACH TO GEOPOTENTIAL FIELD MODELING

JOHN M. QUINN
DONALD L. SHIEL

Approved for public release; distribution is unlimited.

Prepared under the authority of
Commander,
Naval Oceanography Command

FOREWORD

Modern theories of static electric, magnetic, and gravitational potential-fields are based upon the early investigations of Sir William Gilbert (1600) and of Sir Isaac Newton (1686) and upon subsequent investigations covering more than two centuries by numerous other well-known mathematicians and natural philosophers, culminating in the synthesis of electricity and magnetism by Sir James Clerk Maxwell (1864) and the synthesis of gravitation and geometry by Albert Einstein (1916). Applications of electromagnetic field theory and gravitational field theory to the remote sensing of geophysical parameters through inverse modeling techniques has been a major theme throughout the remainder of the 20th century. The Navy's interest in these subjects stems from its Anti-Submarine-Warfare mission, from its concern for locating undersea Hazards-to-Navigation, and from its interest in Attitude-Heading-Reference systems.

This report reviews and synthesizes, and in so doing self-consistently unifies through tensor analysis, the subject of static geopotential-field theory with respect to rectangular-prismatic bodies, which may be considered as the basic building blocks of natural geophysical phenomena. Although this report originated from geophysical considerations, the mathematical expositions it contains are generic in the sense that they are also applicable to remote sensing problems in the fields of classical physics, biophysics, and engineering.

D J Whitford

D. J. WHITFORD
Commander, U.S. Navy
Commanding Officer
Acting

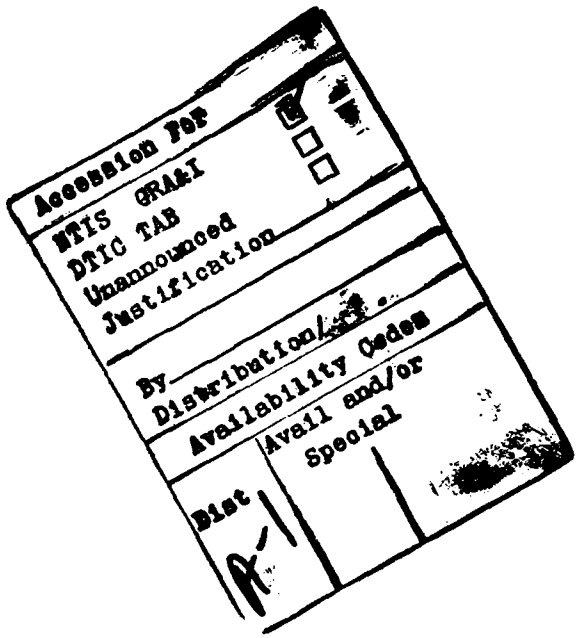

DISCLAIMER NOTICE

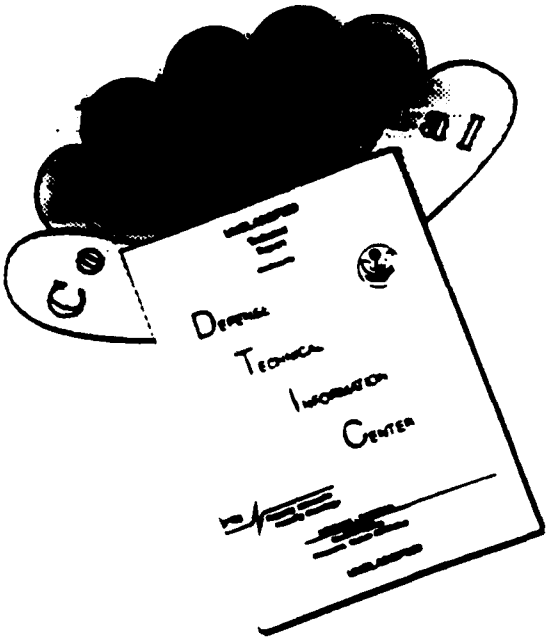

THIS DOCUMENT IS BEST QUALITY AVAILABLE. THE COPY FURNISHED TO DTIC CONTAINED A SIGNIFICANT NUMBER OF COLOR PAGES WHICH DO NOT REPRODUCE LEGIBLY ON BLACK AND WHITE MICROFICHE.

REPORT DOCUMENTATION PAGE

Form Approved
OMB No 0704-0188

1. AGENCY USE ONLY (Leave blank)	2. REPORT DATE	3. REPORT TYPE AND DATES COVERED
	July 1993	Technical Report

4. TITLE AND SUBTITLE
A UNIFIED APPROACH TO GEOPOTENTIAL FIELD MODELING

5. FUNDING NUMBERS

6. AUTHOR(S)
John M. Quinn
Donald L. Shiel

7. PERFORMING ORGANIZATION NAME(S) AND ADDRESS(ES)
Naval Oceanographic Office
1002 Balch Blvd.
Stennis Space Center, MS 39522-5001

8. PERFORMING ORGANIZATION REPORT NUMBER
TR 308

9. SPONSORING / MONITORING AGENCY NAME(S) AND ADDRESS(ES)
Commander
Naval Oceanography Command
1020 Balch Blvd.
Stennis Space Center, MS 39529-5005

10. SPONSORING / MONITORING AGENCY REPORT NUMBER

11. SUPPLEMENTARY NOTES

12a. DISTRIBUTION / AVAILABILITY STATEMENT
Approved for public release;
distribution is unlimited.

12b. DISTRIBUTION CODE

13. ABSTRACT *(Maximum 200 words)*

It is shown that when both vector and gradient tensor components of a potential field are simultaneously available, inverse problems, such as determining the depth to the oceanic magnetic basement, can be split into a purely "geometric" problem, which seeks to determine the dimension and position parameters of one or more prisms and a purely "geophysical" problem, which seeks to determine the physical properties (i.e., the magnetization, polarization, density, etc.) of the prism. The geometrical problem is nonlinear and must be solved iteratively using standard stochastic or least-squares inversion techniques, while the geophysical problem is linear and may be solved by direct inversion once the geometric parameters have been established.

14. SUBJECT TERMS
Magnetic, Electric, Gravity, Inverse Modeling, Poisson Relations, Potential Fields, Rectangular Prisms

15. NUMBER OF PAGES
119

16. PRICE CODE

17. SECURITY CLASSIFICATION OF REPORT	18. SECURITY CLASSIFICATION OF THIS PAGE	19. SECURITY CLASSIFICATION OF ABSTRACT	20. LIMITATION OF ABSTRACT
Unclassified	Unclassified	Unclassified	SAR

TABLE OF CONTENTS

LIST OF FIGURES

LIST OF TABLES

APPENDICES

ABSTRACT

We review from first principles the forward and inverse geopotential modeling problem with respect to the magnetic, electric, and gravitational fields. Under the assumption that any region of the Earth's crust can be conveniently subdivided into rectangular prisms composed of uniformly distributed geophysical parameters (i.e., magnetization, polarization, density, etc.), a wide variety of generalized Poisson relations among the three potentials and their corresponding vector and gradient fields as well as their corresponding geophysical parameters is established.

It is shown that when both vector and gradient tensor components of a potential field are simultaneously available, inverse problems, such as determining the depth to the oceanic magnetic basement, can be split into a purely "geometric" problem, which seeks to determine the dimension and position parameters of one or more prisms and a purely "geophysical" problem, which seeks to determine the physical properties (i.e., the magnetization, polarization, density, etc.) of the prism. The geometrical problem is nonlinear and must be solved iteratively using standard stochastic or least-squares inversion techniques, while the geophysical problem is linear and may be solved by direct inversion once the geometric parameters have been established. By splitting the inverse problem into two parts in this manner, the more troublesome aspects of the well-known non-uniqueness problem associated with geopotential inversions are minimized relative to other inverse modeling methods that attempt to solve for the geometric and geophysical parameters simultaneously using scalar or vector data alone. This approach to inverse modeling does not require direct measurement of the gradient field since any 2-dimensional regional survey of just one vector field component can, through rectangular harmonic analysis, yield a potential function, which in turn can be used to compute all vector and gradient tensor components of the measured field.

1. INTRODUCTION

The Earth's crust is generally composed of a variety of inhomogeneities, the geometric parameters (i.e., dimensions, orientation, distribution, etc.) and the geophysical parameters (i.e., magnetization, polarization, density, etc.) of which we seek to determine from scalar, vector, and gradient tensor measurements of one or more geopotential fields (i.e., magnetic, electric, gravity, etc.). As is well-known, the geopotential inversion problem is inherently non-unique in the sense that for a specified potential field measurement, an arbitrary choice of the geometric parameters defining the source of the potential field has a corresponding set of geophysical parameters that will leave the observed potential field unchanged. Alternatively, an arbitrary choice of the geophysical parameters has a corresponding set of geometric parameters that again will leave the observed potential field unchanged. Fortunately, many of the infinite variety of possible source geometry and geophysical parameter combinations that could produce a measured field are physically unrealistic. Unfortunately, many other possibilities are reasonable. Selecting among all the reasonable solutions, that one which is actually the source of the observed field is rarely, if ever, achieved. Instead, using supplemental information and optimization techniques, the "most likely" solution is generally considered acceptable. Historically, however, only the scalar and vector component measurements of a potential field have been used to determine the geometric and geophysical source parameters. Gravity and geomagnetic data processing and interpretation techniques used during the decade of the 1960's are summarized by Grant (1972). Inverse methods using the scalar field have been put forth by Bott (1959, 1963, and 1967), Talwani (1965), Richards et al. (1967), Bhattacharyya and Navolio (1975), Bhattacharyya and Chan (1977), Pedersen (1977), and Bhattacharyya (1980), while those using vector fields have been based on techniques developed by Plouff (1976) and Barnett

(1976), among others. These methods generally require a simultaneous solutions for both the geophysical and geometric parameters of the inverse problem, a process which leads to certain well-known ambiguities as discussed for instance by Skeels (1947) and Roy (1962).

The inversion technique developed in this report takes further advantage of the gradient tensor field, which is presumed to be either measured or derived from a rectangular harmonic potential. The potential in turn is generated from survey measurements of its corresponding vector field which covers the 2-dimensional region of interest. The addition of gradient tensor information permits the separation of the geometric and geophysical portions of the problem. This improves the stability of the inversion process. Advantage is further taken of the simplicity of the rectangular prism geometry and of the assumption of uniformly distributed geophysical parameters within each prism, which permits the closed form (i.e., non-numerical) evaluation of otherwise complicated integrals. Any geological region can be reduced to a collection of such prisms.

As a prelude to the inverse problem, it is first necessary to solve the forward geopotential modeling problem corresponding to that of a geophysical parameter uniformly distributed within a prism. This is an old problem which dates back almost 200 years and which has been solved, forgotten, and resolved in piecemeal fashion over that time by a long list of researchers, perhaps the first of whom was Poisson himself, who first formulated (1826) the connection between the magnetic and gravity potentials, now referred to as Poisson's relation. Modern interest in potential field modeling based on simple geometric structures resurged during the early part of this century with the works of Kellog (1929) and Barton (1929), which laid the foundation for the analytic results concerning rectangular prisms for vector and/or gradient tensor components

of the magnetic and/or gravity fields by Nettleton (1947), Sorokin (1951), Haaz (1953), Bhattacharyya (1964), Nagy (1966), Goodacre (1973), Plouff (1975a, 1975b), and Okabe (1979 and 1982), among many others. These efforts, however, did not fully exploit the high degree of unification that exists between the gravity and electromagnetic fields. This, we attempt to do in a methodical fashion. In doing so and to remain self-contained and internally consistent from a notational point of view, many well-known results will be rederived, others will be generalized, and new results generated to fill in a few gaps that still remain in the forward problem of modeling geopotential fields generated from rectangular prisms uniformly filled with an appropriate geophysical parameter. Along the way, the usefulness of rotational invariants that may be constructed from the various geopotential-field vector and gradient-tensor components will be pointed out, and generalized Poisson relations will be constructed and tabulated.

Also, through the generalized Poisson relations that are derived from the forward modeling results, the connection between the potential fields and the Riemann curvature tensor in the weak gravity-field limit of General Relativity is made, along with the observation that any classical unified field theory (i.e., any extension of General Relativity) must reduce in the weak gravitational/electromagnetic field limit to the Newtonian/Maxwell geopotential fields of the forward model. This in turn necessarily places a constraint on, and provides a possible starting point for, the development of a classical unified field theory.

In the discussions that follow, a local Cartesian coordinate system will be used such that the **X**-axis is oriented toward the North, the **Y**-axis is oriented East, and the **Z**-axis is oriented vertically down into the Earth. The observed potential field data sets derived from geophysical surveys, which are originally collected in geodetic coordinates, must therefore be appropriately preprocessed to isolate the crustal contribution to the fields as they appear in the local Cartesian

frame. Our procedure is first to remove temporal variations, which in the magnetic case amounts to removing such effects as the Solar Quiet Daily Variation (Sq DV) and its corresponding induction field, using nearby magnetic observatory data, and subsequent removal of the Earth's core-generated, long-wavelength features from the data, using an appropriate spherical harmonic model (e.g., WMM-90 to degree 12 for magnetic field data and WGS-84 to degree 18 for gravity data). Second, a rotation of the residual potential field vector and gradient components from geodetic to rectangular coordinates is performed using the spherical coordinate system as an intermediate stage. The corresponding coordinate transformations are also performed. Finally, biases and linear regional trends are removed from the residual field components. The resulting residuals of each field component are then assumed to be generated by the geophysical properties of the local crustal materials. It is with these properties that we are concerned.

2. THE MAGNETIC FIELD

2.1 Theoretical Background

Because the electromagnetic field obeys the superposition principle, modeling the magnetic field due to non-uniformly magnetized oceanic crust in some region of the Earth, which may be characterized as a collection of uniformly magnetized prisms, reduces to the analysis of only one prism. This analysis begins as usual with Maxwell's equations, which in Gaussian units are given by the following relations:

$$\nabla \bullet \mathbf{D} = 4\pi\sigma \tag{1a}$$

$$\nabla \bullet \mathbf{B} = 0 \tag{1b}$$

$$\nabla \times \mathbf{E} + \frac{\partial \mathbf{B}}{\partial t} = 0 \tag{1c}$$

$$\nabla \times \mathbf{H} - \frac{1}{c}\frac{\partial \mathbf{D}}{\partial t} = \frac{4\pi}{c}\mathbf{J} \tag{1d}$$

where all of the parameters have their usual meanings as do those in the accompanying constitutive relations:

$$\mathbf{D} = \mathbf{E} + 4\pi\mathbf{P} \tag{2a}$$

$$\mathbf{H} = \mathbf{B} + 4\pi\mathbf{M} \tag{2b}$$

and the generalized form of Ohm's law:

$$\mathbf{J} = \eta \bullet \mathbf{E} \tag{3}$$

where η is the conductivity tensor. A dimensional analysis of the constitutive relations shows that the units of the electric displacement **D**, the electric field **E**, and the electric polarization **P** are equivalent in Gaussian units, which are taken to be statvolts/cm. Likewise, the respective units of the magnetic induction **B**, the magnetic field **H**, and the magnetization **M** in Gaussian units are also equivalent and are taken to be nanoTeslas (nT). The electric charge density σ has units of statcoulombs/cm^3, the current density **J** has units of statamps/cm^2 , and the conductivity tensor η has units of sec^{-1}. The speed of light c has units of cm/sec.

In the discussions that follow, a local Cartesian coordinate system is used, which is oriented so that the positive **X**-axis is directed North, the positive **Y**-axis is directed East, and the positive

Z-axis is directed vertically down into the Earth. It is assumed that the field observations have been reduced as explained in the introduction and that we are dealing with the resulting residuals that are generated by the Earth's crust alone. Then, under the assumption that no electric fields, currents, or charges are present, the magnetic fields are necessarily time independent, and Maxwell's equations reduce to their magnetostatic forms:

$$\nabla \bullet \mathbf{B} = 0 \tag{4a}$$

$$\nabla \times \mathbf{H} = 0 \tag{4b}$$

with eq. (2b) as the only remaining constitutive relation. The second of these equations implies that the magnetic field, $\mathbf{H}(\mathbf{r})$, is the gradient of some scalar magnetic potential $\Phi(\mathbf{r})$, (units: nT-cm). That is:

$$\mathbf{H} = -\nabla\Phi \tag{5}$$

By taking the divergence of eq. (2b) and combining the result with eqs. (4a) and (5), the following familiar Poisson equation is obtained:

$$\nabla^2\Phi = 4\pi \nabla \bullet \mathbf{M} \tag{6}$$

It has the well-known solution:

$$\Phi(\mathbf{r}) = -\int_{V'} \frac{\nabla' \bullet \mathbf{M}}{|\mathbf{r}-\mathbf{r}'|} \, d^3\mathbf{r}' \tag{7}$$

Here, we use the notation of Jackson (1975), where the primed coordinates range over the magnetized volume V', while the unprimed coordinates refer to the point of observation. This expression for the magnetic potential is valid regardless of whether or not the point of observation **r** is inside or outside the magnetized volume.

Eq. (7) may be written in more convenient form by employing the following identity:

$$\nabla \bullet (\Psi \mathbf{M}) = \mathbf{M} \bullet \nabla\Psi + \Psi \nabla \bullet \mathbf{M} \tag{8}$$

where, if the scalar function Ψ is identified as:

$$\Psi(\mathbf{r}, \mathbf{r}') = \frac{1}{|\mathbf{r} - \mathbf{r}'|} \tag{9}$$

then:

$$\Phi(\mathbf{r}) = -\int_{V'} \nabla' \bullet \frac{\mathbf{M}(\mathbf{r}')}{|\mathbf{r} - \mathbf{r}'|}\, d^3\mathbf{r}' + \int_{V'} \mathbf{M}(\mathbf{r}') \bullet \nabla' \left(\frac{1}{|\mathbf{r} - \mathbf{r}'|}\right) d^3\mathbf{r}' \tag{10}$$

Using the divergence theorem, it can be shown that the first integral vanishes over any volume that completely encloses the volume V'. In the second integral, use may be made of the rule:

$$\nabla' \left(\frac{1}{|\mathbf{r} - \mathbf{r}'|}\right) = -\nabla\left(\frac{1}{|\mathbf{r} - \mathbf{r}'|}\right) \tag{11}$$

Thus, the magnetic potential reduces to its most useful form:

$$\Phi(\mathbf{r}) = -\nabla \bullet \int_{V'} \frac{\mathbf{M}(\mathbf{r}')}{|\mathbf{r}-\mathbf{r}'|}\, d^3\mathbf{r}' \tag{12}$$

Now, measurements of the magnetic field are usually made in regions of space that are void of any magnetic materials, as is the case with aeromagnetic surveys, for instance. In such regions the magnetization vector $\mathbf{M}(\mathbf{r})$ is zero, so that by eq. (2b), $\mathbf{H}(\mathbf{r}) = \mathbf{B}(\mathbf{r})$. Consequently, eq. (5) reduces to:

$$\mathbf{B}(\mathbf{r}) = -\nabla\Phi(\mathbf{r}) \tag{13}$$

The gradient of $\mathbf{B}(\mathbf{r})$ yields the magnetic gradient tensor $\mathscr{B}(\mathbf{r})$ (units: nT/cm):

$$\mathscr{B}(\mathbf{r}) = \nabla\mathbf{B}(\mathbf{r}) \tag{14}$$

Both $\mathbf{B}(\mathbf{r})$ and $\mathscr{B}(\mathbf{r})$ are measurable quantities. The state of the art in magnetic gradiometry is discussed by Fram et al. (1974), Kekelis (1984), and Hastings et al. (1985).

In the local Cartesian reference frame, the magnetic induction and its corresponding gradient tensor, expressed in terms of their respective vector and tensor components, are written as:

$$\mathbf{B}(\mathbf{r}) = B_x(\mathbf{r})\mathbf{i} + B_y(\mathbf{r})\mathbf{j} + B_z(\mathbf{r})\mathbf{k} \tag{15}$$

$$\mathscr{B}(\mathbf{r}) = \begin{pmatrix} \frac{\partial B_x}{\partial x} & \frac{\partial B_x}{\partial y} & \frac{\partial B_x}{\partial z} \\ \frac{\partial B_y}{\partial x} & \frac{\partial B_y}{\partial y} & \frac{\partial B_y}{\partial z} \\ \frac{\partial B_z}{\partial x} & \frac{\partial B_z}{\partial y} & \frac{\partial B_z}{\partial z} \end{pmatrix} \tag{16}$$

Rather than using the above notation to describe the vector and gradient tensor components of the magnetic field, we will find it more convenient to use tensor notation. In tensor notation, the coordinates and corresponding subscripts x, y, and z are replaced by numerical indices ranging from 1 to 3 such that $x^1 = x$, $x^2 = y$, and $x^3 = z$. Then, for instance, $B_2 = B_y$ and $\mathscr{B}_{23} = \partial B_2/\partial x^3 = \partial B_y/\partial z$. We further employ the single slash notation " / " to denote Euclidean differentiation and the double slash " // " to denote non-Euclidean differentiation, where the curvature of the metric space must be considered. For the moment, we will be concerned only with Euclidean space, for which our example reduces to: $\mathscr{B}_{23} = \partial B_y/\partial z = B_{2/3}$. So, in general, the vector and tensor components of the magnetic field are denoted as B_μ and $\mathscr{B}_{\mu\nu}$ respectively, where the Greek indices μ and ν range from 1 to 3. As a further notational point, we emphasize that in a Euclidean or Cartesian coordinate system, there is no distinction between contravariant vector and tensor components with raised indices (e.g., $\mathscr{B}^{\mu\nu}$) and covariant vector and tensor components with lowered indices (e.g., $\mathscr{B}_{\mu\nu}$). Consequently, we will use the convention that all indices are to remain lowered unless they are being summed over. Then, in accordance with Einstein summation notation, the index being summed over, which must necessarily appear twice in a given mathematical expression, will have one index raised and one lowered. Then, as an example:

$$\mathscr{B}_\mu{}^\nu \mathscr{B}_{\nu\lambda} \equiv \sum_{\nu=1}^{3} \mathscr{B}_\mu^\nu \mathscr{B}_{\nu\lambda} \tag{17}$$

This convention will be used exclusively unless otherwise explicitly stated to the contrary. Using this tensor notation, which corresponds to that of Adler, Bazin, and Schiffer (1975),

eq. (13) becomes:

$$B_{\mu} = -\Phi_{/\mu} \tag{18}$$

while eq. (14) becomes:

$$\mathcal{B}_{\mu\nu} = B_{\mu/\nu} \tag{19}$$

Also, recalling that the point of observation **r** is assumed to be outside of the magnetized volume V' so that **H(r) = B(r)**, the magnetostatic eqs. (4a) and (4b) reduce to the following:

$$B^{\mu}{}_{/\mu} = 0 \tag{20a}$$

$$B_{\mu/\nu} - B_{\nu/\mu} = 0 \tag{20b}$$

Using eq. (19), eqs. (20a) and (20b) may also be written as:

$$\mathcal{B}^{\mu}{}_{\mu} = 0 \tag{21a}$$

$$\mathcal{B}_{\mu\nu} = \mathcal{B}_{\nu\mu} \tag{21b}$$

Furthermore, since $\mathcal{B}_{\mu\nu}$ is the gradient of a vector, it is by definition a tensor. Equation (21a) states that the trace (i.e., the diagonal element sum) of the tensor is zero, while eq. (21b) says that this tensor is also symmetric. These two symmetry conditions, which may be viewed as constraints on the magnetic field gradient tensor, reduce the number of the tensor's independent

components from 9 to 5. Designers of magnetic gradiometers take this fact into account to reduce the electronic complexity of the instrument. However, some redundency may be useful in actual field situations.

2.2 Related Magnetic Vectors, Tensors, and Rotational Invariants

From the vector B_μ and the gradient tensor $\mathcal{B}_{\mu\nu}$, a variety of potentially useful vectors, tensors, and scalar invariants can be constructed. These invariants can be used as additional tools to help identify and interpret the underlying crustal geology. For instance, the following vector may be constructed:

$$\beta_\mu \equiv \mathcal{B}_\mu{}^\lambda B_\lambda \tag{22}$$

The vector β_μ (units: nT^2/cm) may be viewed as the projection of the magnetic gradient tensor onto the magnetic induction vector. From it may be constructed its characteristic rotational invariant (units: nT^2/cm):

$$\beta \equiv \sqrt{\beta_\mu \beta^\mu} \tag{23}$$

Additionally, limiting the discussion only to tensors of rank two, it is possible to construct the following four new tensors:

$$\beta_{\mu\nu} \equiv \beta_\mu \beta_\nu \tag{24a}$$

$$\mathcal{Q}_{\mu\nu} \equiv \beta_\mu B_\nu \tag{24b}$$

$$\mathcal{S}_{\mu\nu} \equiv \mathcal{R}_{\mu}{}^{\lambda}\mathcal{R}_{\lambda\nu} \tag{24c}$$

$$B_{\mu\nu} \equiv B_{\mu}B_{\nu} \tag{24d}$$

Similar tensors can also be constructed from the electric and gravitational fields. Three of these tensors, $\beta_{\mu\nu}$ (units: nT^4/cm^2), $\mathcal{S}_{\mu\nu}$ (units: nT^2/cm^2), and $B_{\mu\nu}$ (units: nT^2) are symmetric, while the tensor $\mathcal{Q}_{\mu\nu}$ (units: nT^3/cm) has both symmetric and antisymmetric parts. By taking the trace of these tensors, several additional rotational invariants can also be constructed. Although we will not dwell upon them, we point them out so that these invariants may be exploited for their long-range and short-range dependencies, as the needs of a particular application dictate. We define these invariants as follows:

$$\beta \equiv \sqrt{\beta^{\mu}{}_{\mu}} \tag{25a}$$

$$\mathcal{Q} \equiv \mathcal{Q}^{\mu}{}_{\mu} \tag{25b}$$

$$\mathcal{S} \equiv \sqrt{\mathcal{S}^{\mu}{}_{\mu}} \tag{25c}$$

$$B \equiv \sqrt{B^{\mu}{}_{\mu}} \tag{25d}$$

The last invariant, B, is just the total magnetic intensity, while $\mathcal{S}$ is the total magnetic gradient. From these invariants, it is possible to generate three other invariants that have dimensions of inverse length (i.e., units: cm^{-1}):

$$Q_1 \equiv \mathscr{I}/B \tag{26a}$$

$$Q_2 \equiv \beta/B^2 \tag{26b}$$

$$Q_3 \equiv \mathscr{Q}/B^3 \tag{26c}$$

It so happens that all three of these invariant functions, in the far field, vary inversely with distance from the source (i.e., as r^{-1}). This can be seen by noting that in the far field, B_μ varies as r^{-3}, while $\mathscr{B}_{\mu\nu}$ varies as r^{-4}. By taking ratios of these invariants, three more dimensionless invariants can be generated which in the far field are constant, but in the near field are highly variable and may be quite sensitive to subtle variations in the source structure or composition. These are:

$$q_1 \equiv Q_1/Q_2 \tag{27a}$$

$$q_2 \equiv Q_2/Q_3 \tag{27b}$$

$$q_3 \equiv Q_3/Q_1 \tag{27c}$$

Some of these invariants may prove to be more useful than others as tools for geological interpretation. One that does seem to be particularly interesting is Q_1, which is simply the ratio of the total magnetic gradient intensity to the total magnetic field intensity. It has the desirable feature of being independent of the orientation of the magnetization vector of the source body. Thus, the source body lateral extention is more sharply defined than with traditional methods.

2.3 The Uniformly Magnetized Rectangular Prism

The static magnetic field generated by an arbitrarily shaped body which has an arbitrary distribution, orientation, and intensity of magnetization can always be represented as having been generated by a collection of uniformly magnetized rectangular prisms. It is, of course, possible to use other elementary geometries such as multifaceted polyhedrons as the basic building blocks. However, for local field analysis we see no special advantage in doing so. Instead, we prefer to maintain the unique compatibility that rectangular prisms have with the Cartesian coordinate system.

Now, consider a single rectangular prism with sides parallel to the coordinate axes, the orientation of which we have previously defined. The center of this prism with respect to the origin of the coordinate system is located at the point $\mathbf{r}_0 = (x_0, y_0, z_0)$. The prism dimensions are taken to be λ_x , λ_y , and λ_z along their respective coordinate axes. When this prism is assigned a uniform magnetization $\mathbf{M}$, having constant components $M_x = M_1$, $M_y = M_2$, and $M_z = M_3$ so that:

$$\mathbf{M} = M_x\mathbf{i} + M_y\mathbf{j} + M_z\mathbf{k} \tag{28}$$

then it is possible, as is shown in Appendix A, to evaluate eq. (12) for the scalar potential, $\Phi(\mathbf{r})$, in closed form and thereby obtain the following expression:

$$\Phi(\mathbf{r}) = -\Omega^{\lambda}{}_{\sigma}\varepsilon^{\sigma}M_{\lambda} \tag{30}$$

where the elements of the $\Omega(\mathbf{r})$ matrix, which are explicitly listed in Table I, are purely

Table 1. Elements of the Ω Matrix

$$\Omega_{11} = + (x - x') \tan^{-1}\left[\frac{(y-y')(z-z')}{(x-x')R}\right] \Big|_{x',y',z'}$$

$$\Omega_{12} = - (y - y') \ln[R + (z - z')] \Big|_{x',y',z'}$$

$$\Omega_{13} = - (z - z') \ln[R + (y - y')] \Big|_{x',y',z'}$$

$$\Omega_{21} = - (x - x') \ln[R + (z - z')] \Big|_{x',y',z'}$$

$$\Omega_{22} = + (y - y') \tan^{-1}\left[\frac{(x-x')(z-z')}{(y-y')R}\right] \Big|_{x',y',z'}$$

$$\Omega_{23} = - (z - z') \ln[R + (x - x')] \Big|_{x',y',z'}$$

$$\Omega_{31} = - (x - x') \ln[R + (y - y')] \Big|_{x',y',z'}$$

$$\Omega_{32} = - (y - y') \ln[R + (x - x')] \Big|_{x',y',z'}$$

$$\Omega_{33} = + (z - z') \tan^{-1}\left[\frac{(x-x')(y-y')}{(z-z')R}\right] \Big|_{x',y',z'}$$

geometric in character, depending only on the position $\mathbf{r}$, the prism dimensions, and the prism location $\mathbf{r}_0$. Both $\mathbf{r}$ and $\mathbf{r}_0$ are referenced to a conveniently chosen origin.

As a matter of notational convenience, we have defined the constant vector $\boldsymbol{\varepsilon}$:

$$\boldsymbol{\varepsilon} = \varepsilon_1 \mathbf{i} + \varepsilon_2 \mathbf{j} + \varepsilon_3 \mathbf{k} \tag{31}$$

so that each of its components is equal to one. That is:

$$\varepsilon_1 = \varepsilon_2 = \varepsilon_3 \equiv 1 \tag{32}$$

The virtue of defining the vector, $\boldsymbol{\varepsilon}$, in this manner is that the mathematical forms of various geopotential field equations are considerably simplified.

In Table 1, the notation $|_{x', y', z'}$ is used to indicate that the primed coordinates are to be evaluated at the boundaries of the prism as indicated in Appendix A. Also in Table 1, the parameter R is defined to be the Euclidean distance between the source prism and the point of observation:

$$R = \sqrt{(x-x')^2 + (y-y')^2 + (z-z')^2} \tag{33}$$

Although it is possible to derive an expression for the magnetic induction vector, $\mathbf{B}(\mathbf{r})$, by directly taking the gradient of eq. (30), it turns out to be simpler to combine eqs. (12) and (13) and then to evaluate the resulting integrals as shown in Appendix B. The vector components of the magnetic induction vector, thus obtained, are expressed quite simply in tensor notation as:

$$B_\mu = \Lambda_\mu{}^\lambda M_\lambda \tag{34}$$

where the elements of the 3 x 3 matrix $\Lambda(\mathbf{r})$, which are listed in Table 2, are, like those of the matrix Ω to which it is related, purely geometrical in character.

Figures (1a), (1b), and (1c) illustrate the three components (x, y, and z respectively) of the magnetic field vector **B** generated according to eq. (34) by a single prism with unit magnetization **M** oriented vertically downward in the positive Z direction. The computations were performed on a surface situated a unit distance above the prism. Figure (1d) illustrates the magnetic total intensity for the same situation. The scale in these figures is arbitrary. Therefore, these figures could represent the magnetic field generated by a rock sample a few centimeters in diameter in the laboratory, or they could represent the magnetic field generated by a large volume of ocean crust several kilometers in diameter. Figures (2a), (2b), and (2c) are vector components of the magnetic induction B_x (North), B_y (East), and B_z (Vertically Down) respectively for a multiple prism situation simulating a region encompassing a magnetic reversal in the oceanic crust. The magnetic reversal axis straddles the East-West coordinate axis. North of this axis, the magnetization is vertically upward, while South of this axis, the magnetization is vertically downward. The magnetizations are of unit magnitude in both directions. The prism dimensions are arbitrarily chosen to be of unit length. Figure (2d) is the total magnetic intensity for this situation. The observation plane is a unit distance above the line of prisms. The magnetic field contribution of each prism is added vectorially at each grid site on the observational plane.

Table 2. Elements of the Λ Matrix

$$\Lambda_{11} = + \tan^{-1}\left[\frac{(y-y')(z-z')}{(x-x')R}\right] \Big|_{x',y',z'}$$

$$\Lambda_{12} = - \ln[R + (z - z')] \Big|_{x',y',z'}$$

$$\Lambda_{13} = - \ln[R + (y - y')] \Big|_{x',y',z'}$$

$$\Lambda_{21} = - \ln[R + (z - z')] \Big|_{x',y',z'}$$

$$\Lambda_{22} = + \tan^{-1}\left[\frac{(x-x')(z-z')}{(y-y')R}\right] \Big|_{x',y',z'}$$

$$\Lambda_{23} = - \ln[R + (x - x')] \Big|_{x',y',z'}$$

$$\Lambda_{31} = - \ln[R + (y - y')] \Big|_{x',y',z'}$$

$$\Lambda_{32} = - \ln[R + (x - x')] \Big|_{x',y',z'}$$

$$\Lambda_{33} = + \tan^{-1}\left[\frac{(x-x')(y-y')}{(z-z')R}\right] \Big|_{x',y',z'}$$

Figure 1a. North-X Component of a Vertically Magnetized Prism.
(units: nT, arbitrary scale)

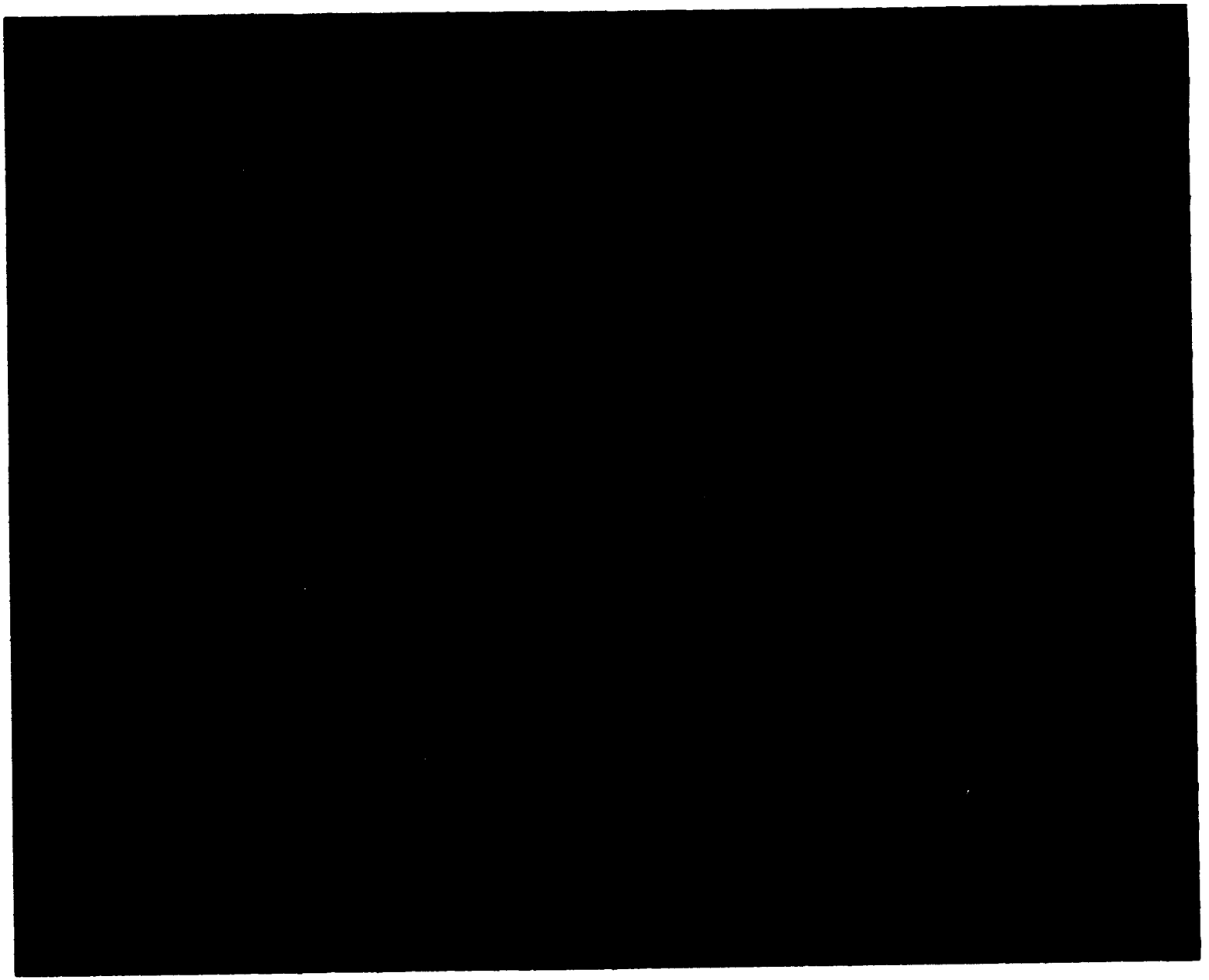

Figure 1b. East-Y Component of a Vertically Magnetized Prism.
(units: nT, arbitrary scale)

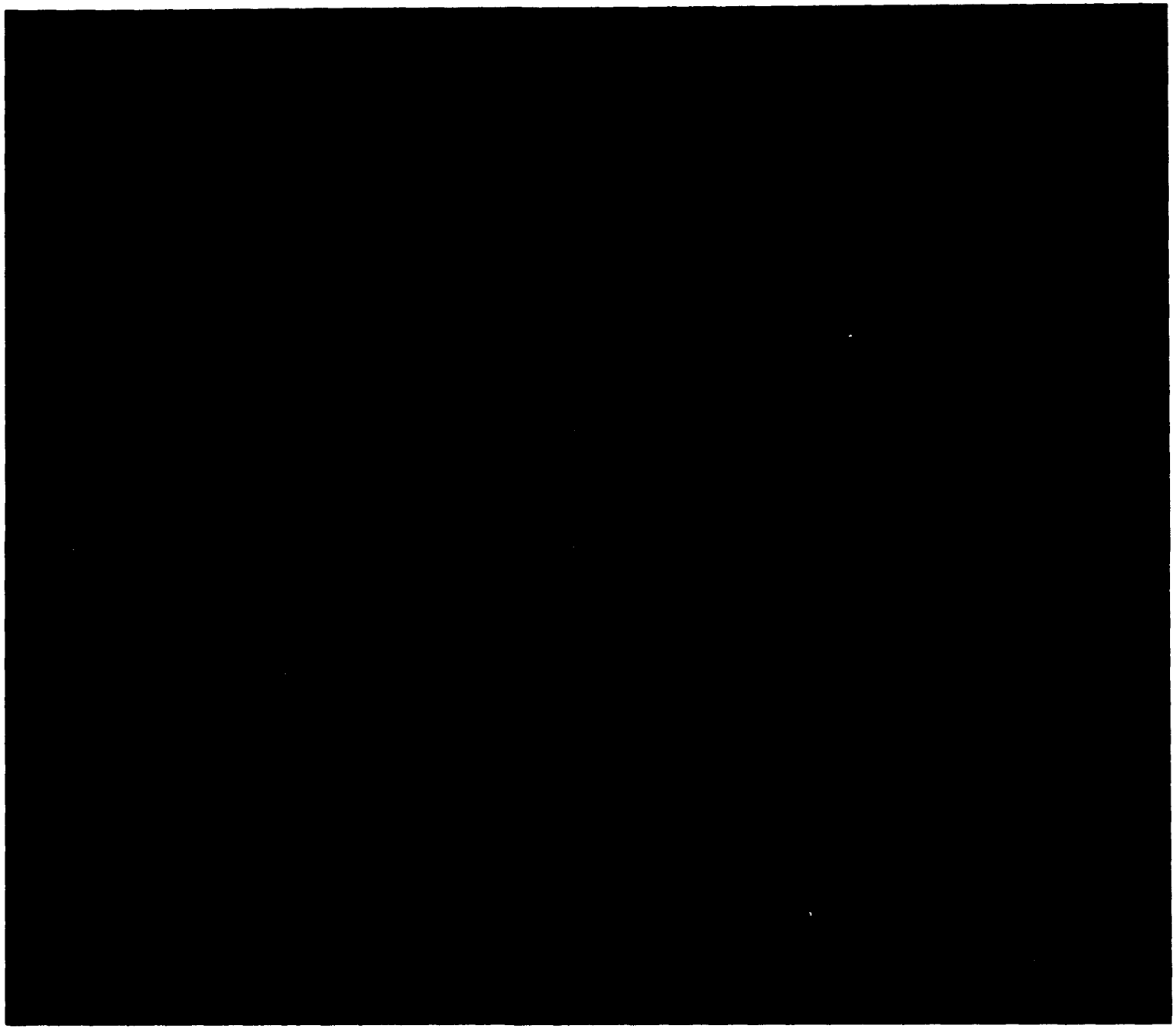

Figure 1c. Vertical-**Z** Component of a Vertically Magnetized Prism.
(units: nT, arbitrary scale)

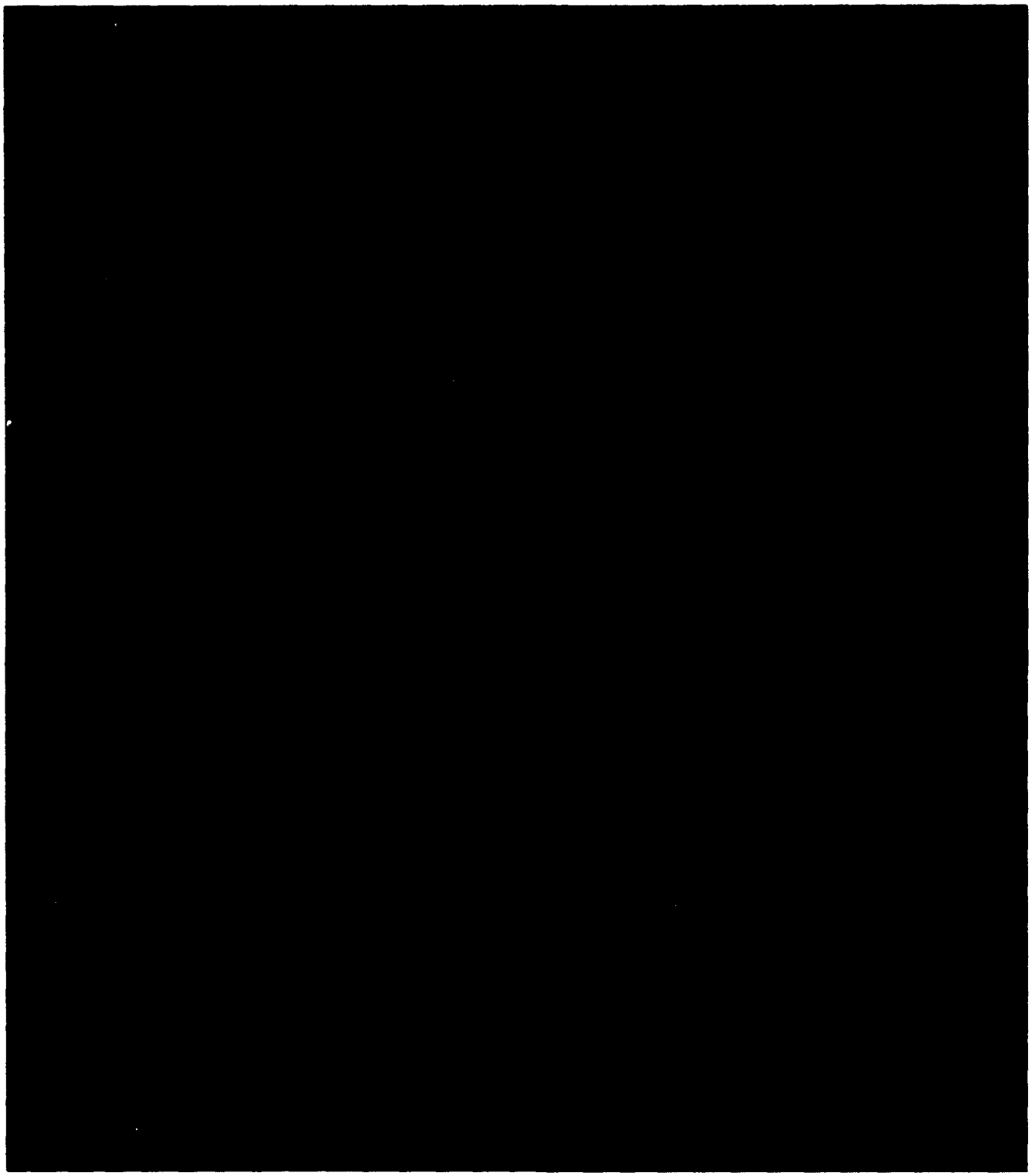

Figure 1d. Total Intensity of a Vertically Magnetized Prism.
(units: nT, arbitrary scale)

Figure 2a. North-X Component in a Region of Vertical Magnetization Reversal.
(units: nT, arbitrary scale)

Figure 2b. East-Y Component in a Region of Vertical Magnetization Reversal.
(units: nT, arbitrary scale)

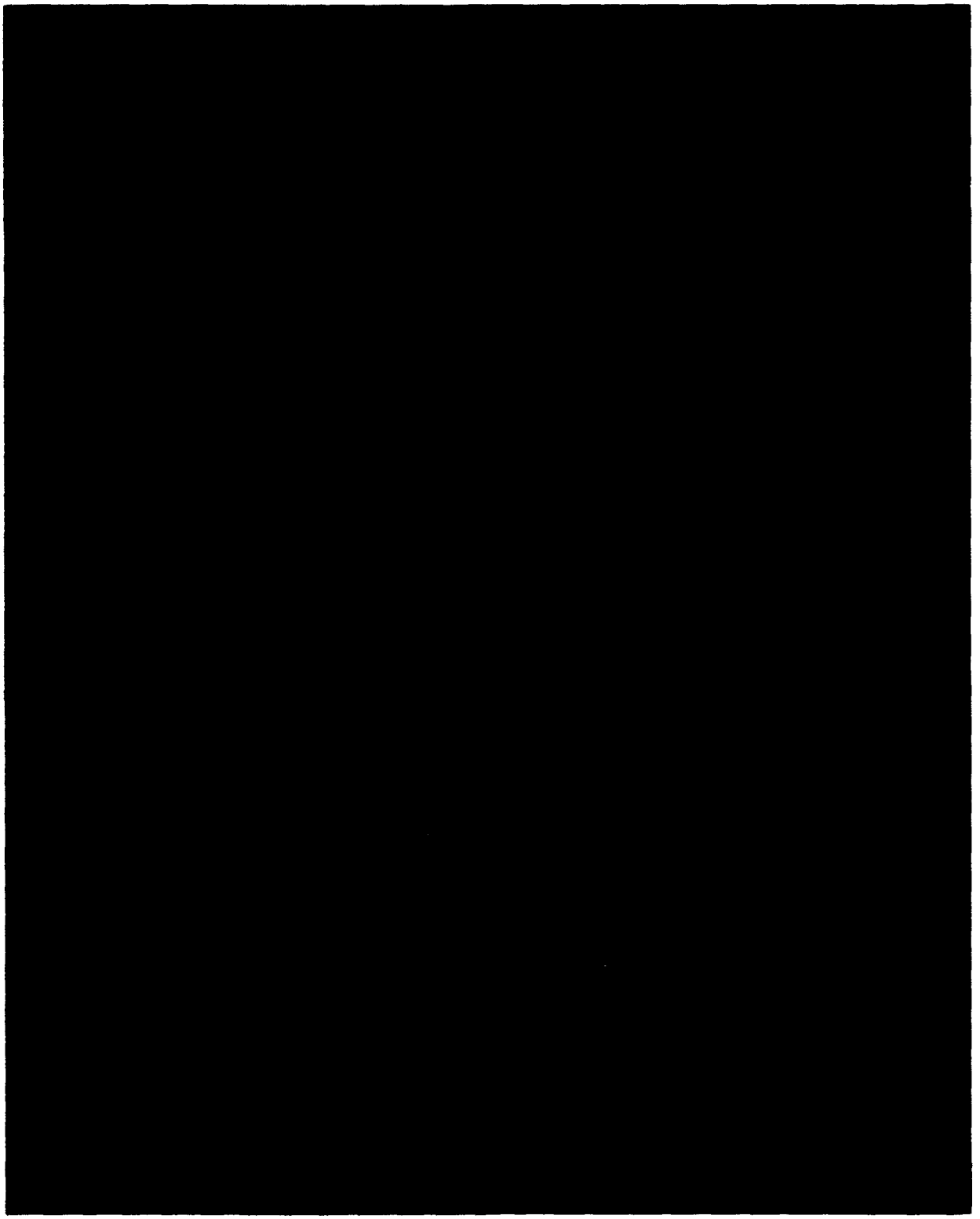

Figure 2c. Vertical-Z Component in a Region of Vertical Magnetization Reversal.
(units: nT, arbitrary scale)

Figure 2d. Total Intensity in a Region of Vertical Magnetization Reversal.
(units: nT, arbitrary scale)

It is perhaps helpful to view the Ω matrix as a transformation that maps the magnetization vector **M** into the magnetic potential Φ, while the matrix Λ acts as a transformation that maps the magnetization vector into the magnetic induction **B**. The relationships among components of these two matrices, which are in fact tensors of rank two, are found by combining eqs. (18), (29), and (34), which yields:

$$\Lambda_{\mu\nu} = \Omega_{\mu\sigma/\nu}\varepsilon^{\sigma} \tag{35}$$

The magnetic gradient due to the rectangular prism is obtained by combining eqs. (19) and (34), which yields:

$$\mathcal{B}_{\mu\nu} = \Lambda_{\mu}{}^{\lambda}{}_{/\nu} M_{\lambda} \tag{36}$$

The gradient of Λ appearing in eq. (36) forms a tensor of rank 3. It maps the magnetization of the rectangular prism into the magnetic gradient tensor. The components of this third-rank tensor are listed in Table 3. These components are obtained by taking the indicated derivatives of the elements of the Λ matrix and simplifying the resulting algebraic forms.

The Λ matrix is symmetric, and if the point of observation **r** extends beyond the boundary of the volume V' (denoted as $\partial V'$), then it is also traceless. If **r** is within this boundary, then the trace of Λ is a nonzero constant. These results may be summarized in the following way:

$$\Lambda_{\mu\nu} = \Lambda_{\nu\mu} \tag{37a}$$

$$\Lambda^{\mu}{}_{\mu} = \begin{cases} -4\pi & \mathbf{r} \le \partial V' \\ 0 & \mathbf{r} > \partial V' \end{cases} \tag{37b}$$

Table 3. Derivatives of the A Matrix Elements

$$\Lambda_{11/1} = + \frac{1}{R}\left[\frac{(z-z')}{R+(y-y')} + \frac{(y-y')}{R+(z-z')}\right]\Big|_{x',y',z'}$$

$$\Lambda_{11/2} = - \frac{1}{R}\left[\frac{(x-x')}{R+(z-z')}\right]\Big|_{x',y',z'}$$

$$\Lambda_{11/3} = - \frac{1}{R}\left[\frac{(x-x')}{R+(y-y')}\right]\Big|_{x',y',z'}$$

$$\Lambda_{12/1} = - \frac{1}{R}\left[\frac{(x-x')}{R+(z-z')}\right]\Big|_{x',y',z'}$$

$$\Lambda_{12/2} = - \frac{1}{R}\left[\frac{(y-y')}{R+(z-z')}\right]\Big|_{x',y',z'}$$

$$\Lambda_{12/3} = - \frac{1}{R}\Big|_{x',y',z'}$$

$$\Lambda_{13/1} = - \frac{1}{R}\left[\frac{(x-x')}{R+(y-y')}\right]\Big|_{x',y',z'}$$

$$\Lambda_{13/2} = - \frac{1}{R}\Big|_{x',y',z'}$$

$$\Lambda_{13/3} = - \frac{1}{R}\left[\frac{(z-z')}{R+(y-y')}\right]\Big|_{x',y',z'}$$

$$\Lambda_{21/1} = - \frac{1}{R}\left[\frac{(x-x')}{R+(z-z')}\right]\Big|_{x',y',z'}$$

$$\Lambda_{21/2} = - \frac{1}{R}\left[\frac{(y-y')}{R+(z-z')}\right]\Big|_{x',y',z'}$$

$$\Lambda_{21/3} = - \frac{1}{R}\Big|_{x',y',z'}$$

$$\Lambda_{22/1} = - \frac{1}{R}\left[\frac{(y-y')}{R+(z-z')}\right]\Big|_{x',y',z'}$$

$$\Lambda_{22/2} = + \frac{1}{R}\left[\frac{(z-z')}{R+(x-x')} + \frac{(x-x')}{R+(z-z')}\right]\Big|_{x',y',z'}$$

Table 3. Derivatives of the A Matrix Elements (con.)

$$\Lambda_{22/3} = -\frac{1}{R}\left[\frac{(y-y')}{R+(x-x')}\right]\Big|_{x',y',z'}$$

$$\Lambda_{23/1} = -\frac{1}{R}\Big|_{x',y',z'}$$

$$\Lambda_{23/2} = -\frac{1}{R}\left[\frac{(y-y')}{R+(x-x')}\right]\Big|_{x',y',z'}$$

$$\Lambda_{23/3} = -\frac{1}{R}\left[\frac{(z-z')}{R+(x-x')}\right]\Big|_{x',y',z'}$$

$$\Lambda_{31/1} = -\frac{1}{R}\left[\frac{(x-x')}{R+(y-y')}\right]\Big|_{x',y',z'}$$

$$\Lambda_{31/2} = -\frac{1}{R}\Big|_{x',y',z'}$$

$$\Lambda_{31/3} = -\frac{1}{R}\left[\frac{(z-z')}{R+(y-y')}\right]\Big|_{x',y',z'}$$

$$\Lambda_{32/1} = -\frac{1}{R}\Big|_{x',y',z'}$$

$$\Lambda_{32/2} = -\frac{1}{R}\left[\frac{(y-y')}{R+(x-x')}\right]\Big|_{x',y',z'}$$

$$\Lambda_{32/3} = -\frac{1}{R}\left[\frac{(z-z')}{R+(x-x')}\right]\Big|_{x',y',z'}$$

$$\Lambda_{33/1} = -\frac{1}{R}\left[\frac{(z-z')}{R+(y-y')}\right]\Big|_{x',y',z'}$$

$$\Lambda_{33/2} = -\frac{1}{R}\left[\frac{(z-z')}{R+(x-x')}\right]\Big|_{x',y',z'}$$

$$\Lambda_{33/3} = +\frac{1}{R}\left[\frac{(y-y')}{R+(x-x')} + \frac{(x-x')}{R+(y-y')}\right]\Big|_{x',y',z'}$$

We are primarily concerned with the situation for which the trace is zero. Together, these last two equations imply that Λ has just 5 independent components. Using eqs. (37a) and (37b), it is possible to deduce, in conjunction with Table 3, the following symmetry relations among the gradient components of Λ:

$$\Lambda_{\mu\nu/\lambda} = \Lambda_{\nu\mu/\lambda} \tag{38a}$$

$$\Lambda_{\mu\nu/\lambda} = \Lambda_{\lambda\mu/\nu} = \Lambda_{\nu\lambda/\mu} \tag{38b}$$

$$\Lambda^{\mu}{}_{\mu/\lambda} = 0 \tag{38c}$$

These symmetry relations substantially reduce the number of independent components of the gradient of the Λ tensor from a possible 27 to just 7 .

2.4 Geomagnetic Inversion

Still considering a single prism, it should be clear that at any observation point **r**, eq. (34) can be formally inverted to give:

$$M_\lambda = \overline{\Lambda}_\lambda{}^{\mu} B_\mu \tag{39}$$

where $\overline{\Lambda}$ is the inverse of the 3x3 matrix Λ and has elements that satisfy the following relation:

$$\overline{\Lambda}_\mu{}^{\lambda} \Lambda_{\lambda\nu} = \delta_{\mu\nu} \tag{40}$$

where $\delta_{\mu\nu}$ is the Kronecker delta function. Subsequent insertion of eq. (39) into eq. (36) yields a

relationship between the magnetic field and its gradient that is independent of the magnetization:

$$\mathcal{B}_{\mu\nu} = \Lambda_{\mu}{}^{\lambda}{}_{/\nu}\,\overline{\Lambda}_{\lambda}{}^{\sigma}\,B_{\sigma} \tag{41}$$

This is the main result. Essentially, a decoupling of the geophysical and geometric parameters has taken place. Since the magnetic field and its gradient are both measurable quantities, eq. (41) is in essence a nonlinear system of five independent equations for the six unknown geometric parameters of the magnetized prism, namely: $\mathbf{r}_0$ and λ_x , λ_y , and λ_z. Since there are more unknowns than equations, this system of equations is underdetermined. For this reason and also because magnetic field measurements contain errors and extraneous environmental noise, it is necessary to make some additional assumptions regarding the size or location of the prism in order to reduce the number of unknown geometric parameters. Alternatively, it is possible to make many field measurements at a variety of locations, in which case, this system of equations will be overdetermined. In either case, or when the two approaches are combined, the problem is a nonlinear one which can be solved via stochastic inversion techniques. Having thus determined the prism's geometric parameters, the tensor $\mathbf{\Lambda(r)}$ is considered to be known and is unique in the least-squares sense as being generated by the "most likely" or "optimal" set of prism parameters. Knowledge of this tensor then permits eq. (39) to be solved via a straightforward linear inversion to obtain the "most likely" or "optimal" magnetization (the geophysical parameter) of the prism, which is referred to as the "equivalent" magnetization of the prism. This is the magnetization one expects to obtain if the actual magnetization were truly smeared out uniformly over the entire prism, and the "most likely" geometric parameter solution is also the environmentally "true" solution.

2.5 Practical Applications to Large Area Aeromagnetic Surveys

To determine the crustal magnetization and depth to the magnetic basement (i.e., to the basalt layer), it is not actually necessary to measure the gradient field in order to apply the inversion technique described above. If a 2-dimensional vector aeromagnetic survey is performed over a given area, it is possible to use the vector magnetic data to compute a rectangular harmonic potential function from which the gradient data may be computed. The procedures used in the July 1981 Juan de Fuca Project MAGNET vector aeromagnetic survey performed by the Naval Oceanographic Office serve as a practical example of the kind of data manipulation that is necessary to use this inverse modeling technique successfully (Quinn and Shiel [1993]).

The Juan de Fuca survey area, which covered the geographical region from 47^0 N latitude to 51^0 N latitude and from 124^0 W longitude to 130^0 W longitude, was densely surveyed at a 500-ft altitude in the East-West direction with approximately 3 nautical miles between these survey tracks. A few North-South tracks were also flown for control. The effective along-track data sample rate was 0.5 Hertz, while the speed of Project MAGNET's RP-3D Orion aircraft was approximately 240 nautical miles per hour. Magnetograms from a nearby geomagnetic observatory at Victoria, British Columbia, were used to monitor and remove temporal magnetic variations. A portable Vector Magnetic Ground Station (VMGS) was also established at Mc Chord Air Force Base near Tacoma, Washington, for the same purpose. This data set was edited for spurious electronic noise spikes, and the Main magnetic field was removed using the 1980 Epoch Goddard Space Flight Center (GSFC 12/83) spherical harmonic model (Langel and Estes [1985]) up to harmonic degree 12. The residual X-, Y-, and Z-components of the entire data set were each uniformly gridded and interpolated as necessary into lat x lon cells of 1.5 arcminutes x 1.5 arcminutes (i.e., roughly half the East-West track line separation) such that

each magnetic component consisted of 256 x 256 grid points. The gridding process has the advantage of smoothing out instrument noise, navigational errors, and other environmental noise that cannot otherwise be accounted for and thus eliminated. The coordinates of each grid point were then transformed from geodetic to rectangular coordinates, using the spherical coordinate system as an intermediate step. At the same time, the vector components at each grid point were rotated from geodetic to rectangular coordinates, also using the spherical coordinate system as an intermediate stage. Biases and linear trends in the North-South and East-West directions were then determined and removed from the residual grids of their corresponding components. These biases and trends were also saved as the "regional" models of the survey area. Subsequently, a 2-dimensional Fast Fourier Transform (2-D FFT) was performed on only the Z-component grid. This procedure results in a set of complex Fourier coefficients in the wavenumber domain which are algebraically related in a simple way to the real coefficients of a rectangular-harmonic magnetic potential-function model of the surveyed area. This model is composed of 256 x 256 = 65,536 coefficients. Having determined the rectangular harmonic model in this way, it is a straightforward process to recompute, using the 2-D FFT, not only the vector magnetic components but the magnetic gradient components as well. The result is a set of 3 vector component grids and 5 independent gradient component grids, each with 256 x 256 grid points. Since all of these magnetic component grids were derived from the original Z-component grid, they are necessarily consistent with each other. The original vector component grids derived directly from the survey data would not have been as consistent because each vector component observation contains unique instrumental errors and environmental noise which are then passed on to the grids generated from those measurements. Therefore, in the inversion process that follows, we use the X- , Y-, and Z-component grids generated from the model, which in turn is

derived from just the observed Z-component gridded data, rather than using the X- and Y-component grids generated directly from the observed data. The computed and observed Z-component grids are identical since this component is used to generate the model.

At this stage each grid point has associated with it the "observed" magnetic vector components B_μ and the "observed" magnetic gradient components $\mathcal{B}_{\mu\nu}$. Here, the word "observed" is used loosely since each grid value of a magnetic vector or gradient component is based indirectly on measured data through the rectangular harmonic model, which in turn is derived from observed data. Magnetic gradients, $\mathcal{B}_{\mu\nu}$, generated from eq. (41) using "only" the "observed" magnetic "vector" components will be referred to as the "computed" magnetic gradients. Thus, for each magnetic gradient component at each grid point there exists an "observed" and a "computed" value. It is therefore possible to solve for the geometric parameters for each grid point by setting up a χ^2 function which is the sum of the square of the differences between the "computed" and "observed" values of the five independent gradient components for each grid point. In the Juan de Fuca case, we first made a few assumptions based on knowledge of magnetic sources in the oceanic crust to constrain the inversion problem in order to eliminate some variables. Since it is known that the oceanic crust typically has two magnetic layers, one about .5 km thick with reasonably high magnetization and another layer about 1 km thick directly below the first layer, but considerably less magnetic, we fixed the thickness of a single prism to be 1.5 km thick. The lateral prism dimensions were also fixed to be 5 km on a side (about the same length as the estimated depth to source). The prism was centered below the particular grid point of interest so that there was a minimum of 2.5 km from the grid point to the edge of the prism. From a geomorphological point of view, dramatic

variations in depth or magnetization should not dominate for such small lateral distances. Consequently, the influence of magnetized material much beyond a prism edge, 2.5 km from the observation point, should be comparatively small and can therefore be neglected. Consequently, the only parameter yet to be determined is the magnetic source depth z_0 of the prism's center. It can be evaluated by minimizing the χ^2 function:

$$\chi^2 = \sum_{\mu=1}^{3} \sum_{\nu=1}^{3} (\mathcal{B}_{\mu\nu} - \mathcal{B}_{\mu\nu\,(obs)})^2 \qquad (42)$$

This function was minimized by varying the depth parameter at .1-km increments from the known bathymetry base on NAVOCEANO's 5-Minute Digital Bathymetric Data Base (DBDB5) downward, well beyond the poorly estimated Curie depths, computing the χ^2 function at each depth and noting where the minimum occurred. Having obtained the magnetic source depth, z_0, in this manner, eq. (39) was used to compute the equivalent magnetization of the prism. This procedure was performed independently for each individual grid point until the entire survey area was covered, yielding a 256 x 256 grid for magnetic source depth and the same size grid for each of the three components of the magnetization vector. The results from one grid point to the next were smoothly varying (i.e., not noisy) over the entire area. This is attributed to smoothing that takes place during the gridding process and also to the additional use of self-consistent magnetic parameters, all derived from the same rectangular harmonic potential. Since the inverted data are generated on the same grid as the input data, the results are easily profiled as functions of either latitude or longitude.

Because the dimensions of the prism were somewhat arbitrarily chosen, the resulting depths, though reasonable, were not taken as absolute. This is not a limitation of the method, since we could have optimized the prism dimensions along with the depth. Prism dimension constraints were applied to the Juan de Fuca survey due to the large size of the survey area and the resulting computational burden it entailed on an older mainframe computer. Also, some additional non-uniqueness concerns arise when all geometric parameters are allowed to float freely.

Finally, improved depth-to-source determinations are possible through more detailed modeling techniques using multiple prisms stacked vertically below a grid point and which are assumed to have varying magnetization, by iterating (i.e., by computing the residual magnetic field and gradient field components after the characteristics of one prism have been determined and solving for the depth and magnetization of a second, less-thick prism constrained to be at shallower depths below the same grid point) and by making other fairly simple refinements.

2.6 Inverse Magnetic Modeling with Multiple Prisms

Although reasonable results can be obtained, even for large ocean areas of complicated geomorphology such as the Juan de Fuca region, improved results ought to be expected through more detailed modeling with multiple prisms. In this case we consider a collection of magnetized prisms foliated within part, or all, of the oceanic crust beneath a surveyed area. Depending on the situation, one may fix the number of prisms a priori or view the number of prisms, N, as another parameter to be determined as part of the least-square or stochastic minimization procedure. One can further allow the prisms to vary in size and to overlap, in which case the resulting magnetizations in the overlapping regions would simply add vectorially. Alternatively, one could constrain the prisms not to overlap and perhaps even fill the entire

volume of the oceanic crust below the surveyed area with adjacent prisms, each of the same fixed dimensions. Regardless of the choices made, the multiprism inversion technique is basically the same, although computationally more demanding, than that for a single prism.

The generalization to the multiprism case is straightforward. It is now assumed that there is a total of K observations of the magnetic field and gradient field components which are presumed to be the composite of all fields generated by a total of N prisms. Then, at the k'th observation point $\mathbf{r}_k$, eqs. (34) and (36) generalize to the following:

$$B_{\mu k} = \sum_{n=1}^{N} \left(\Lambda_\mu{}^\lambda\right)_{kn} M_{\lambda n} \qquad k = 1,2,\ldots K \tag{43}$$

$$\mathcal{B}_{\mu\nu k} = \sum_{n=1}^{N} \left(\Lambda_\mu{}^\lambda{}_{/\nu}\right)_{kn} M_{\lambda n} \qquad k = 1,2,\ldots K \tag{44}$$

where the notation has been chosen to convey the following meanings: $B_{\mu k} \equiv B_\mu(\mathbf{r}_k)$, $\mathcal{B}_{\mu\nu k} \equiv \mathcal{B}_{\mu\nu}(\mathbf{r}_k)$, $(\Lambda_\mu{}^\lambda)_{kn} \equiv \Lambda_\mu{}^\lambda(\mathbf{r}_k, \mathbf{r}'_n)$, and $(\Lambda_\mu{}^\lambda{}_{/\nu})_{kn} \equiv \Lambda_\mu{}^\lambda{}_{/\nu}(\mathbf{r}_k, \mathbf{r}'_n)$. Additionally, $M_{\lambda n}$ is the λ–component of magnetization of the n'th prism, which is centered about the point $\mathbf{r}'_{0n}$.

Equations (43) and (44) can be written more succinctly in matrix form as follows:

$$\mathcal{B}_\mu = \Upsilon_\mu{}^\lambda \mathcal{M}_\lambda \tag{45}$$

$$\mathcal{B}_{\mu\nu} = \Psi_\mu{}^\lambda{}_\nu \mathcal{M}_\lambda \tag{46}$$

where, for a total of K observations and N prisms, the matrices in the above equations take the following forms:

$$\mathbb{B}_{\mu} = \begin{pmatrix} B_{\mu 1} \\ B_{\mu 2} \\ B_{\mu 3} \\ \bullet \\ \bullet \\ \bullet \\ B_{\mu K} \end{pmatrix} \tag{47}$$

$$\mathbb{B}_{\mu\nu} = \begin{pmatrix} \mathcal{B}_{\mu\nu 1} \\ \mathcal{B}_{\mu\nu 2} \\ \mathcal{B}_{\mu\nu 3} \\ \bullet \\ \bullet \\ \bullet \\ \mathcal{B}_{\mu\nu K} \end{pmatrix} \tag{48}$$

$$\Upsilon_{\mu}{}^{\nu} = \begin{pmatrix} (\Lambda_{\mu}{}^{\nu})_{11} & (\Lambda_{\mu}{}^{\nu})_{12} & (\Lambda_{\mu}{}^{\nu})_{13} & \bullet & \bullet & (\Lambda_{\mu}{}^{\nu})_{1N} \\ (\Lambda_{\mu}{}^{\nu})_{21} & \bullet & & & & \bullet \\ (\Lambda_{\mu}{}^{\nu})_{31} & & \bullet & & & \bullet \\ \bullet & & & & & \bullet \\ \bullet & & & \bullet & & \bullet \\ \bullet & & & & \bullet & \bullet \\ (\Lambda_{\mu}{}^{\nu})_{K1} & \bullet & \bullet & \bullet & \bullet & (\Lambda_{\mu}{}^{\nu})_{KN} \end{pmatrix} \tag{49}$$

$$\Psi_{\mu}{}^{\lambda}{}_{/\nu} = \begin{pmatrix} (\Lambda_{\mu}{}^{\lambda}{}_{/\nu})_{11} & (\Lambda_{\mu}{}^{\lambda}{}_{/\nu})_{12} & (\Lambda_{\mu}{}^{\lambda}{}_{/\nu})_{13} & \bullet & \bullet & (\Lambda_{\mu}{}^{\lambda}{}_{/\nu})_{1N} \\ (\Lambda_{\mu}{}^{\nu}{}_{/\nu})_{21} & \bullet & & & & \bullet \\ (\Lambda_{\mu}{}^{\lambda}{}_{/\nu})_{31} & & \bullet & & & \bullet \\ \bullet & & & \bullet & & \bullet \\ \bullet & & & & \bullet & \bullet \\ \bullet & & & & & \bullet \\ (\Lambda_{\mu}{}^{\lambda}{}_{/\nu})_{K1} & \bullet & \bullet & \bullet & \bullet & (\Lambda_{\mu}{}^{\lambda}{}_{/\nu})_{KN} \end{pmatrix} \tag{50}$$

$$\mathfrak{M}_\lambda = \begin{pmatrix} M_{\lambda 1} \\ M_{\lambda 2} \\ M_{\lambda 3} \\ \bullet \\ \bullet \\ \bullet \\ M_{\lambda N} \end{pmatrix} \tag{51}$$

A formal inversion of eq. (45) then gives the magnetization matrix $\mathfrak{M}_\lambda$ in terms of the matrix $\mathfrak{B}_\mu$ containing the magnetic field vector component observations:

$$\mathfrak{M}_\lambda = \Pi_{\lambda\nu} \bar{\Upsilon}^{\nu\mu} \mathfrak{B}_\mu \tag{52}$$

where $\bar{\Upsilon}^{\nu\mu}$ is the transpose of $\Upsilon^{\nu\mu}$ with respect to the Latin indices n and k, and where the matrix $\Pi_{\lambda\nu}$ is the inverse of the N x N matrix $\Pi_{\nu\lambda}$, which is defined as follows:

$$\Pi_{\nu\lambda} = \bar{\Upsilon}_\nu^{\ \mu} \Upsilon_{\mu\lambda} \tag{53}$$

Inserting eq. (52) into eq. (46) accomplishes the desired separation of the geophysical and geometric parameters and yields:

$$\mathfrak{B}_{\mu\nu} = \Psi_\mu^{\ \lambda}{}_\nu \Pi_{\lambda\alpha} \bar{\Upsilon}^{\alpha\beta} \mathfrak{B}_\beta \tag{54}$$

The right side of this equation, by virtue of the three Einstein summations involving the indices α, β, and λ, contains 27 terms, each term being the product of 4 matrices. Equation (54) is therefore a rather large system of nonlinear equations involving only the geometric parameters

associated with the N prisms and must be solved iteratively using stochastic or generalized inversion techniques. Thereby, a unique solution in the "optimized" least-squares sense can be obtained. The number of prisms, N, can also be included as one of the unknown parameters or the number of prisms may be set a priori. The solution for the geometric parameters, thus determined from eq. (54), then provides, in conjunction with eq. (52), a straightforward linear inversion problem for the determination of the vector components of the magnetization in each of the N prisms.

2.7 The Computational Algorithm MAGREP

Subroutine MAGREP (MAGnetic field due to a REctangular Prism) computes the magnetic scalar potential $\Phi(\mathbf{r})$ from eq. (30), the magnetic induction vector $\mathbf{B}(\mathbf{r})$ from eq. (34), and the nine elements of the magnetic gradient tensor $\mathcal{B}(\mathbf{r})$ from eq. (36) given the magnetization, position, and dimensions of prism. It is assumed that the user of this routine has written a driver program for the MAGREP subroutine that defines the prism parameters and passes them to MAGREP through a common block called /MAGBLK/. It is further assumed that the position of the prism is referenced to an origin located at the lower left-hand corner of a user-defined surface. The point of observation is also referenced to this origin. The rectangular components of the observation point are passed to MAGREP through the CALL statement, which also returns the computed magnetic field values. The field observed at a single observation point generated by multiple prisms is the sum of outputs of MAGREP for each prism. The prism can be rotated with respect to the rectangular coordinate axes associated with the coordinate origin through a set of three Euler angles that are also passed to MAGREP from the driving program through the common block. When the Euler angles are zero, the prism is unrotated, and its sides

are parallel to the coordinate axes. Documentation with a detailed description of these and other parameters is contained in the FORTRAN code of the subroutine which is listed in Appendix E. This subroutine is well suited for simulating magnetic fields generated by a variety of geophysical entities such as seamounts, as well as those of man-made origin, such as ships, planes, trains, etc.

3. THE GRAVITY FIELD

3.1 Theoretical Background

Modeling a gravitational field that is generated by some crustal feature or collection of features begins with a pair of equations that may be considered as the gravitational analogue of Maxwell's magnetostatic equations. The static gravitational field equations are:

$$\nabla \cdot \mathbf{g} = -4\pi G\rho \tag{55a}$$

$$\nabla \times \mathbf{g} = 0 \tag{55b}$$

where $\mathbf{g}$ is the gravitational acceleration vector (units: gal = cm/sec^2), G is the universal gravitational constant ($G = 6.6720 \times 10^{-8}$ $cm^3/gm\text{-}sec^2$), and ρ is the density contrast of the Earth's crust (units: gm/cm^3).

Equation (55b) indicates that the gravitational acceleration vector may be considered as the gradient of some scalar potential $U(\mathbf{r})$ (units: cm^2/sec^2), the units of which correspond to those of energy per unit mass. Consequently:

$$\mathbf{g} = -\nabla U \tag{56}$$

This equation, when combined with eq. (55a), yields the familiar Poisson equation for the gravitational field:

$$\nabla^2 U = 4\pi G\rho \tag{57}$$

which has the well-known solution:

$$U(\mathbf{r}) = -G \int_{V'} \frac{\rho(\mathbf{r}')}{|\mathbf{r}-\mathbf{r}'|} d^3\mathbf{r}' \tag{58}$$

Equation (58) is valid for any observation point $\mathbf{r}$ regardless of whether or not $\mathbf{r}$ is inside or outside the gravity field source volume V'. In the event that the observation point $\mathbf{r}$ is outside of this volume, then eq. (58) must also satisfy Laplace's equation:

$$\nabla^2 U = 0 \tag{59}$$

The solutions to this equation are also well-known, depending on the coordinate geometry as rectangular harmonic functions, spherical harmonic functions, etc.

The gradient of the gravity acceleration vector, $\mathbf{g}$, yields the gravity gradient tensor (units: sec^{-2}):

$$\mathscr{G}(\mathbf{r}) = \nabla \mathbf{g}(\mathbf{r}) \tag{60}$$

Both $\mathbf{g}(\mathbf{r})$ and $\mathscr{G}(\mathbf{r})$ are measurable quantities. The state of the art in gravity gradiometry is discussed by Jordan (1978, 1985) and Wells (1983).

As in the magnetic case, the gravity acceleration vector and the gravity gradient tensor may be decomposed into their respective Cartesian components such that:

$$\mathbf{g}(\mathbf{r}) = g_x(\mathbf{r})\,\mathbf{i} + g_y(\mathbf{r})\,\mathbf{j} + g_z(\mathbf{r})\,\mathbf{k} \tag{61}$$

and

$$\mathcal{G}(\mathbf{r}) = \begin{pmatrix} \frac{\partial g_x}{\partial x} & \frac{\partial g_y}{\partial x} & \frac{\partial g_z}{\partial x} \\ \frac{\partial g_x}{\partial y} & \frac{\partial g_y}{\partial y} & \frac{\partial g_z}{\partial y} \\ \frac{\partial g_x}{\partial z} & \frac{\partial g_y}{\partial z} & \frac{\partial g_z}{\partial z} \end{pmatrix} \tag{62}$$

In tensor notation, the components of the gravity acceleration vector are denoted as g_μ, while the components of the gravity gradient tensor are denoted as $\mathcal{G}_{\mu\nu}$, where, as in the magnetic case, the Greek subscripts μ, ν, λ, etc., range from 1 to 3 so that $g_1 = g_x$, $g_2 = g_y$, $g_3 = g_z$, and $\mathcal{G}_{12} = \partial g_x/\partial y$, etc. Using this notation, eqs. (55a) and (55b) are cast into the following forms:

$$g^{\mu}{}_{/\mu} = -4\pi G\rho \tag{63a}$$

$$g_{\mu/\nu} - g_{\nu/\mu} = 0 \tag{63b}$$

Also, eq. (56) becomes:

$$g_\mu = -U_{/\mu} \tag{64}$$

while eq. (57) takes the form:

$$U^{/\mu}{}_{/\mu} = 4\pi G\rho \tag{65}$$

Finally, eq. (60) in tensor notation becomes:

$$\mathcal{G}_{\mu\nu} = g_{\mu/\nu} \tag{66}$$

Now, by combining eq. (66) with eqs. (63a) and (63b) it is found that:

$$\mathcal{G}^{\mu}{}_{\mu} = -4\pi G\rho \tag{67a}$$

$$\mathcal{G}_{\mu\nu} = \mathcal{G}_{\nu\mu} \tag{67b}$$

That is, the gravity gradient tensor is symmetric, and its trace is proportional to the density ρ at the point of observation **r**. In particular, when r is outside the volume V', the trace is zero, so that:

$$\mathcal{G}^{\mu}{}_{\mu} = 0 \tag{68}$$

Finally, we know that $\mathcal{G}_{\mu\nu}$ is a tensor because it is the gradient of the gravity acceleration vector, and by definition, the gradient of any vector or tensor is also a tensor.

3.2 Related Gravity Vectors, Tensors, and Rotational Invariants

As in the magnetic case, the components of the gravitational acceleration vector g_μ and the components of the gravity gradient tensor $\mathcal{G}_{\mu\nu}$ may be combined in various ways to form a variety of other vectors, tensors, and rotational invariants, in direct analogy with the magnetic field. These quantities are additional tools that may be used to examine the field observations in ways that hitherto have been overlooked or which may become more useful as sophisticated gradiometric instruments become more widely available. They can yield supplementary information concerning the underlying structure and density contrast of a surveyed area that may be used to constrain the density morphology model of that area. From the vector g_μ and the tensor $\mathcal{G}_{\mu\nu}$ we can, for instance, construct the vector γ_μ and its corresponding scalar invariant γ (units: cm/sec^4):

$$\gamma_\mu \equiv \mathcal{G}_\mu{}^\lambda g_\lambda \tag{69a}$$

$$\gamma \equiv \sqrt{\gamma^\mu \gamma_\mu} \tag{69b}$$

Additionally, the following four tensors of rank two may also be constructed:

$$\gamma_{\mu\nu} \equiv \gamma_\mu \gamma_\nu \tag{70a}$$

$$\mathcal{P}_{\mu\nu} \equiv \gamma_\mu g_\nu \tag{70b}$$

$$\mathcal{T}_{\mu\nu} \equiv \mathcal{G}_\mu{}^\lambda \mathcal{G}_{\lambda\nu} \tag{70c}$$

$$g_{\mu\nu} \equiv g_\mu g_\nu \tag{70d}$$

Three of these tensors, $\gamma_{\mu\nu}$ (units: cm^2/sec^8), $\mathcal{T}_{\mu\nu}$ (units: sec^{-4}), and $g_{\mu\nu}$ (units: cm^2/sec^4) are symmetric, while the tensor $\mathcal{P}_{\mu\nu}$ (units: cm^2/sec^6) has both symmetric and antisymmetric parts. Rotational invariants constructed from the traces of these tensors are defined as follows:

$$\gamma \equiv \sqrt{\gamma^{\mu}{}_{\mu}} \tag{71a}$$

$$\mathcal{P} \equiv \mathcal{P}^{\mu}{}_{\mu} \tag{71b}$$

$$\mathcal{T} \equiv \sqrt{\mathcal{T}^{\mu}{}_{\mu}} \tag{71c}$$

$$g \equiv \sqrt{g^{\mu}{}_{\mu}} \tag{71d}$$

The last invariant, g (units: cm/sec^2), is simply the total gravitational acceleration (i.e., the magnitude of the gravitational acceleration vector), while $\mathcal{T}$ (units: sec^{-2}) is the total gravitational gradient. Equations (69b) and (71a) are different expressions for the same parameter, γ. The invariant $\mathcal{P}$ has the same units as the tensor $\mathcal{P}_{\mu\nu}$ itself.

In the far field, the gravitational acceleration, g, will vary as $1/R^2$, where R is the distance from the source of the gravitational field, while the gravitational gradient $\mathcal{T}$ will vary as $1/R^3$. Consequently, in the far field, γ will vary as $1/R^5$, and $\mathcal{P}$ will vary as $1/R^7$. Furthermore, several combinations of these invariant parameters form other invariant parameters that have a 1/R dependence in the far field and also have units of inverse length (i.e., units of cm^{-1}). These are:

$$P_1 \equiv \mathscr{T}/g \tag{72a}$$

$$P_2 \equiv \mathscr{P}/g^3 \tag{72b}$$

$$P_3 \equiv \mathscr{J}^2/\gamma \tag{72c}$$

Ratios of these parameters in turn will yield dimensionless parameters that are constants in the far field, but which may be quite sensitive to subtle variations in the source geometry or composition in the near field. These are:

$$p_1 \equiv P_1/P_2 \tag{73a}$$

$$p_2 \equiv P_2/P_3 \tag{73b}$$

$$p_3 \equiv P_3/P_1 \tag{73c}$$

These parameters simply provide a different way of looking at the gravitational field and ought to be viewed as additional tools in the repertoire of modern geopotential analysis, which may, under the appropriate circumstances, be exploited. Their value stems from the fact that their dependence on the radial distance from the source is quite different from that of the gravity field or its corresponding gradient tensor field.

3.3 The Uniformly Dense Rectangular Prism

The last section reviewed the essence of Newtonian gravitational field theory without specifying the nature of the gravitating body or bodies. Now, as in the magnetic case, we

represent sources of gravitational fields as being composed of a collection of rectangular prisms, each of which is assigned a uniform density, which may be different from one prism to another.

Considering just one such prism oriented with its sides parallel to the coordinate axes, we again characterize the prism as having its center at the point $\mathbf{r}_0 = (x_0 , y_0 , z_0)$ with respect to some coordinate origin and as having dimensions λ_x , λ_y , and λ_z along their respective coordinate axes. Then, given that the density, ρ, of the prism is constant, eq. (58) can be evaluated for the gravity potential $U(\mathbf{r})$, as is shown in Appendix C, yielding the result:

$$U(\mathbf{r}) = -\varepsilon^{\sigma} \Gamma_{\sigma\lambda} D^{\lambda} \tag{74}$$

where the elements of the Γ matrix are listed in Table 4, where ε_{σ} represents the components of the constant vector $\boldsymbol{\varepsilon}$, which was previously defined in eqs. (31) and (32), and where D_{λ} represents the components of the density vector $\mathbf{D}$ (units: sec^{-2}), which is defined by analogy to the magnetization vector $\mathbf{M}$ so that:

$$\mathbf{D} \equiv G\rho\boldsymbol{\varepsilon} \tag{75}$$

Then, in terms of its components D_{λ} , we have:

$$D_{\lambda} = G\rho\varepsilon_{\lambda} \tag{76}$$

This equation simply means that $D_1 = D_2 = D_3 = G\rho$. Introduction of the density vector allows us to put eq. (74) and related equations into a convenient and compact form that is comparable to eq. (30) for the magnetic case. The Γ matrix (units: cm^2) is symmetric, as can be directly

Table 4. Elements of the Γ Matrix

$$\Gamma_{11} = + (x - x')^2 \tan^{-1}\left[\frac{(y-y')(z-z')}{(x-x')R}\right] \Big|_{x',y',z'}$$

$$\Gamma_{12} = - (x - x')(y - y') \ln[R + (z - z')] \Big|_{x',y',z'}$$

$$\Gamma_{13} = - (x - x')(z - z') \ln[R + (y - y')] \Big|_{x',y',z'}$$

$$\Gamma_{21} = - (y - y')(x - x') \ln[R + (z - z')] \Big|_{x',y',z'}$$

$$\Gamma_{22} = + (y - y')^2 \tan^{-1}\left[\frac{(x-x')(z-z')}{(y-y')R}\right] \Big|_{x',y',z'}$$

$$\Gamma_{23} = - (y - y')(z - z') \ln[R + (x - x')] \Big|_{x',y',z'}$$

$$\Gamma_{31} = - (z - z')(x - x') \ln[R + (y - y')] \Big|_{x',y',z'}$$

$$\Gamma_{32} = - (z - z')(y - y') \ln[R + (x - x')] \Big|_{x',y',z'}$$

$$\Gamma_{33} = + (z-z')^2 \tan^{-1}\left[\frac{(x-x')(y-y')}{(z-z')R}\right] \Big|_{x',y',z'}$$

verified by an examination of Table 4. Therefore:

$$\Gamma_{\mu\nu} = \Gamma_{\nu\mu} \tag{77}$$

However, it has a nonzero trace regardless of whether or not the point of observation is inside or outside the gravitational source volume V' .

Taking the gradient of eq. (70) will yield the gravity acceleration vector **g** due to a prism of uniform density. It turns out to be somewhat easier to obtain the mathematical expression of the acceleration vector by taking the gradient of eq. (58) and subsequently evaluating the resulting integrals, as is shown in Appendix D. These integrals are the same as those previously encountered for the magnetic potential. Performing the necessary computations yields the following result for the gravity acceleration vector components:

$$g_\mu = \Omega_\mu{}^\lambda D_\lambda \tag{78}$$

where the elements of the $\boldsymbol{\Omega}$ matrix (units: cm) have been previously encountered and are listed in Table 1. This matrix has no special symmetry or trace properties. However, by combining eqs. (64), (74), and (78), its relationship to the Γ matrix can be established as:

$$\Omega_{\mu\lambda} = -\Gamma_{\sigma\lambda/\mu}\,\varepsilon^\sigma \tag{79}$$

Combining this result with eq. (35) we also note that:

$$\Lambda_{\mu\nu} = -\Gamma_{\sigma\lambda/\mu/\nu}\,\varepsilon^\sigma\varepsilon^\lambda \tag{80}$$

Since the density ρ is constant, so is the density vector $\mathbf{D}$. Consequently, inserting eq. (78) into eq. (66) yields the following form for the gravity gradient tensor:

$$\mathcal{G}_{\mu\nu} = \Omega_{\mu}{}^{\lambda}{}_{/\nu} D_{\lambda} \tag{81}$$

The derivatives of the Ω matrix, obtained by direct computation and subsequent simplification, are listed in Table 5. When eq. (81) is combined with eqs. (35) and (76), the following basic result is obtained:

$$\mathcal{G}_{\mu\nu} = G\rho \Lambda_{\mu\nu} \tag{82}$$

Since the gravity gradient $\mathcal{G}_{\mu\nu}$ is known to be a tensor by virtue of the fact that it is the gradient of a vector, and since the factor $G\rho$ is just a constant, eq. (82) implies that the Λ transformation matrix encountered in the magnetic case is also a tensor as is its gradient. Furthermore, combining eqs. (67a), (68), and (82) leads to eq. (37b).

A variety of additional relationships among the various components of the gradient of the Ω matrix can be obtained by examining the symmetry properties of the Λ tensor in the context of eq. (35) and also by direct examination of Table 5. Several of these relationships are listed in Table 6.

3.4 Gravity Inversion

Although there are some differences, the gravitational inversion procedure follows the same basic line of thought as was outlined for the magnetic case. We first note that multiplication of

Table 5. Derivatives of the Ω Matrix Elements

$$\Omega_{11/1} = \Lambda_{11} + \frac{(x-x')}{R}\left[\frac{(z-z')}{R+(y-y')} + \frac{(y-y')}{R+(z-z')}\right] \Big|_{x',y',z'}$$

$$\Omega_{11/2} = -\frac{1}{R}\left[\frac{(x-x')^2}{R+(z-z')}\right] \Big|_{x',y',z'}$$

$$\Omega_{11/3} = -\frac{1}{R}\left[\frac{(x-x')^2}{R+(y-y')}\right] \Big|_{x',y',z'}$$

$$\Omega_{12/1} = -\frac{1}{R}\left[\frac{(x-x')(y-y')}{R+(z-z')}\right] \Big|_{x',y',z'}$$

$$\Omega_{12/2} = \Lambda_{12} - \frac{1}{R}\left[\frac{(y-y')^2}{R+(z-z')}\right] \Big|_{x',y',z'}$$

$$\Omega_{12/3} = -\frac{(y-y')}{R} \Big|_{x',y',z'}$$

$$\Omega_{13/1} = -\frac{1}{R}\left[\frac{(x-x')(z-z')}{R+(y-y')}\right] \Big|_{x',y',z'}$$

$$\Omega_{13/2} = -\frac{(z-z')}{R} \Big|_{x',y',z'}$$

$$\Omega_{13/3} = \Lambda_{13} - \frac{1}{R}\left[\frac{(z-z')^2}{R+(y-y')}\right] \Big|_{x',y',z'}$$

$$\Omega_{21/1} = \Lambda_{21} - \frac{1}{R}\left[\frac{(x-x')^2}{R+(z-z')}\right] \Big|_{x',y',z'}$$

$$\Omega_{21/2} = -\frac{1}{R}\left[\frac{(x-x')(y-y')}{R+(z-z')}\right] \Big|_{x',y',z'}$$

$$\Omega_{21/3} = -\frac{(x-x')}{R} \Big|_{x',y',z'}$$

$$\Omega_{22/1} = -\frac{1}{R}\left[\frac{(y-y')^2}{R+(z-z')}\right] \Big|_{x',y',z'}$$

$$\Omega_{22/2} = \Lambda_{22} + \frac{(y-y')}{R}\left[\frac{(z-z')}{R+(x-x')} + \frac{(x-x')}{R+(z-z')}\right] \Big|_{x',y',z'}$$

Table 5. Derivatives of the Ω Matrix Elements (con.)

$$\Omega_{22/3} = -\frac{1}{R}\left[\frac{(y-y')^2}{R+(x-x')}\right]\Big|_{x',y',z'}$$

$$\Omega_{23/1} = -\frac{(z-z')}{R}\Big|_{x',y',z'}$$

$$\Omega_{23/2} = -\frac{1}{R}\left[\frac{(y-y')(z-z')}{R+(x-x')}\right]\Big|_{x',y',z'}$$

$$\Omega_{23/3} = \Lambda_{23} - \frac{1}{R}\left[\frac{(z-z')^2}{R+(x-x')}\right]\Big|_{x',y',z'}$$

$$\Omega_{31/1} = \Lambda_{31} - \frac{1}{R}\left[\frac{(x-x')^2}{R+(y-y')}\right]\Big|_{x',y',z'}$$

$$\Omega_{31/2} = -\frac{(x-x')}{R}\Big|_{x',y',z'}$$

$$\Omega_{31/3} = -\frac{1}{R}\left[\frac{(x-x')(z-z')}{R+(y-y')}\right]\Big|_{x',y',z'}$$

$$\Omega_{32/1} = -\frac{(y-y')}{R}\Big|_{x',y',z'}$$

$$\Omega_{32/2} = \Lambda_{32} - \frac{1}{R}\left[\frac{(y-y')^2}{R+(x-x')}\right]\Big|_{x',y',z'}$$

$$\Omega_{32/3} = -\frac{1}{R}\left[\frac{(y-y')(z-z')}{R+(x-x')}\right]\Big|_{x',y',z'}$$

$$\Omega_{33/1} = -\frac{1}{R}\left[\frac{(z-z')^2}{R+(y-y')}\right]\Big|_{x',y',z'}$$

$$\Omega_{33/2} = -\frac{1}{R}\left[\frac{(z-z')^2}{R+(x-x')}\right]\Big|_{x',y',z'}$$

$$\Omega_{33/3} = \Lambda_{33} + \frac{(z-z')}{R}\left[\frac{(y-y')}{R+(x-x')} + \frac{(x-x')}{R+(y-y')}\right]\Big|_{x',y',z'}$$

Table 6. Summary of Matrix Identities and Symmetries

$$\Gamma_{\mu\nu} = \Gamma_{\nu\mu}$$

$$\Gamma_{\mu\nu}{}^{/\lambda}{}_{/\lambda}\,\varepsilon^{\mu}\varepsilon^{\nu} = 0$$

$$\Gamma_{\mu\nu/\lambda/\sigma}\varepsilon^{\mu}\varepsilon^{\nu} = \Gamma_{\mu\nu/\sigma/\lambda}\varepsilon^{\mu}\varepsilon^{\nu}$$

$$\Omega_{\mu\nu} = -\Gamma_{\sigma\nu/\mu}\varepsilon^{\sigma}$$

$$\Omega_{\mu\sigma/\nu}\varepsilon^{\sigma} = \Omega_{\nu\sigma/\mu}\varepsilon^{\sigma}$$

$$\Omega^{\mu}{}_{\sigma/\lambda/\mu}\varepsilon^{\sigma} = 0$$

$$\Omega^{\mu}{}_{\sigma/\mu}\varepsilon^{\sigma} = \begin{cases} -4\pi & r \le \partial V' \\ 0 & r > \partial V' \end{cases}$$

$$\Lambda_{\mu\nu} = -\Gamma_{\lambda\sigma/\mu/\nu}\varepsilon^{\lambda}\varepsilon^{\sigma}$$

$$\Lambda_{\mu\nu} = \Omega_{\mu\sigma/\nu}\varepsilon^{\sigma}$$

$$\Lambda_{\mu\nu} = \Lambda_{\nu\mu}$$

$$\Lambda^{\mu}{}_{\mu} = \begin{cases} -4\pi & r \le \partial V' \\ 0 & r > \partial V' \end{cases}$$

$$\Lambda^{\mu}{}_{\lambda/\mu} = 0$$

$$\Lambda_{\mu\nu/\lambda} = \Lambda_{\lambda\mu/\nu} = \Lambda_{\nu\lambda/\mu}$$

eq. (82) by $\bar{\Lambda}^{\lambda\mu}$, the elements of the inverse of Λ, and subsequent contraction (i.e., setting two indices equal to each other causing a summation) of the indices immediately yields the inverse relationship:

$$G\rho = \frac{1}{3}\bar{\Lambda}^{\mu\nu}\mathcal{G}_{\mu\nu} \tag{83}$$

This equation permits the determination of the density ρ of a single prism given the geometry (i.e., the location and dimensions) of that prism through the inverse matrix $\bar{\Lambda}$ and given measurements of the gravity gradient field that surrounds the prism. However, we really want to be able to determine not only the density, but also the geometry (size and location) of the prism. This more general problem is intrinsically non-unique if all that we have to work with is eq. (83). Fortunately, there is more that can be said.

Begin by denoting the inverse of the 3 x 3 matrix Ω as $\bar{\Omega}$. The elements of these two matrices satisfy the relation:

$$\bar{\Omega}_{\mu}{}^{\lambda}\Omega_{\lambda\nu} = \delta_{\mu\nu} \tag{84}$$

where $\delta_{\mu\nu}$ is the Kronecker delta. The elements of this inverse matrix are defined by the relation:

$$\bar{\Omega}_{\mu\nu} = \frac{\text{cofactor}(\Omega_{\nu\mu})}{\det(\Omega)} \tag{85}$$

Then, quite formally the inverse of eq. (78) is:

$$D_{\lambda} = \bar{\Omega}_{\lambda}{}^{\mu}g_{\mu} \tag{86}$$

Combining this result with eq. (81) then gives the basic result:

$$g_{\mu\nu} = \Omega_{\mu}{}^{\lambda}{}_{/\nu}\Pi_{\lambda}{}^{\sigma}g_{\sigma} \tag{87}$$

Consequently, a decoupling of the geometric parameters (i.e., x_0 , y_0 , z_0 , λ_x , λ_y , and λ_z) from the geophysical parameter (i.e., the density ρ) has been accomplished. The intention, then, is to solve the nonlinear problem indicated by eq. (87) for the geometric parameters and subsequently solve the linear problem indicated by eq. (83) for the geophysical parameter. Due to the symmetry and trace properties of the gravity gradient tensor which leave five independent components, there are more unknown geometric parameters, a total of six, than there are equations to solve for them. Consequently, either one uses gravity measurements obtained at several locations, or one may make some restrictive assumptions about either the dimensions or location of the prism. In either case, the solution can be obtained by stochastic or generalized inversion techniques that attempt to minimize a chi-square (χ^2) function constructed from the differences between the gravitational gradients computed from eq. (87) and the measured (observed) gravity gradients. Note, however, that it is not necessary to measure the gravity gradients directly since they may be computed from a rectangular harmonic potential function derived from measurements of the Z-component of the gravity acceleration. Also, advantage can be taken of the fact that the X-component and Y-component of the gravity acceleration vector can be computed in terms of the Z-component. The general procedure is the same as that outlined for the magnetic survey of the Juan de Fuca region.

It is useful to examine eq. (78) in more detail. It represents the following three equations:

$$g_1 = G\rho(\Omega_{11} + \Omega_{12} + \Omega_{13}) \tag{88a}$$

$$g_2 = G\rho(\Omega_{21} + \Omega_{22} + \Omega_{23}) \tag{88b}$$

$$g_3 = G\rho(\Omega_{31} + \Omega_{32} + \Omega_{33}) \tag{88c}$$

Taking the ratio of eq. (88a) with eq. (88c) and taking the ratio of eq. (88b) with eq. (88c) then yields:

$$g_1 = \frac{(\Omega_{11} + \Omega_{12} + \Omega_{13})}{(\Omega_{31} + \Omega_{32} + \Omega_{33})} g_3 \tag{89a}$$

$$g_2 = \frac{(\Omega_{21} + \Omega_{22} + \Omega_{23})}{(\Omega_{31} + \Omega_{32} + \Omega_{33})} g_3 \tag{89b}$$

These equations show explicitly the dependence of the g_1 and g_2 components of the gravitational acceleration vector on the third component, g_3 , which is the component that is most frequently measured. From eq. (88c) we also find that:

$$G\rho = \frac{g_3}{(\Omega_{31} + \Omega_{32} + \Omega_{33})} = D_1 = D_2 = D_3 \tag{90}$$

This equation can be used to determine the density of the prism once eq. (87) has been used to determine the geometric parameters and hence Ω .

3.5 Inverse Gravity Modeling with Multiple Prisms

Generalizing to multiple prisms, we now consider the Earth's crust beneath a gravitationally surveyed area to be foliated with a total of N prisms, each of which has its own uniform

density, ρ_n . The gravitational acceleration vector and the gravitational gradient tensor at the k'th observation point, $\mathbf{r}_k$, are then composite sums of the gravity fields generated by the individual prisms. Therefore:

$$g_{\mu k} = \sum_{n=1}^{N} \left(\Omega_\mu{}^\lambda\right)_{kn} D_{\lambda n} \tag{91a}$$

$$\mathcal{G}_{\mu\nu k} = \sum_{n=1}^{N} \left(\Omega_\mu{}^\lambda{}_{/\nu}\right)_{kn} D_{\lambda n} \tag{91b}$$

where, as in the magnetic case, the subscript, k, identifies a particular point of observation, $\mathbf{r}_k$ such that $g_{\mu k} \equiv g_\mu(\mathbf{r}_k)$, $\mathcal{G}_{\mu\nu k} \equiv \mathcal{G}_{\mu\nu}(\mathbf{r}_k)$, $\left(\Omega_\mu{}^\lambda\right)_{kn} \equiv \Omega_\mu{}^\lambda(\mathbf{r}_k, \mathbf{r}'_n)$, and $\left(\Omega_\mu{}^\lambda{}_{/\nu}\right)_{kn} \equiv \Omega_\mu{}^\lambda{}_{/\nu}(\mathbf{r}_k, \mathbf{r}'_n)$. $D_{\lambda n}$ is the λ component of the density vector in the n'th prism, which is centered about the point $\mathbf{r}'_{0n}$.

In more succinct fashion, eqs. (91a) and (91b) may be written in terms of matrices as:

$$\mathbf{G}_\mu = \Theta_\mu{}^\lambda \mathbf{D}_\lambda \tag{92}$$

$$\mathbf{G}_{\mu\nu} = \Xi_\mu{}^\lambda{}_\nu \mathbf{D}_\lambda \tag{93}$$

where, assuming there exists a total of K observations for each component of the gravity field and the gravity gradient field, the matrices in the above equations take the following explicit forms:

$$\mathcal{G}_{\mu} = \begin{pmatrix} g_{\mu 1} \\ g_{\mu 2} \\ g_{\mu 3} \\ \bullet \\ \bullet \\ \bullet \\ g_{\mu K} \end{pmatrix} \tag{94}$$

$$\mathcal{G}_{\mu\nu} = \begin{pmatrix} \mathcal{G}_{\mu\nu 1} \\ \mathcal{G}_{\mu\nu 2} \\ \mathcal{G}_{\mu\nu 3} \\ \bullet \\ \bullet \\ \bullet \\ \mathcal{G}_{\mu\nu K} \end{pmatrix} \tag{95}$$

$$\Theta_{\mu\nu} = \begin{pmatrix} \left(\Omega_{\mu}{}^{\lambda}\right)_{11} & \left(\Omega_{\mu}{}^{\lambda}\right)_{12} & \bullet & \bullet & \bullet & \left(\Omega_{\mu}{}^{\lambda}\right)_{1N} \\ \left(\Omega_{\mu}{}^{\lambda}\right)_{21} & \bullet & & & & \bullet \\ \left(\Omega_{\mu}{}^{\lambda}\right)_{31} & & \bullet & & & \bullet \\ \bullet & & & \bullet & & \bullet \\ \bullet & & & & \bullet & \bullet \\ \bullet & & & & & \bullet \\ \left(\Omega_{\mu}{}^{\lambda}\right)_{K1} & \bullet & \bullet & \bullet & \bullet & \left(\Omega_{\mu}{}^{\lambda}\right)_{KN} \end{pmatrix} \tag{96}$$

$$\Xi_{\mu}{}^{\lambda}{}_{\nu} = \begin{pmatrix} \left(\Omega_{\mu}{}^{\lambda}{}_{/\nu}\right)_{11} & \left(\Omega_{\mu}{}^{\lambda}{}_{/\nu}\right)_{12} & \bullet & \bullet & \bullet & \left(\Omega_{\mu}{}^{\lambda}{}_{/\nu}\right)_{1N} \\ \left(\Omega_{\mu}{}^{\lambda}{}_{/\nu}\right)_{21} & \bullet & & & & \bullet \\ \left(\Omega_{\mu}{}^{\lambda}{}_{/\nu}\right)_{31} & & \bullet & & & \bullet \\ \bullet & & & \bullet & & \bullet \\ \bullet & & & & \bullet & \bullet \\ \bullet & & & & & \bullet \\ \left(\Omega_{\mu}{}^{\lambda}{}_{/\nu}\right)_{K1} & \bullet & \bullet & \bullet & \bullet & \left(\Omega_{\mu}{}^{\lambda}{}_{/\nu}\right)_{KN} \end{pmatrix} \tag{97}$$

$$\mathfrak{D}_\lambda = \begin{pmatrix} D_{\lambda 1} \\ D_{\lambda 2} \\ D_{\lambda 3} \\ \bullet \\ \bullet \\ \bullet \\ D_{\lambda N} \end{pmatrix} \tag{98}$$

A formal inversion of eq. (92) yields the density matrix $\mathfrak{D}_\lambda$ in terms of the gravity acceleration matrix $\mathfrak{G}_\mu$:

$$\mathfrak{D}_\lambda = \bar{\Delta}_{\nu\lambda} \bar{\Theta}^{\mu\nu} \mathfrak{G}_\mu \tag{99}$$

where $\bar{\Theta}^{\mu\nu}$ is the transpose of the matrix $\Theta^{\mu\nu}$ with respect to the Latin indices n and k, and where the matrix $\bar{\Delta}_{\nu\lambda}$ is the inverse of the N x N matrix $\Delta_{\nu\lambda}$, which is defined as follows:

$$\Delta_{\nu\lambda} = \bar{\Theta}^{\mu}{}_{\nu} \Theta_{\mu\lambda} \tag{100}$$

Inserting eq. (99) into eq. (93) yields the desired separation of the geometric and geophysical parameters:

$$\mathfrak{G}_{\mu\nu} = \Xi_\mu{}^\lambda{}_\nu \bar{\Delta}_{\beta\lambda} \bar{\Theta}^{\alpha\beta} \mathfrak{G}_\alpha \tag{101}$$

The right-hand side of this equation consists of 27 terms which result from the three Einstein summations over the dummy indices α, β, and λ. Choosing as an example, just one of these terms which corresponds to the index specification: $\mu = 1$, $\nu = 2$, $\lambda = 3$, $\alpha = 1$, and $\beta = 2$, we obtain the typical term: $\Xi_1{}^3{}_2 \bar{\Delta}_{23} \bar{\Theta}^{12} \mathfrak{G}_\alpha$, where $\Xi_1{}^3$ is a K x N matrix, $\bar{\Delta}_{23}$ is an N x N matrix, $\bar{\Theta}^{12}$ is an N x K matrix, and $\mathfrak{G}_1$ is a K x 1 matrix.

Equation (101) is a complicated *nonlinear system of equations* involving 6N+1 unknown geometric parameters; the number of prisms N, being the one extra unknown. Had we not already pre-specified the orientation of the prisms as being aligned parallel to the coordinate axes, there would be an additional three unknown Euler angles per prism to be evaluated, yielding 9N+1 unknowns. Problems such as these can be solved by stochastic inversion or generalized inversion techniques. Such solutions, having been optimized, are therefore unique in the least-squares sense as being the "best estimate" of the unknown parameters. Once determined, the geophysical parameters follow directly from eq. (99).

3.6 The Computational Algorithm GRVREP

Subroutine GRVREP (GRaVity field due to a REctangular Prism) computes the gravity potential $U(\mathbf{r})$ from eq. (74), the gravity acceleration vector $\mathbf{g}(\mathbf{r})$ from eq. (78), and the nine elements of the gravity gradient tensor $\mathcal{G}(\mathbf{r})$ from eq. (81) or equivalently, eq. (82). It is assumed that the user of this routine has written a driver program for the GRVREP subroutine that defines the prism parameters and passes them to GRVREP through a common block called /GRVBLK/. It is further assumed that the location and orientation of the prism are related to the origin in the same manner as for Subroutine MAGREP, as discussed in Section 2.7. The FORTRAN code for this subroutine is internally documented and is listed in Appendix F.

4. THE ELECTRIC FIELD

Considering again only static sources, the electric field can be analyzed using the results already obtained for the magnetic and gravity fields. There are two separate situations that can be considered. The first assumes that the source of the field consists of a charge density $\sigma(\mathbf{r}')$

that is contained in some volume V'. The second assumes that the source of the field is a material within the volume V' containing an electric polarization $\mathbf{P}(\mathbf{r}')$. In either situation, it is assumed that there are no electric currents and that the volume V' can be broken into one or more subvolumes in each of which the charge density and the polarization may be considered uniformly distributed.

4.1 Fields Generated by an Electrically Charged Medium

The mathematical analysis of a static electrically charged medium has a one-to-one correspondence to that of the gravitational case previously described since, under the electrostatic assumptions, Maxwell's equations reduce to the following:

$$\nabla \bullet \mathbf{E} = 4\pi\sigma \tag{102a}$$

$$\nabla \times \mathbf{E} = 0 \tag{102b}$$

These equations are identical in form to eqs. (55a) and (55b). Therefore, the results regarding gravity fields in section (3) may be taken over completely if we replace **g** by **E** and $-G\rho$ by σ. We also chose to make appropriate notational replacements such that $U \rightarrow \mathscr{V}$, $\mathcal{G}_{\mu\nu} \rightarrow \mathscr{E}_{\mu\nu}$ and $D_\lambda \rightarrow Q_\lambda$ correspond to the electrostatic potential (units: statvolts), the electric field gradient tensor (units: statvolts/cm^2), and the electric charge density vector (units: statCoulombs/cm^3), respectively. Using this notation, the results for a single rectangular prism containing a uniform charge density are summarized along with magnetic and gravity results in Table 7.

Table 7. Summary of Field Equations for the Single Prism Geometry

GRAVITY	ELECTRIC	ELECTRIC	MAGNETIC
Source: uniform mass density	**Source: uniform charge density**	**Source: uniform polarization**	**Source: uniform magnetization**
$U = -\Gamma_{\sigma\lambda}\varepsilon^{\sigma} D^{\lambda}$	$\mathcal{V} = -\Gamma_{\sigma\lambda}\varepsilon^{\sigma} Q^{\lambda}$	$\mathcal{V}_p = -\Omega^{\lambda}{}_{\sigma}\varepsilon^{\sigma} P_{\lambda}$	$\Phi = -\Omega^{\lambda}{}_{\sigma}\varepsilon^{\sigma} M_{\lambda}$
$U = -\Gamma_{\sigma\lambda}\overline{\Omega}^{\lambda\mu}\varepsilon^{\sigma} g_{\mu}$	$\mathcal{V} = -\Gamma_{\sigma\lambda}\overline{\Omega}^{\lambda\mu}\varepsilon^{\sigma} E_{\mu}$	$\mathcal{V}_p = -\Omega^{\lambda}{}_{\sigma}\overline{\Lambda}_{\lambda}{}^{\mu}\varepsilon^{\sigma} E_{p\mu}$	$\Phi = -\Omega^{\lambda}{}_{\sigma}\overline{\Lambda}_{\lambda}{}^{\mu}\varepsilon^{\sigma} B_{\mu}$
$g_{\mu} = \Omega_{\mu}{}^{\lambda} D_{\lambda}$	$E_{\mu} = \Omega_{\mu}{}^{\lambda} Q_{\lambda}$	$E_{p\mu} = \Lambda_{\mu}{}^{\lambda} P_{\lambda}$	$B_{\mu} = \Lambda_{\mu}{}^{\lambda} M_{\lambda}$
$\mathcal{G}_{\mu\nu} = \Omega_{\mu}{}^{\lambda}{}_{/\nu} D_{\lambda}$	$\mathcal{E}_{\mu\nu} = \Omega_{\mu}{}^{\lambda}{}_{/\nu} Q_{\lambda}$	$\mathcal{E}_{p\mu\nu} = \Lambda_{\mu}{}^{\lambda}{}_{/\nu} P_{\lambda}$	$\mathcal{B}_{\mu\nu} = \Lambda_{\mu}{}^{\lambda}{}_{/\nu} M_{\lambda}$
$\mathcal{G}_{\mu\nu} = \Omega_{\mu}{}^{\lambda}{}_{/\nu}\overline{\Omega}_{\lambda}{}^{\sigma} g_{\sigma}$	$\mathcal{E}_{\mu\nu} = \Omega_{\mu}{}^{\lambda}{}_{/\nu}\overline{\Omega}_{\lambda}{}^{\sigma} E_{\sigma}$	$\mathcal{E}_{p\mu\nu} = \Lambda_{\mu}{}^{\lambda}{}_{/\nu}\overline{\Lambda}_{\lambda}{}^{\sigma} E_{p\sigma}$	$\mathcal{B}_{\mu\nu} = \Lambda_{\mu}{}^{\lambda}{}_{/\nu}\overline{\Lambda}_{\lambda}{}^{\sigma} B_{\sigma}$
$\mathcal{G}_{\mu\nu} = G\rho\Lambda_{\mu\nu}$	$\mathcal{E}_{\mu\nu} = -\sigma\Lambda_{\mu\nu}$		
$\mathcal{G}_{\mu\nu} = \mathcal{G}_{\nu\mu}$	$\mathcal{E}_{\mu\nu} = \mathcal{E}_{\nu\mu}$	$\mathcal{E}_{p\mu\nu} = \mathcal{E}_{p\nu\mu}$	$\mathcal{B}_{\mu\nu} = \mathcal{B}_{\nu\mu}$
$\mathcal{G}^{\mu}{}_{\mu} = \begin{cases} -4\pi G\rho & r \le \partial V' \\ 0 & r > \partial V' \end{cases}$	$\mathcal{E}^{\mu}{}_{\mu} = \begin{cases} 4\pi\sigma & r \le \partial V' \\ 0 & r > \partial V' \end{cases}$	$\mathcal{E}_{p}{}^{\mu}{}_{\mu} = 0 \quad r > \partial V'$	$\mathcal{B}^{\mu}{}_{\mu} = 0 \quad r > \partial V'$
$D_{\lambda} = \overline{\Omega}_{\lambda}{}^{\mu} g_{\mu}$	$Q_{\lambda} = \overline{\Omega}_{\lambda}{}^{\mu} E_{\mu}$	$P_{\lambda} = \overline{\Lambda}_{\lambda}{}^{\mu} E_{p\mu}$	$M_{\lambda} = \overline{\Lambda}_{\lambda}{}^{\mu} B_{\mu}$
$D_{\lambda} = G\rho\varepsilon_{\lambda}$	$Q_{\lambda} = -\sigma\varepsilon_{\lambda}$		
$G\rho = \frac{1}{3}\overline{\Lambda}^{\mu\nu}\mathcal{G}_{\mu\nu}$	$\sigma = -\frac{1}{3}\overline{\Lambda}^{\mu\nu}\mathcal{E}_{\mu\nu}$	$P = \sqrt{P^{\lambda} P_{\lambda}}$	$M = \sqrt{M^{\lambda} M_{\lambda}}$

4.2 Fields Generated by an Electrically Polarized Medium

Maxwell's equations for this case take the following electrostatic form:

$$\nabla \bullet \mathbf{D} = 0 \tag{103a}$$

$$\nabla \times \mathbf{E}_p = 0 \tag{103b}$$

These equations are identical in form to eqs. (4a) and (4b) of the magnetic case. Consequently, the results of that case may be taken over completely if we make the appropriate notational replacements $\mathbf{M} \rightarrow \mathbf{P}$, $\Phi \rightarrow \mathscr{V}_p$, and $\mathscr{B}_{\mu\nu} \rightarrow \mathscr{E}_{p\mu\nu}$. Here, $\mathscr{V}_p$ is the electric potential (units: statvolts), and $\mathscr{E}_{p\mu\nu}$ is the electric field gradient tensor (units: statvolts/cm^2) due to the polarization $\mathbf{P}$. The subscript (p) has been introduced to distinguish the present electrically polarized medium case from the electrically charged medium case of the previous section. Using this notation, the results for a single uniformly polarized prism are also summarized in Table 7. These seem to be the least used of the geopotential relations derived in this report. However, it should be noted that other non-geophysics applications for them do exist.

5. CONNECTIONS AMONG THE ELECTRIC, MAGNETIC, AND GRAVITY FIELDS

Over a century and a half ago, Poisson (1826) noticed that close a relationship exists between the magnetic potential and the gravity potential when the sources of those potentials are uniformly distributed over the same volume. Similar relationships exist between the electric field and the gravity field potentials, as well as between the electric and magnetic potentials. These relationships can be extended to include the vector and gradient components of these fields as well.

Taking just the relationship between the magnetic and gravity fields as an example, we find that if eq. (31) is multiplied by the factor Gρ and subsequent note of eq. (82) is taken, one of the many possible forms of Poisson's relation is obtained:

$$G\rho B_{\mu} = \mathcal{G}_{\mu}{}^{\lambda} M_{\lambda} \tag{104}$$

which, after multiplication by B_{μ}, gives:

$$G\rho = \left(\frac{B^{\mu}}{B^{\sigma} B_{\sigma}} \mathcal{G}_{\mu}{}^{\lambda} \right) M_{\lambda} \tag{105}$$

or, after inverting eq. (104), we have:

$$M_{\lambda} = (\overline{\mathcal{G}}_{\lambda}{}^{\mu} B_{\mu})\, G\rho \tag{106}$$

Also, after inserting eqs. (18), (64), and (66) into eq. (104) and subsequently integrating with respect to dx^{μ}, Poisson's relation can be expressed in standard form with respect to the gravity and magnetic potentials, as:

$$\Phi = \left(\frac{1}{G\rho} \right) U_{/\lambda} M^{\lambda} \tag{107}$$

where the arbitrary constant of integration has been set to zero. Furthermore, by taking the gradient of eq. (104) another form of Poisson's relation is found to be:

$$G\rho B_{\mu/\nu} = \mathcal{G}_{\mu}{}^{\lambda}{}_{/\nu} M_{\lambda} \tag{108}$$

All of the above forms of Poisson's relation for the gravity and magnetic fields are expressed in terms of the geophysical sources parameters (i.e., magnetization and density) of those fields. However, if eqs. (106) and (108) are combined, then the source parameters may be eliminated. The result is a most interesting relationship between the fields themselves:

$$\mathcal{B}_{\mu\nu} = \mathcal{G}_{\mu}{}^{\lambda}{}_{/\nu}\overline{\mathcal{G}}_{\lambda}{}^{\sigma}\, B_{\sigma} \tag{109}$$

Thus, given a priori knowledge of the gravitational field, this equation may be considered as a coupled system of linear first-order differential equations for the three components of the magnetic field. This can be seen more clearly if eq. (19) is inserted on the left-hand side of eq. (109), thereby yielding:

$$B_{\mu/\nu} = \mathcal{G}_{\mu}{}^{\lambda}{}_{/\nu}\overline{\mathcal{G}}_{\lambda}{}^{\sigma}\, B_{\sigma} \tag{110}$$

This equation embodies the essence of a classical unification of fields since it permits one of the two otherwise unrelated fields (i.e., gravity and magnetism) to be derived from the other without reference to any additional fields or source parameters. This relationship goes well beyond the standard Poisson relations for these fields. From this point of view, it seems reasonable to suggest that eq. (110) and other equations similarly derived for the electric field might be considered as classical, static, weak-field-limit approximations of a true classical unified field theory (i.e., an extension of General Relativity) and that eq. (110) ought to be considered as supporting evidence for the existence of such a theory.

In defense of this notion, we mention as an aside that there is a connection between the Λ

matrix and certain components of the Riemann curvature tensor, $\mathcal{R}^{ij}{}_{kl}$, of General Relativity. The Riemann curvature tensor is a tensor of rank four, which characterizes the geometry of a 4-dimensional Riemann space. Here, Latin indices range from 0 to 3, while Greek indices still range from 1 to 3. In a 4-dimensional Riemann space, the zero'th coordinate is related to time, which, when multiplied by the speed of light, c, has units of length. Then, in addition to the three space coordinates $x^1 = x$, $x^2 = y$, and $x^3 = z$, we also have $x^0 = c\,t$. Details regarding the definition of the Riemann curvature tensor and its relationship with the gravitational field equations of General Relativity and its Newtonian approximation are discussed by Adler, Bazin, and Schiffer (1975). Here we simply note that linearization of the gravitational field equations of General Relativity in the static, weak-field approximation yields the following result:

$$\mathcal{R}^{\alpha 0}{}_{\beta 0} \equiv -\frac{2}{c^2} U^{/\alpha}{}_{/\beta} = \frac{2}{c^2} \mathcal{G}^{\alpha}{}_{\beta} = \frac{2G\rho}{c^2} \Lambda^{\alpha}{}_{\beta} \tag{111}$$

which establishes the connection between the Riemann curvature tensor and the Λ matrix. Furthermore, if we denote the inverse of the 3 x 3 matrix $\mathcal{R}^{\alpha 0}{}_{\beta 0}$ as $\overline{\mathcal{R}}^{\alpha 0}{}_{\beta 0}$ so that:

$$\overline{\mathcal{R}}^{\gamma 0}{}_{\alpha 0}\, \mathcal{R}^{\alpha 0}{}_{\beta 0} = \delta^{\gamma}{}_{\beta} \tag{112}$$

we find that eq. (110) can be put into the form:

$$B_{\mu\,/\,\nu} \equiv \mathcal{R}_{\mu}{}^{o\lambda}{}_{o\,/\,\nu}\, \overline{\mathcal{R}}_{\lambda}{}^{0\sigma}{}_{0}\, B_{\sigma} \tag{113}$$

A similar result can be obtained for the static electric field. Using results such as these, it may

be possible to extend these field relationships to covariant 4-dimensional form and thereby obtain a system of classical unified field equations, which in the limit of weak electromagnetic fields reduce to the tensor form of Maxwell's equations and the equations of General Relativity. That such a classical unified field theory should exist, regardless of what further unifications may exist at the quantum level, is discussed by Tonnelat (1966a, 1966b).

Several other Poisson relationships exist between the electric and magnetic fields and between the electric and gravitational fields. They can be derived almost by inspection in a manner that is essentially the same as that described above between the magnetic and gravitational fields. For one more example, take the case of the electric field $\mathbf{E}_p(\mathbf{r})$ due to the polarization $\mathbf{P}(\mathbf{r})$ and their relationship to the magnetic induction $\mathbf{B}(\mathbf{r})$ due to the magnetization $\mathbf{M}(\mathbf{r})$. Using the correspondences established in Section 4.2, we can say that:

$$E_{p\mu} = \Lambda_\mu{}^\lambda P_\lambda \tag{114}$$

This has the following inverse relationship:

$$P_\lambda = \bar{\Lambda}_\lambda{}^\mu E_{p\mu} \tag{115}$$

Taking the vector dot product between the polarization vector and the magnetic induction vector using eqs. (115) and (34) and subsequently taking note of the symmetry of the Λ matrix and using eq. (40), we obtain the following Poisson relation:

$$B_\mu P^\mu = M_\lambda E_p^\lambda \tag{116}$$

Taking the gradient of this equation and noting the definition of the magnetic gradient tensor given by eq. (19) and that the electric field gradient due to polarization $\mathscr{E}_p(\mathbf{r})$ is similarly defined in terms of the electric field due to polarization $\mathbf{E}_p(\mathbf{r})$, we find, due to the uniformity of the magnetization vector and the polarization vector, another Poisson relation:

$$\mathscr{B}_{\mu\nu} P^{\nu} = \mathscr{E}_{p\mu\lambda} M^{\lambda} \tag{117}$$

By multiplying through eq. (117) by the inverse of the magnetic gradient tensor, we find that:

$$P_{\nu} = \bar{\mathscr{B}}_{\nu}{}^{\mu} \mathscr{E}_{p\mu}{}^{\lambda} M_{\lambda} \tag{118}$$

Alternatively, multiplying eq. (117) by the inverse of the electric field gradient tensor, we find that:

$$M_{\lambda} = \mathscr{B}^{\mu}{}_{\nu} \bar{\mathscr{E}}^{\nu}_{p\lambda} P_{\mu} \tag{119}$$

The symmetry property of the two gradient tensors was also used to derive eqs. (118) and (119). These and other Poisson relations are listed in Table 8 and Table 9. However, this list of relations is not an exhaustive one. Furthermore, they are not exclusively applicable to geophysics problems. They can also be applied to problems in biophysics, engineering, etc.

Table 8. Poisson Relations Among the Gravity, Electric, and Magnetic Fields I

Sources: mass density & polarization	Sources: mass density & magnetization	Sources: charge density & polarization	Sources: charge density & magnetization
$G\rho = \left(\frac{P_\lambda E_p^\mu}{E_{p\circ} E_p^\circ}\right) \mathcal{G}_\mu{}^\lambda$	$G\rho = \left(\frac{M_\lambda B^\mu}{B_\circ B^\circ}\right) \mathcal{G}_\mu{}^\lambda$	$\sigma = -\left(\frac{P_\lambda E_p^\mu}{E_{p\circ} E_p{}^\circ}\right) \mathcal{E}_\mu{}^\lambda$	$\sigma = -\left(\frac{M_\lambda B^\mu}{B_\circ B^\circ}\right) \mathcal{E}_\mu{}^\lambda$
$P_\lambda = G\rho\, E_{p\mu}\, \bar{\mathcal{G}}_\lambda{}^\mu$	$M_\lambda = G\rho\, B_\mu\, \bar{\mathcal{G}}_\lambda{}^\mu$	$P_\lambda = -\sigma E_{p\mu}\, \bar{\mathcal{E}}_\lambda{}^\mu$	$M_\lambda = -\sigma B_\mu\, \bar{\mathcal{E}}_\lambda{}^\mu$
$\mathcal{V}_p = \frac{1}{G\rho} U_{/\lambda} P^\lambda$	$\Phi = \frac{1}{G\rho} U_{/\lambda} M^\lambda$	$\mathcal{V}_p = -\frac{1}{\sigma} P^\lambda \mathcal{V}_{/\lambda}$	$\Phi = -\frac{1}{\sigma} M^\lambda \mathcal{V}_{/\lambda}$
$E_{p\mu} = \frac{1}{G\rho} P^\lambda \mathcal{G}_{\mu\lambda}$	$B_\mu = \frac{1}{G\rho} M^\lambda \mathcal{G}_{\mu\lambda}$	$E_{p\mu} = -\frac{1}{\sigma} P^\lambda \mathcal{E}_{\mu\lambda}$	$B_\mu = -\frac{1}{\sigma} M^\lambda \mathcal{E}_{\mu\lambda}$
$\mathcal{E}_{p\mu\nu} = \mathcal{G}_\mu{}^\lambda{}_{/\nu} \bar{\mathcal{G}}_\lambda{}^\sigma E_{p\sigma}$	$\mathcal{B}_{\mu\nu} = \mathcal{G}_\mu{}^\lambda{}_{/\nu}\, \bar{\mathcal{G}}_\lambda{}^\sigma B_\sigma$	$\mathcal{E}_{p\mu\nu} = \mathcal{E}_\mu{}^\lambda{}_{/\nu} \bar{\mathcal{E}}_\lambda{}^\sigma E_{p\sigma}$	$\mathcal{B}_{\mu\nu} = \mathcal{E}_\mu{}^\lambda{}_{/\nu} \bar{\mathcal{E}}_\lambda{}^\sigma B_\sigma$

Table 9. Poisson Relations Among the Gravity, Electric, and Magnetic Fields II

Sources: mass density & charge density	Sources: magnetization & polarization
$G\rho = -\frac{\sigma}{3}\bar{\mathscr{E}}^{\mu\nu}\mathscr{G}_{\mu\nu}$	$M_\lambda = \mathscr{B}^{\mu}{}_{\nu}\bar{\mathscr{E}}^{\nu}_{p\ \lambda}P_\mu$
$\sigma = -\frac{G\rho}{3}\bar{\mathscr{G}}^{\mu\nu}\mathscr{E}_{\mu\nu}$	$P_\mu = \mathscr{E}^{\lambda}_{p\ \nu}\bar{\mathscr{B}}^{\nu}{}_{\mu}M_\lambda$
$U = -\frac{G\rho}{\sigma}\mathscr{V}$	
$g_\mu = -\frac{G\rho}{\sigma}E_\mu$	$P^\mu B_\mu = E_{p\lambda}M^\lambda$
$g_\mu = \frac{1}{3}\bar{\mathscr{E}}^{\lambda\nu}\mathscr{G}_{\lambda\nu}E_\mu$	
$\mathscr{G}_{\mu\nu} = -\frac{G\rho}{\sigma}\mathscr{E}_{\mu\nu}$	$P^\mu\mathscr{B}_{\mu\nu} = \mathscr{E}_{p\nu\lambda}M^\lambda$

REFERENCES

Adler, R., M. Bazin, and M. Schiffer; **Introduction to General Relativity**, *Mc Graw-Hill Book Company*, New York (1975)

Barnett, C. T.; Theoretical Modeling of the Magnetic and Gravitational Fields of an Arbitrarily Shaped Three Dimensional Body, *Geophysics,* Vol. 41, No. 6, pp. 1353-1364 (1976)

Barton, D. C.; Calculations in the Interpretations of Observations with the Eötvös Torsion Balance, AIME, pp. 481-486 (1929)

Bhattacharyya, B. K.; Magnetic Anomalies Due to Prism Shaped Bodies with Arbitrary Polarization, *Geophysics*, Vol. XXIX, No. 4, pp. 517-531 (1964)

Bhattacharyya, B. K. and M. E. Navolio; Digital Convolution for Computing Gravity and Magnetic Anomalies Due to Arbitrary Bodies, *Geophysics*, Vol. 40, No. 6, pp. 981-992 (1975)

Bhattacharyya, B. K. and K. C. Chan; Computation of Gravity and Magnetic Anomalies Due to Inhomogeneous Distribution of Magnetization and Density in a Localized Region, *Geophysics*, Vol. 42, No. 3, pp. 602-609 (1977)

Bhattacharyya, B. K.; A Generalized Multibody Model for Inversion of Magnetic Anomalies, *Geophysics*, Vol. 45, No. 2, pp. 255-270 (1980)

Bott, M. H. P.; The Use of Electronic Digital Computers For the Evaluation of Gravimetric Terrain Corrections, *Geophysical Prospecting*, Vol. 7, pp. 45-54 (1959)

Bott, M. H. P.; Two Methods Applicable to Computers for Evaluating Magnetic Anomalies Due to Finite Three Dimensional Bodies, *Geophysical Prospecting*, Vol. 11, pp. 292-299 (1963)

Bott, M. H. P.; Solution of the Linear Inverse Problem in Magnetic Interpretation with Application to Oceanic Magnetic Anomalies, *Geophys. J. R. astr. Soc.*, Vol. 13, pp. 313-323 (1967)

Frahm, C. P., R. H. Clark, W. M. Wynn, M. J. Wynn, J. Wellhoner, and P. J. Carroll; Advanced Superconducting Gradiometer/Magnetometer Arrays and a Novel Signal Processing Technique, *Naval Coastal Systems Laboratory Report*, (1974)

Goodacre, A. K.; Some Comments on the Calculation of the Gravitation and Magnetic Attraction of a Homogeneous Rectangular Prism, *Geophysical Prospecting*, Vol. 21, pp. 66-69 (1973)

Gradshteyn, I. S. and I. M. Ryzhik; **Table of Integrals, Series, and Products**, *Academic Press*, New York (1980)

Grant, F. S.; Review of Data Processing and Interpretation Methods in Gravity and Magnetics, 1964-1971, *Geophysics*, Vol. 37, pp. 647-661 (1972)

Haaz, I. B.; Relations Between the Potential of the Attraction of the Mass Contained in a Finite Rectangular Prism and Its First and Second Derivatives (in Hungarian), *Geofizikai Kozlemenyek*, Vol. II, No. 7 (1953)

Hastings, R., R. P. S. Mahler, R. Schnieider, Jr., and J. H. Eraker; Cryogenic Magnetic Gradiometers for Space Applications, *IEEE Transactions on Geoscience and Remote Sensing*, Vol. GE-23, No. 4, pp. 552-561 (1985)

Hinze, W. J., L. W. Braile, W. W. Chandler, andF. E. Massella; Combined Magnetic and Gravity Analysis, *Final Report NASA Contract No. S-500 29A Modification No. 8*, U. S. Geological Survey, Reston Virginia, pp. 34-87 (1975)

Jackson, J. D.; **Classical Electrodynamics**, 2nd Ed., Chapter 5, *John Wiley & Sons*, New York (1975)

Jordan, S.; Moving-Base Gravity Gradiometer Surveys and Interpretation, *Geophysics*, Vol. 43, No. 1, pp. 94-101 (1978)

Jordan, S.; Status of Moving-Base Gravity Gradiometer, *Geospace Systems Corp.*, Presented at the Third International Symposium on Inertial Technology for Surveying and Geodesy, Banff, Canada (1985)

Kekelis, G.; Field Deployable Superconducting Gradiometers, *Naval Coastal Systems Center*, Technical Report No. SP84-111-U26 (1984)

Kellog, O. D.; **Foundations of Potential Theory**, *Julius Springer*, Berlin (1929)

Langel, R. A. and R. H. Estes; The Near-Earth Magnetic Field and 1980 Determined from Magsat Data, *Journal of Geophysical Research*, Vol. 90, No. B3, pp. 2495-2509 (1985)

Nagy, D.; The Gravitational Attraction of a Right Rectangular Prism, *Geophysics*, Vol. XXXI, No. 2, pp. 362-371 (1966)

Nettleton, L. L.; Gravity and Magnetic Calculations, *Geophysics*, Vol. 7, pp. 293-310 (1942)

Okabe, M.; Analytic Expressions for Gravity Due to Homogeneous Polyhedral Bodies and Translations into Magnetic Anomalies, *Geophysics*, Vol. 44, No. 4, pp. 730-741 (1979)

Okabe, M.; Analytical Expressions for Gravity Due to Homogeneous Revolutional Compartments in the Gaussian Divergence Approach, *Geophysical Prospecting*, Vol. 30, pp. 166-187 (1982)

Pedersen, L. B.; Interpretation of Potential Field Data - A Generalized Approach, *Geophysical Prospecting*, Vol. 25, pp. 199-230 (1977)

Plouff, D.; Derivation of Formulas and FORTRAN Program to Compute Magnetic Anomalies of Prisms, *Natl. Tech. Inf. Service*, No. PB-243-525, U. S. Dept. of Commerce, Springfield, Va. (1975a)

Plouff, D.; Derivation Formulas and FORTRAN Programs to Compute Gravity Anomalies of Prisms, *Natl. Tech. Inf. Service*, No. PB-243-526, U. S. Dept. of Commerce, Springfield, Va. (1975b)

Plouff, D.; Gravity and Magnetic Fields of Polygonal Prisms and Application to Magnetic Terrain Corrections, *Geophysics*, Vol. 41, No. 4, pp. 727-741 (1976)

Poisson, S. D.; Memoire sur la Theorie du Magnetisme, *Memoires de l'Acadamie Royale des Sciences de l'Institut de France*, pp. 247-348 (1826)

Quinn, J. M. and D. L. Shiel; Magnetic Field Modeling of the Northern Juan de Fuca and Explorer Plates, *Technical Report No.* 309, Naval Oceanographic Office, Stennis Space Center, MS (1993)

Richards, M. L., V. Vacquier, and C. D. Van Voorhis; Calculation of the Magnetization of Uplifts from Combining Topographic and Magnetic Surveys, *Geophysics*, Vol. XXXII, No. 4, pp. 678-707 (1967)

Roy, A.; Ambiguity in Geophysical Interpretation, *Geophysics*, Vol. XXVII, No. 1, pp. 90-91 (1962)

Skeels, D. C.; Ambiguity in Gravity Interpretation, *Geophysics*, Vol. 12, pp. 43-56 (1947)

Sorokin, L. V.; Gravimetry and Gravimetrical Prospecting (in Russian), *State Tech. Publ.*, Moscow (1951)

Talwani, K.; Computation with the Help of a Digital Computer of Magnetic Anomalies Caused by Bodies of Arbitrary Shape, *Geophysics*, Vol. XXX, No. 5, pp. 797 - 817 (1965)

Tonnelat, M.; **The Principles of Electromagnetic Theory and of Relativity**, Chapter XIII, *Gordon and Breach*, New York (1966a)

Tonnelat, M.; **Einstein's Unified Field Theory**, *Gordon and Breach*, New York (1966b)

Wells, W. C., Ed.; Spaceborne Gravity Gradiometers, *NASA*, Conference Publication No. 2305 (1983)

APPENDIX A

DERIVATION OF THE Ω MATRIX ELEMENTS

Recalling eq. (12), which is an expression for the magnetic scalar potential $\Phi(\mathbf{r})$ in terms of the vector magnetization $\mathbf{M}(\mathbf{r}')$, we now specify that this magnetization be uniformly distributed over the volume V' of a single rectangular prism and hence is a constant vector **M**, so that:

$$\Phi(\mathbf{r}) = -\mathbf{M} \cdot \int_{V'} \nabla \left(\frac{1}{|\mathbf{r} - \mathbf{r}'|} \right) d^3\mathbf{r}' \tag{A1}$$

In Cartesian coordinates this equation takes the form:

$$\Phi(x,y,z) = M_x I_x + M_y I_y + M_z I_z \tag{A2}$$

where M_x , M_y , and M_z are the constant components of the magnetization vector **M**, and where the following notation has been used:

$$I_x(x,y,z) = \int_{V'} \frac{\partial}{\partial x} \left(\frac{1}{R} \right) dx'\, dy'\, dz' \tag{A3a}$$

$$I_y(x,y,z) = \int_{V'} \frac{\partial}{\partial y} \left(\frac{1}{R} \right) dx'\, dy'\, dz' \tag{A3b}$$

$$I_z(x,y,z) = \int_{V'} \frac{\partial}{\partial z} \left(\frac{1}{R} \right) dx'\, dy'\, dz' \tag{A3c}$$

where:

$$R \equiv |r - r'| = \sqrt{\left(x - x'\right)^2 + \left(y - y'\right)^2 + \left(z - z'\right)^2} \tag{A4}$$

The integrals I_x , I_y , and I_z are just cyclic permutations of the same mathematical form. Therefore, it is sufficient to evaluate just one of these integrals, for instance I_x , and obtain the others by permuting x, y and z appropriately wherever they occur. Thus, taking I_x and performing the indicated derivative with respect to x gives:

$$I_x(x,y,z) = \int_{V'} \frac{(x - x')}{R^3}\, dx'\, dy'\, dz' \tag{A5}$$

The volume of integration, V' , is taken to be a rectangular prism centered about the point $r_0 = (x_0 , y_0 , z_0)$ with its sides parallel to the coordinate axes and having dimensions λ_x , λ_y , and λ_z . Consequently,

$$I_x(x,y,z) = \int_{z_L}^{z_U} \int_{y_L}^{y_U} \int_{x_L}^{x_U} \frac{(x - x')}{R^3}\, dx'\, dy'\, dz' \tag{A6}$$

where the upper and lower limits of integration are defined as follows:

$$x_L = x_0 - \frac{\lambda_x}{2} \tag{A7a}$$

$$x_U = x_0 + \frac{\lambda_x}{2} \tag{A7b}$$

$$y_L = y_0 - \frac{\lambda_y}{2} \tag{A7c}$$

$$y_U = y_0 + \frac{\lambda_y}{2} \tag{A7d}$$

$$z_L = z_0 - \frac{\lambda_z}{2} \tag{A7e}$$

$$z_U = z_0 + \frac{\lambda_z}{2} \tag{A7f}$$

In the event that we were dealing with multiple prisms, each term in the above set of equations would include the additional subscript n, which identifies a particular prism. Integrating first with respect to x' , gives:

$$I_x(x,y,z) = \int_{z_L}^{z_U} \int_{y_L}^{y_U} \frac{dy'\,dz'}{R} \Big|_{x'} \tag{A8}$$

where we have used the shorthand notation:

$$\Big|_{x'} \equiv \Big|_{x'=x_L}^{x'=x_U} \tag{A9}$$

to indicate the limits of evaluation of the x' coordinate. Subsequently, the same notation will also be used for the limits of the y' and z' integrations.

Next, integrating over the y' coordinate, the following result is obtained:

$$I_x(x,y,z) = -\int_{z_L}^{z_U} \ln[(y - y') + R]dz' \quad |_{x',y'} \tag{A10}$$

The first two integrals over x' and y' are found in standard mathematics tables of integrals. The last integral over z' is not as easy to evaluate. In order to perform this last integration, first define:

$$u = (y - y') + R \tag{A11}$$

Using eq. (A4) for R, the above equation can be solved for (z - z') in terms of the variable u:

$$z - z' = \pm S(u) \tag{A12}$$

where:

$$S(u) = \sqrt{\left[u - \left(y - y'\right)\right]^2 - \left(x - x'\right)^2 - \left(y - y'\right)^2} \tag{A13}$$

Taking the derivative of eq. (A12) then gives:

$$dz' = \pm dS(u) \tag{A14}$$

Now, S(u) is always positive since it is just equal to $|z - z'|$. So, the $\pm$ signs above must be chosen to correspond with the sign of (z-z'). Thus, the positive sign (+) is chosen if $z - z' \geq 0$, while the negative sign (-) is chosen if $z - z' < 0$, the sign changing at the point

$z = z'$. Consequently, the integral I_x is broken into two parts as follows:

$$I_x(x,y,z) = -\left\{ \int_{z_L}^{z} \ln\left[\left(y - y'\right) + R\right]dz' + \int_{z}^{z_U} \ln\left[\left(y - y'\right) + R\right]dz' \right\} \Big|_{x',y'} \qquad (A15)$$

Then, in terms of the variable u, the integrals in eq. (A15) may be written in the following manner:

$$I_x(x,y,z) = -\left\{ -\int_{u_L}^{u(z)} \ln(u)\,dS(u) + \int_{u(z)}^{u_U} \ln(u)\,dS(u) \right\} \Big|_{x',y'} \qquad (A16)$$

where, by the notation u_L and u_U we mean $u(z' = z_L)$ and $u(z' = z_U)$ respectively. Integrating by parts gives:

$$I_x(x,y,z) = -\left\{ -S(u)\ln(u)\Big|_{u_L}^{u(z)} + S(u)\ln(u)\Big|_{u(z)}^{u_U} + \int_{u_L}^{u(z)} \frac{S(u)}{u}\,du - \int_{u(z)}^{u_U} \frac{S(u)}{u}\,du \right\} \Big|_{x',y'} \qquad (A17)$$

The argument underneath the square root in S(u) is just quadratic in u. Therefore, the two integrals in eq. (A17) may be partially evaluated using Gradshteyn and Ryzhik (2.2671), yielding:

$$I_x(x,y,z) = -\left\{ -S(u)\ln(u)\Big|_{u_L}^{u(z)} + S(u)\ln(u)\Big|_{u(z)}^{u_U} + S(u)\Big|_{u_L}^{u(z)} - S(u)\Big|_{u(z)}^{u_U} - (x-x')^2 \int_{u_L}^{u(z)} \frac{du}{u\,S(u)} \right.$$

$$\left. + (x - x')^2 \int_{u(z)}^{u_U} \frac{du}{u\,S(u)} - (y - y') \int_{u_L}^{u(z)} \frac{du}{S(u)} + (y - y') \int_{u(z)}^{u_U} \frac{du}{S(u)} \right\} \Big|_{x',y'} \qquad (A18)$$

Finally, using Gradshteyn and Rhyzik (1980) sections 2.261 and 2.266 it is found that:

$$I_x(x,y,z) = -\left\{\left[1-\ln(u)\right]S(u)\Big|_{u_L}^{u(z)} - \left[1-\ln(u)\right]S(u)\Big|_{u(z)}^{u_U} - (x-x')\tan^{-1}\left[\frac{-\left(x-x'\right)^2-\left(y-y'\right)u}{\left(x-x'\right)S(u)}\right]\Big|_{u_L}^{u(z)}\right.$$

$$+ (x-x')\tan^{-1}\left[\frac{-(x-x')^2-(y-y')u}{\left(x-x'\right)S(u)}\right]\Big|_{u(z)}^{u_U} - (y-y')\ln\left[S(u)+u-(y-y')\right]\Big|_{u_L}^{u(z)}$$

$$\left. + (y-y')\ln\left[S(u)+u-(y-y')\right]\Big|_{u(z)}^{u_U}\right\}\Big|_{x',y'} \qquad \text{(A19)}$$

Recalling the definition of u given in eq. (A10), the above equation becomes:

$$I_x(x,y,z) = -\left\{|z-z'|\left\{1-\ln\left[R+(y-y')\right]\right\}\Big|_{z_L}^{z} - |z-z'|\left\{1-\ln\left[R+(y-y')\right]\right\}\Big|_{z}^{z_U}\right.$$

$$-(x-x')\tan^{-1}\left[\frac{-(x-x')^2-(y-y')^2-(y-y')R}{(x-x')|z-z'|}\right]\Big|_{z_L}^{z} + (x-x')\tan^{-1}\left[\frac{-(x-x')^2-(y-y')^2-(y-y')R}{(x-x')|z-z'|}\right]\Big|_{z}^{z_U}$$

$$\left. -(y-y')\ln\left[R+|z-z'|\right]\Big|_{z_L}^{z} + (y-y')\ln\left[R+|z-z'|\right]\Big|_{z}^{z_U}\right\}\Big|_{x',y'} \qquad \text{(A20)}$$

This result simplifies somewhat when it is noted that the following identity holds:

$$\tan^{-1}(-Q) = -\tan^{-1}(Q) \qquad \text{(A21)}$$

Then, when the factor | z - z' | is replaced by $\pm(z - z')$ depending on the limits of the z' integration, it is found that:

$$I_x(x,y,z) = -\left\{(z-z')\left\{1-\ln\left[R+(y-y')\right]\right\}\Big|_{z_L}^{z_U} + (x-x')\tan^{-1}\left[\frac{(x-x')^2+(y-y')^2+(y-y')R}{(x-x')(z-z')}\right]\Big|_{z_L}^{z_U}\right.$$

$$\left. -(y-y')\ln\left[R+(z-z')\right]\Big|_{z_L}^{z} + (y-y')\ln\left[R-(z-z')\Big|_{z}^{z_U}\right]\right\}\Big|_{x',y'} \qquad \text{(A22)}$$

Further note that any term that does not involve all three coordinates x', y', and z' will, upon evaluation at the limits of integration, be equal to zero. Consequently, the first term in eq. (A22) is zero. That is:

$$(z-z')\,\Big|_{x',\,y',\,z'} = 0 \tag{A23}$$

Using the identity:

$$\ln[R-(z-z')]\,\Big|_{x',\,y',\,z'} = -\ln[R+(z-z')]\,\Big|_{x',\,y',\,z'} \tag{A24}$$

the validity of which depends on the fact that these logarithms are being evaluated at fixed limits, $I_x(x,y,z)$ reduces to:

$$I_x(x,y,z) = -\left\{(x-x')\tan^{-1}\left[\frac{(x-x')^2+(y-y')^2+(z-z')^2}{(x-x')(z-z')}\right] - (z-z')\ln[R+(y-y')]\right.$$

$$\left. -(y-y')\ln[R+(z-z')]\right\}\,\Big|_{x',\,y',\,z'} \tag{A25}$$

Next, applying the identity:

$$\left[\tan^{-1}(Q)+\tan^{-1}(Q^{-1})\right]\,\Big|_{x',\,y',\,z'} = \varepsilon\,\frac{\pi}{2}\,\Big|_{x',\,y',\,z'} = 0 \tag{A26}$$

where:

$$\varepsilon = \begin{cases} +1 & Q > 0 \\ -1 & Q < 0 \end{cases} \tag{A27}$$

and subsequently performing some straightforward manipulations to simplify the result, we find:

$$-\tan^{-1}\left[\frac{(x-x')(z-z')}{(x-x')^2+(y-y')R+(y-y')^2}\right]\Big|_{x',y',z'} = \tan^{-1}\left[\frac{(y-y')(z-z')}{(x-x')R}\right]\Big|_{x',y',z'} \quad \text{(A28)}$$

Consequently, the final result is obtained:

$$I_x(x,y,z) = -\left\{+(x-x')\tan^{-1}\left[\frac{(y-y')(z-z')}{(x-x')R}\right] - (y-y')\ln[R+(z-z')] - (z-z')\ln[R+(y-y')]\right\}\Big|_{x',y',z'}$$

(A29a)

The integrals $I_y(x,y,z)$ and $I_z(x,y,z)$ can be obtained from the above expression for $I_x(x,y,z)$ by cyclic permutations of the coordinate differences, i.e.:

$$(x-x') \rightarrow (y-y') \rightarrow (z-z') \rightarrow (x-x')$$

yielding:

$$I_y(x,y,z) = -\left\{-(x-x')\ln[R+(z-z')] + (y-y')\tan^{-1}\left[\frac{(x-x')(z-z')}{(y-y')R}\right] - (z-z')\ln[R+(x-x')]\right\}\Big|_{x',y',z'}$$

(A29b)

and

$$I_z(x,y,z) = -\left\{-(x-x')\ln[R+(y-y')] - (y-y')\ln[R+(x-x')] + (z-z')\tan^{-1}\left[\frac{(x-x')(y-y')}{(z-z')R}\right]\right\}\Big|_{x',y',z'}$$

(A29c)

The magnetic scalar potential is therefore determined and is:

$$\Phi(x,y,z) = M_x I_x(x,y,z) + M_y I_y(x,y,z) + M_z I_z(x,y,z) \qquad \text{(A30)}$$

The elements of the Ω matrix, listed in Table 1, are defined to be the nine terms contained in the three functions $I_x(x,y,z)$, $I_y(x,y,z)$ and $I_z(x,y,z)$. Defining the matrix elements in this way and given the definition of the vector ε, eq. (A30) can be put into the form of eq. (30) of the main text.

APPENDIX B

DERIVATION OF THE Λ MATRIX ELEMENTS

In terms of the magnetic scalar potential $\Phi(x,y,z)$ the magnetic field vector $\mathbf{B}(x,y,z)$, generated by a single prism, is:

$$\mathbf{B}(x,y,z) = -\nabla\Phi(x,y,z) \tag{B1}$$

Using the form for the scalar potential given in eq. (A2) with I_x given in the form of eq. (A10), while I_y and I_z are obtained from eq. (A10) by cyclic permutation of the coordinate differences as previously described in Appendix A, the magnetic induction **B** can be cast into the following form:

$$\mathbf{B}(x,y,z) = M_x \mathcal{I}_x + M_y \mathcal{I}_y + M_z \mathcal{I}_z \tag{B2}$$

where the vectors $\mathcal{I}_x$, $\mathcal{I}_y$, and $\mathcal{I}_z$ are defined as follows:

$$\mathcal{I}_x(x,y,z) = \int_{z_L}^{z_U} \nabla \ln[(y-y') + R]dz' \Big|_{x',y'} \tag{B3a}$$

$$\mathcal{I}_y(x,y,z) = \int_{x_L}^{x_U} \nabla \ln[(z-z') + R]dx' \Big|_{y',z'} \tag{B3b}$$

$$\mathcal{I}_z(x,y,z) = \int_{y_L}^{y_U} \nabla \ln[(x-x') + R]dy' \Big|_{x',z'} \tag{B3c}$$

Since the vectors $\mathcal{I}_x$, $\mathcal{I}_y$, and $\mathcal{I}_z$ are all of the same mathematical form, it is sufficient to evaluate just one of them, for instance $\mathcal{I}_x$, and then to obtain expressions for the other two vectors, via cyclic permutation of the coordinate differences as was done in Appendix A.

Additionally, since we are now dealing with vectors, a simultaneous cyclic permutation of the unit vectors **i** , **j** and **k** is also necessary. That is:

$$(x-x') \rightarrow (y-y') \rightarrow (z-z') \rightarrow (x-x')$$

$$\mathbf{i} \rightarrow \mathbf{j} \rightarrow \mathbf{k} \rightarrow \mathbf{i}$$

Now, the gradient of the natural logarithm in eq. (B3a) is easily computed, yielding:

$$\mathcal{J}_x(x,y,z) = \int_{z_L}^{z_U} \left\{ \left[\frac{(x-x')}{(x-x')^2+(z-z')^2} - \frac{(x-x')(y-y')}{[(x-x')^2+(z-z')^2]R} \right] \mathbf{i} + \left(\frac{1}{R}\right)\mathbf{j} \right.$$

$$\left. + \left[\frac{(z-z')}{[(x-x')^2+(z-z')^2]} - \frac{(y-y')(z-z')}{[(x-x')^2+(z-z')^2]R} \right] \mathbf{k} \right\} dz' \Big|_{x',y'} \qquad \text{(B4)}$$

Noticing that the first term of the integral will contribute nothing to the final result, when evaluated at the limits, since it is independent of the y' coordinate and further noticing that the same is true of the fourth term, $\mathcal{J}_x$ (x,y,z) simplifies to:

$$\mathcal{J}_x(x,y,z) = \left\{ \int_{z_L}^{z_U} \frac{(x-x')(y-y')}{[(x-x')^2+(y-y')^2]R} dz' \, \mathbf{i} + \int_{z_L}^{z_U} \frac{dz'}{R} \mathbf{j} - \int_{z_L}^{z_U} \frac{(x-x')(z-z')}{[(x-x')^2+(z-z')^2]R} dz' \, \mathbf{k} \right\} \Big|_{x',y',z'} \qquad \text{(B5)}$$

These final three integrals may be evaluated using Gradshteyn and Ryzhik (2.124, 2.261 and 2.284), yielding:

$$\mathcal{J}_x(x,y,z) = \left\{ \tan^{-1}\left[\frac{(y-y')(z-z')}{(x-x')R} \right] \mathbf{i} - \ln[R + (z-z')]\,\mathbf{j} - \frac{1}{2} \ln\left[\frac{(y-y')-R}{(y-y')+R} \right] \mathbf{k} \right\} \Big|_{x',y',z'} \qquad \text{(B6)}$$

The last term can be simplified by multiplying the numerator and denominator of the logarithm argument by the factor $(y - y') + R$. Then, the logarithm can be broken into the sum of two terms, one of which will be independent of y' and therefore will contribute nothing when evaluated at the limits. In this way, the following identity (and cyclic permutations thereof) is obtained:

$$\tfrac{1}{2}\ln\left[\frac{(y-y')-R}{(y-y')+R}\right]\Big|_{x',y',z'} = -\ln[R + (y-y')]\Big|_{x',y',z'} \qquad \text{(B7)}$$

Consequently, $\mathcal{I}_x(x,y,z)$ finally reduces to:

$$\mathcal{I}_x(x,y,z) = \left\{\tan^{-1}\left[\frac{(y-y')(z-z')}{(x-x')R}\right]\mathbf{i} - \ln[R + (z-z')]\,\mathbf{j} - \ln[R + (y-y')]\,\mathbf{k}\right\}\Big|_{x',y',z'} \qquad \text{(B8a)}$$

Cyclic permutations then yield similar expressions for $\mathcal{I}_y(x,y,z)$ and $\mathcal{I}_z(x,y,z)$:

$$\mathcal{I}_y(x,y,z) = \left\{-\ln[R + (z-z')]\,\mathbf{i} + \tan^{-1}\left[\frac{(x-x')(z-z')}{(y-y')R}\right]\mathbf{j} - \ln[R + (x-x')]\,\mathbf{k}\right\}\Big|_{x',y',z'} \qquad \text{(B8b)}$$

and

$$\mathcal{I}_z(x,y,z) = \left\{-\ln[R + (y-y')]\,\mathbf{i} - \ln[R + (x-x')]\,\mathbf{j} + \tan^{-1}\left[\frac{(x-x')(y-y')}{(z-z')R}\right]\mathbf{k}\right\}\Big|_{x',y',z'} \qquad \text{(B8c)}$$

The nine terms in the three eqs. (B8a), (B8b), and (B8c), each evaluated independently at the prism limits, form the nine elements of the Λ matrix listed in Table 2. These matrix elements, so defined, allow eq. (B2) to be written in the form of eq. (34) of the main text.

APPENDIX C

DERIVATION OF THE Γ MATRIX ELEMENTS

If the mass density, ρ , is specified to be uniform over the volume of integration V' and consequently is independent of r', then eq. (58) for the gravitational potential U(**r**) may be written as:

$$U(\mathbf{r}) = -G\rho \int_{V'} \frac{d^3\mathbf{r}'}{|\mathbf{r}-\mathbf{r}'|} \qquad \text{(C1)}$$

Taking the volume of integration V', as in Appendix A, to be a rectangular prism, centered about the point $\mathbf{r}_0 = (x_0 , y_0 , z_0)$ and having dimensions λ_x , λ_y , and λ_z , the above equation may be written as:

$$U(x,y,z) = -G\rho\, I(x,y,z) \qquad \text{(C2)}$$

where:

$$I(x,y,z) = \int_{z_L}^{z_U}\int_{y_L}^{y_U}\int_{x_L}^{x_U} \frac{dx'\,dy'\,dz'}{R} \qquad \text{(C3)}$$

and where the limits of integration are the same as those defined in Appendix A. The first integral over x' is found in most standard mathematics tables of integrals and yields the following result:

$$I(x,y,z) = \int_{z_L}^{z_U}\int_{y_L}^{y_U} \ln[(x - x') + R]\,dy'\,dz' \;\Big|_{x'} \qquad \text{(C4)}$$

The integral over y' is of the same mathematical form as that of eq. (A10), which, after some effort, was evaluated, yielding $I_y(x,y,z)$ in Appendix A. Consequently, we have:

$$I(x,y,z) = \left\{(x-x')\int_{z_L}^{z_U} \ln[R + (y-y')]dz' + (y-y')\int_{z_L}^{z_U} \ln[R + (x-x')]dz' \right.$$

$$\left. - \int_{z_L}^{z_U} (z-z') \tan\left[\frac{(x-x')(y-y')}{(z-z')R}\right]dz'\right\} \Big|_{x',y'} \qquad \text{(C5)}$$

The first two integrals over z' in the above expression are of the same form as the one just performed over y' . So we have immediately:

$$I(x,y,z) = \left\{(x-x')\left\{(x-x')\tan^{-1}\left[\frac{(y-y')(z-z')}{(x-x')R}\right] - (y-y')\ln[R + (z-z')] - (z-z')\ln[R + (y-y')]\right\}\right|_{z'}$$

$$+ (y-y')\left\{-(x-x')\ln[R + (z-z')] - (z-z')\ln[R + (x-x')] + (y-y')\tan^{-1}\left[\frac{(x-x')(z-z')}{(y-y')R}\right]\right\}\Big|_{z'}$$

$$\left. - \int_{z_L}^{z_U} (z-z')\tan^{-1}\left[\frac{(x-x')(y-y')}{(z-z')R}\right]dz'\right\} \Big|_{x',y'} \qquad \text{(C6a)}$$

The final integral in eq. (C6a) is rather formidable. However, there is a little trick that can be used. Note that the order of integration of eq. (C3) is arbitrary because the limits of integration are fixed. So instead of integrating first over x' and then over y' , as was just done, we could have integrated first over y' and then over z', or alternatively, we could have integrated first over x' and then over z'. The results of these alternative orders of integrations is obtained from eq. (C6a) by cyclic permutation of the coordinate differences, yielding:

$$I(x,y,z) = \left\{ - \int_{x_L}^{x_U} (x-x') \tan^{-1}\left[\frac{(y-y')(z-z')}{(x-x')R}\right] dx' + (y-y')\left\{(y-y')\tan^{-1}\left[\frac{(x-x')(z-z')}{(y-y')R}\right]\right.\right.$$

$$- (z-z')\ln[R+(x-x')] - (x-x')\ln[R+(z-z')]\}\Big|_{x'} + (z-z')\{-(y-y')\ln[R+(x-x')]$$

$$\left.\left. - (x-x')\ln[R+(y-y')] + (z-z')\tan^{-1}\left[\frac{(x-x')(y-y')}{(z-z')R}\right]\right\}\Big|_{x'}\right\}\Big|_{y',z'} \qquad \text{(C6b)}$$

and

$$I(x,y,z) = \left\{(x-x')\left\{-(z-z')\ln[R+(y-y')] - (y-y')\ln[R+(z-z')] + (x-x')\tan^{-1}\left[\frac{(y-y')(z-z')}{(x-x')R}\right]\right\}\Big|_{y'}\right.$$

$$- \int_{y_L}^{y_U} (y-y')\tan^{-1}\left[\frac{(x-x')(z-z')}{(y-y')R}\right] dy' + (z-z')\left\{(z-z')\tan^{-1}\left[\frac{(x-x')(y-y')}{(z-z')R}\right]\right.$$

$$\left. - (x-x')\ln[R+(y-y')] - (y-y')\ln[R+(x-x')]\}\Big|_{y'}\right\}\Big|_{x',z'} \qquad \text{(C6c)}$$

The three forms of I(x,y,z) given in eqs. (C6a), (C6b), and (C6c) must be equivalent. Therefore, by comparing these three equations, it may be inferred that :

$$\int_{x_L}^{x_U} (x-x')\tan^{-1}\left[\frac{(y-y')(z-z')}{(x-x')R}\right] dx' \Big|_{y',z'} = -\left\{(x-x')\left\{(x-x')\tan^{-1}\left[\frac{(y-y')(z-z')}{(x-x')R}\right]\right.\right.$$

$$\left.\left. - (y-y')\ln[R+(z-z')] - (z-z')\ln[R+(y-y')]\}\right\}\Big|_{x',y',z'} \qquad \text{(C7)}$$

Cyclic permutations of this equation are also valid. Thus, when eq. (C7) and its permutations with respect to the coordinate differences are inserted into equations (C6a), (C6b), and (C6c), it is found that the gravitational potential of a rectangular prism takes the following final form:

$$U(x,y,z) = -G\rho\left\{(x-x')\left\{(x-x')\tan^{-1}\left[\frac{(y-y')(z-z')}{(x-x')R}\right] - (y-y')\ln[R+(z-z')] - (z-z')\ln[R+(y-y')]\right\}\right.$$

$$+(y-y')\left\{-(x-x')\ln[R+(z-z')] + (y-y')\tan^{-1}\left[\frac{(x-x')(z-z')}{(y-y')R}\right] - (z-z')\ln[R+(x-x')]\right\}$$

$$\left.+(z-z')\left\{-(x-x')\ln[R+(y-y')] - (y-y')\ln[R+(x-x')] + (z-z')\tan^{-1}\left[\frac{(x-x')(y-y')}{(z-z')R}\right]\right\}\right\}\Big|_{x',y',z'} \qquad \text{(C8)}$$

The elements of the Γ matrix listed in Table 4 are defined to be the nine geometric terms contained in eq. (C8). Defining the matrix elements in this way allows eq. (C8) to be written in the compact form of eq. (74) of the main text.

APPENDIX D

DERIVATION OF THE GRAVITY ACCELERATION VECTOR COMPONENTS

The gravitational potential generated by a rectangular prism with a uniform mass density ρ is of the form:

$$U(x,y,z) = -G\rho\, I(x,y,z) \tag{D1}$$

where, as in Appendix C, we have:

$$I(x,y,z) = \int_{z_L}^{z_U}\int_{y_L}^{y_U}\int_{x_L}^{x_U} \frac{dx'\,dy'\,dz'}{R} \tag{D2}$$

and where the limits of integration are the same as those defined in Appendix A.

The gravitational acceleration vector, **g**, is the negative gradient of the potential, so that:

$$\mathbf{g}(x,y,z) = -\nabla U(x,y,z) \tag{D3}$$

So if the x' integration in eq. (D2) is performed first, then the gravitational acceleration takes the following form:

$$\mathbf{g}(x,y,z) = -G\rho \int_{z_L}^{z_U}\int_{y_L}^{y_U} \nabla \ln[R + (x - x')]\,dy'\,dz' \;|_{x'} \tag{D4a}$$

On the other hand, since the limits of integration are fixed, the y' integration could have been performed first, giving:

$$\mathbf{g}(x,y,z) = -G\rho \int_{z_L}^{z_U}\int_{x_L}^{x_U} \nabla \ln[R + (y - y')]\,dx'\,dz' \;|_{y'} \tag{D4b}$$

Another possibility is to perform the z' integration first, which then yields:

$$\mathbf{g}(x,y,z) = -G\rho \int_{y_L}^{y_U} \int_{x_L}^{x_U} \nabla \ln[R + (z-z')]\,dx'\,dy' \Big|_{z'} \qquad \text{(D4c)}$$

These last three equations are just cyclic permutations with respect to the coordinate differences of the same basic mathematical form. Furthermore, note that the y' integration of eq. (D4a) is the same as the one previously encountered in eq. (B3c), while the z' integration in eq. (D4b) is the same as that already encountered in eq. (B3a). Likewise, the x' integration in eq. (D4c) is the same as that previously encountered in eq. (B3b). The results of these three integrations are given in eqs. (B8a), (B8b), and (B8c) of Appendix B, so that eqs. (D4a), (D4b), and (D4c) can immediately be written, respectively, as:

$$\mathbf{g}(x,y,z) = -G\rho \int_{z_L}^{z_U} \left\{ -\ln[R + (y-y')]\mathbf{i} - \ln[R + (x-x')]\mathbf{j} + \tan^{-1}\left[\frac{(x-x')(y-y')}{(z-z')R}\right]\mathbf{k} \right\} dz' \Big|_{x',y'} \qquad \text{(D5a)}$$

$$\mathbf{g}(x,y,z) = -G\rho \int_{x_L}^{x_U} \left\{ +\tan^{-1}\left[\frac{(y-y')(z-z')}{(x-x')R}\right]\mathbf{i} - \ln[R + (z-z')]\mathbf{j} - \ln[R + (y-y')]\mathbf{k} \right\} dx' \Big|_{y',z'} \qquad \text{(D5b)}$$

$$\mathbf{g}(x,y,z) = -G\rho \int_{y_L}^{y_U} \left\{ -\ln[R + (z-z')]\mathbf{i} + \tan^{-1}\left[\frac{(x-x')(z-z')}{(y-y')R}\right]\mathbf{j} - \ln[R + (x-x')]\mathbf{k} \right\} dy' \Big|_{x',z'} \qquad \text{(D5c)}$$

These three expressions for the gravitational acceleration vector must be equal. Therefore, by comparing like components of these expressions, we find the following set of identities:

$$\int_{x_L}^{x_U} \tan^{-1}\left[\frac{(y-y')(z-z')}{(x-x')R}\right] dx' \Big|_{y',z'} = -\int_{y_L}^{y_U} \ln[R + (z-z')]\,dy' \Big|_{x',z'} = -\int_{z_L}^{z_U} \ln[R + (y-y')]\,dz' \Big|_{x',y'}$$

(D6)

Cyclic permutations of these relations with respect to the coordinate differences are also valid. The reason for going through the above exercise is that the integrations involving the arc-tangents are very difficult to evaluate, unless they are cast into some other equivalent forms, which has now been done.

Picking any one of the three forms of g(x,y,z), for instance that of eq. (D5c), and using one of the identities in eq. (D6) for the arc-tangent, we may write the gravitational acceleration vector in the following form:

$$\mathbf{g}(x,y,z) = G\rho\left\{\int_{y_L}^{y_U} \ln[R+(z-z')]\,dy' \;\Big|_{x',z'}\,\mathbf{i} + \int_{z_L}^{z_U} \ln[R+(x-x')]\,dz' \;\Big|_{x',y'}\,\mathbf{j} + \int_{y_L}^{y_U} \ln[R+(x-x')]\,dy' \;\Big|_{x',z'}\,\mathbf{k}\right\} \tag{D7}$$

All of the integrals in this equation are of the same basic mathematical form as eq. (A10) of Appendix A. Consequently, when evaluated, the above integrations will yield forms of the type given in eqs. (A30a), (A30b), and (A30c), the particular form depending on which permutation of the coordinate differences is involved. In this way, the following result is obtained:

$$\mathbf{g}(x,y,z) = g_x\,\mathbf{i} + g_y\,\mathbf{j} + g_z\,\mathbf{k} \tag{D8}$$

where:

$$g_x(x,y,z) = G\rho\left\{+(x-x')\tan^{-1}\left[\frac{(y-y')(z-z')}{(x-x')R}\right] - (y-y')\ln[R+(z-z')] - (z-z')\ln[R+(y-y')]\right\}\Big|_{x',y',z'}$$

$$g_y(x,y,z) = G\rho\left\{-(x-x')\ln[R+(z-z')] + (y-y')\tan^{-1}\left[\frac{(x-x')(z-z')}{(y-y')R}\right] - (z-z')\ln[R+(x-x')]\right\}\Big|_{x',y',z'}$$

$$g_x(x,y,z) = G\rho\left\{-(x-x')\ln[R+(y-y')] - (y-y')\ln[R+(x-x')] + (z-z')\tan^{-1}\left[\frac{(x-x')(y-y')}{(z-z')R}\right]\right\}\Big|_{x',y',z'}$$

Using the elements of the Ω matrix derived in Appendix A and listed in Table 1, the vector components of the gravitational acceleration given in eq. (D8) can be cast into the form of eq. (78) of the main text.

APPENDIX E

THE MAGREP FORTRAN ALGORITHM

```
C*********************************************************************
C
C
C     SUBROUTINE MAGREP (MAGNETIC FIELD DUE TO A RECTANGULAR PRISM)
C
C
C*********************************************************************
C
C
C     PROGRAMMED BY:  JOHN M. QUINN  AND  DONALD L. SHIEL   8/8/86
C                     NAVAL OCEANOGRAPHIC OFFICE
C                     STENNIS SPACE CENTER, MS  39522-5001
C
C
C*********************************************************************
C
C
C     PURPOSE:  THIS ROUTINE COMPUTES THE MAGNETIC FIELD COMPONENTS DUE
C               TO A RECTANGULAR PRISM LOCATED AT (XB,YB,ZB) RELATIVE TO
C               SOME ORIGIN LOCATED AT THE OCEAN SURFACE AT THE LOWER
C               LEFT-HAND CORNER OF THE SURVEY AREA.  THE PRISM HAS
C               DIMENSIONS (LAMX,LAMY,LAMZ).  ITS ORIENTATION IS
C               DESCRIBED BY EULER ANGLES (ALPHA,BETA,GAMA)
C               CORRESPONDING TO YAW, PITCH, AND ROLL ACCORDING TO THE
C               3-2-1 CONVENTION, RELATIVE TO THE USUAL GEODETIC
C               COORDINATES FOR WHICH X=NORTH, Y=EAST, AND Z=DOWN.  THE
C               PRISM HAS UNIFORM MAGNETIZATION (MX,MY,MZ) WITH RESPECT
C               TO THE PRISM-FIXED COORDINATES.
C
C
C*********************************************************************
C
C
C     REFERENCE:  A UNIFIED APPROACH TO GEOPOTENTIAL FIELD MODELING;
C                 BY: JOHN M. QUINN AND DONALD L. SHIEL; U. S. NAVAL
C                 OCEANOGRAPHIC OFFICE TECHNICAL REPORT No. 308 (1993)
C
C
C*********************************************************************
C
C
C     PARAMETER DESCRIPTIONS:
C
C       X      - INERTIAL X (NORTH) COORDINATE OF OBSERVATION POINT (KM)
C       Y      - INERTIAL Y (EAST) COORDINATE OF OBSERVATION POINT (KM)
C       Z      - INERTIAL Z (DOWN) COORDINATE OF OBSERVATION POINT (KM)
C       XB     - INERTIAL X (NORTH) COORDINATE OF CENTER OF PRISM (KM)
C       YB     - INERTIAL Y (EAST) COORDINATE OF CENTER OF PRISM (KM)
C       ZB     - INERTIAL Z (DOWN) COORDINATE OF CENTER OF PRISM (KM)
C       XP     - PRISM FIXED X-AXIS COORD. OF OBSERVATION POINT (KM)
C       YP     - PRISM FIXED Y-AXIS COORD. OF OBSERVATION POINT (KM)
C       ZP     - PRISM FIXED Z-AXIS COORD. OF OBSERVATION POINT (KM)
C       LAMX   - DIMENSION OF PRISM ALONG X-AXIS (KM)
C       LAMY   - DIMENSION OF PRISM ALONG Y-AXIS (KM)
C       LAMZ   - DIMENSION OF PRISM ALONG Z-AXIS (KM)
C       ALPHA  - YAW ROTATION ANGLE ABOUT Z-XIS OF PRISM (DEG.)
C       BETA   - PITCH ROTATION ANGLE ABOUT Y-AXIS OF PRISM (DEG.)
C       GAMA   - ROLL ROTATION ANGLE ABOUT X-AXIS OF PRISM (DEG.)
C       MX     - X-COMPONENT OF MAGNETIZATION OF PRISM (NT)
C       MY     - Y-COMPONENT OF MAGNETIZATION OF PRISM (NT)
```

```
C       MZ      - Z-COMPONENT OF MAGNETIZATION OF PRISM (NT)
C       ROT     - ROTATION MATRIX FROM INERTIAL TO PRISM FIXED COORDS.
C       ROTI    - INVERSE ROT. MATRIX -- PRISM-FIXED TO INERTIAL COORDS.
C       V       - GEOMAGNETIC POTENTIAL IN INERTIAL COORDINATES (NT-KM)
C       BX      - INERTIAL X-COMPONENT OF OBSERVED MAGNETIC FIELD (NT)
C       BY      - INERTIAL Y-COMPONENT OF OBSERVED MAGNETIC FIELD (NT)
C       BZ      - INERTIAL Z-COMPONENT OF OBSERVED MAGNETIC FIELD (NT)
C       GB      - INERTIAL MAGNETIC FIELD GRADIENT MATRIX (NT/KM)
C                 GB(1,1)=DBX/DX
C                 GB(1,2)=DBX/DY
C                 GB(1,3)=DBX/DZ
C                 GB(2,1)=DBY/DX
C                 GB(2,2)=DBY/DY
C                 GB(2,3)=DBY/DZ
C                 GB(3,1)=DBZ/DX
C                 GB(3,2)=DBZ/DY
C                 GB(3,3)=DBZ/DZ
C       OMEGA   - MAGNETIC POTENTIAL TRANSFORMATION MATRIX (KM)
C       LAMDA   - MAGNETIC FIELD TRANSFORMATION MATRIX (DIMENSIONLESS)
C       DLAMD   - GRADIENT OF LAMDA MATRIX (KM**(-1))
C
C
C*********************************************************************
C
C
C     NOTE:  THE PRISM IS ROTATED THROUGH EULER ANGLES ALPHA,
C            BETA AND GAMA.  THESE ANGLES DEFINE A NET
C            ROTATION R(GAMA,BETA,ALPHA).  THESE ROTATION ANGLES
C            ARE DEFINED IN ACCORDANCE WITH THE 3-2-1 CONVENTION
C            THAT IS IN GENERAL USE BY BRITISH AND AMERICAN
C            AERODYNAMICISTS.  IN THIS CONVENTION THE ANGLE ALPHA
C            CORRESPONDS TO A COUNTERCLOCKWISE ROTATION ABOUT THE
C            POSITIVE Z-AXIS, THE ANGLE BETA CORRESPONDS TO A
C            CLOCKWISE ROTATION ABOUT THE NEW Y-AXIS, AND THE ANGLE
C            GAMMA CORRESPONDS TO A COUNTERCLOCKWISE ROTATION ABOUT THE
C            FINAL X AXIS.  THE CONSECUTIVE ROTATIONS MUST BE PERFORMED
C            IN THE ABOVE ORDER.  THE INVERSE ROTATION MUST BE
C            PERFORMED IN THE REVERSE ORDER.
C
C            THE INERTIAL COORDINATE SYSTEM IS REFERENCED TO AN
C            ORIGIN AT THE LOWER LEFT-HAND CORNER OF THE SURVEY AREA.
C
C            THE PRISM-FIXED COORDINATE SYSTEM IS REFERENCED TO AN
C            ORIGIN THAT IS AT THE CENTER OF THE PRISM.  THE PRISM
C            FIXED COORDINATES ROTATE WITH THE PRISM RELATIVE TO
C            THE INERTIAL COORDINATES.
C
C*********************************************************************
C
C
      SUBROUTINE MAGREP(X,Y,Z,V,BX,BY,BZ,GB)
C
C
      IMPLICIT DOUBLE PRECISION (A-H,O-Z)
      DOUBLE PRECISION MX,MY,MZ,LAMX,LAMY,LAMZ,LAMDA(3,3)
      DIMENSION OMEGA(3,3),DLAMD(3,3,3),GB(3,3),GBP(3,3)
      DIMENSION ROT(3,3),ROTI(3,3)
      COMMON /MAGBLK/ MX,MY,MZ,LAMX,LAMY,LAMZ,XB,YB,ZB,ALPHA,BETA,GAMA
C
C
```

```
      PI=3.141593D0
      ALPH=ALPHA*PI/180.D0
      BET=BETA*PI/180.D0
      GAM=GAMA*PI/180.D0
C
C        COMPUTE FORWARD AND INVERSE ROTATION MATRICES
C
      ROT(1,1)=+DCOS(ALPH)*DCOS(BET)
      ROT(1,2)=+DSIN(ALPH)*DCOS(BET)
      ROT(1,3)=-DSIN(BET)
      ROT(2,1)=-DSIN(ALPH)*DCOS(GAM)+DCOS(ALPH)*DSIN(BET)*DSIN(GAM)
      ROT(2,2)=+DCOS(ALPH)*DCOS(GAM)+DSIN(ALPH)*DSIN(BET)*DSIN(GAM)
      ROT(2,3)=+DCOS(BET)*DSIN(GAM)
      ROT(3,1)=+DSIN(ALPH)*DSIN(GAM)+DCOS(ALPH)*DSIN(BET)*DCOS(GAM)
      ROT(3,2)=-DCOS(ALPH)*DSIN(GAM)+DSIN(ALPH)*DSIN(BET)*DCOS(GAM)
      ROT(3,3)=+DCOS(BET)*DCOS(GAM)
C
      ROTI(1,1)=+DCOS(ALPH)*DCOS(BET)
      ROTI(1,2)=+DCOS(ALPH)*DSIN(BET)*DSIN(GAM)-DSIN(ALPH)*DCOS(GAM)
      ROTI(1,3)=+DCOS(ALPH)*DSIN(BET)*DCOS(GAM)+DSIN(ALPH)*DSIN(GAM)
      ROTI(2,1)=+DSIN(ALPH)*DCOS(BET)
      ROTI(2,2)=+DSIN(ALPH)*DSIN(BET)*DSIN(GAM)+DCOS(ALPH)*DCOS(GAM)
      ROTI(2,3)=+DSIN(ALPH)*DSIN(BET)*DCOS(GAM)-DCOS(ALPH)*DSIN(GAM)
      ROTI(3,1)=-DSIN(BET)
      ROTI(3,2)=+DCOS(BET)*DSIN(GAM)
      ROTI(3,3)=+DCOS(BET)*DCOS(GAM)
C
C        ROTATE FROM INERTIAL TO PRISM-FIXED COORDINATES
C
      XP=ROT(1,1)*(X-XB)+ROT(1,2)*(Y-YB)+ROT(1,3)*(Z-ZB)
      YP=ROT(2,1)*(X-XB)+ROT(2,2)*(Y-YB)+ROT(2,3)*(Z-ZB)
      ZP=ROT(3,1)*(X-XB)+ROT(3,2)*(Y-YB)+ROT(3,3)*(Z-ZB)
C
C        COMPUTE THE GEOMAGNETIC POTENTIAL, THE VECTOR FIELD AND THE
C        GRADIENT TENSOR FIELD IN THE PRISM FIXED COORDIANTES
C
      VP=0.0D0
      BXP=0.0D0
      BYP=0.0D0
      BZP=0.0D0
      GBP(1,1)=0.0D0
      GBP(1,2)=0.0D0
      GBP(1,3)=0.0D0
      GBP(2,1)=0.0D0
      GBP(2,2)=0.0D0
      GBP(2,3)=0.0D0
      GBP(3,1)=0.0D0
      GBP(3,2)=0.0D0
      GBP(3,3)=0.0D0
      DO 30 JB=1,2
      IF (JB .EQ. 1) XL=+LAMX/2.0D0
      IF (JB .EQ. 2) XL=-LAMX/2.0D0
      IF (JB .EQ. 1) SX=+1.0D0
      IF (JB .EQ. 2) SX=-1.0D0
      XD=XP-XL
      DO 20 KB=1,2
      IF (KB .EQ. 1) YL=+LAMY/2.0D0
      IF (KB .EQ. 2) YL=-LAMY/2.0D0
      IF (KB .EQ. 1) SY=+1.0D0
      IF (KB .EQ. 2) SY=-1.0D0
```

```
      YD=YP-YL
      DO 10 LB=1,2
      IF (LB .EQ. 1) ZL=+LAMZ/2.0D0
      IF (LB .EQ. 2) ZL=-LAMZ/2.0D0
      IF (LB .EQ. 1) SZ=+1.0D0
      IF (LB .EQ. 2) SZ=-1.0D0
      ZD=ZP-ZL
      S=SX*SY*SZ
      R2=XD**2+YD**2+ZD**2
      R=DSQRT(R2)
      IF (R+ZD .EQ. 0.0D0) PRINT *, ' A'
      IF ((R-YD)/(R+YD) .EQ. 0.0D0) PRINT *, ' B'
      IF ((R-XD)/(R+XD) .EQ. 0.0D0) PRINT *, ' C'
      IF (R+XD .EQ. 0.0D0) PRINT *, ' D'
      LAMDA(1,1)=+S*DATAN(YD*ZD/(XD*R))
      LAMDA(1,2)=-S*DLOG(ABS(R+ZD))
      LAMDA(1,3)=-S*DLOG(ABS(R+YD))
      LAMDA(2,1)=LAMDA(1,2)
      LAMDA(2,2)=+S*DATAN(XD*ZD/(YD*R))
      LAMDA(2,3)=-S*DLOG(ABS(R+XD))
      LAMDA(3,1)=LAMDA(1,3)
      LAMDA(3,2)=LAMDA(2,3)
      LAMDA(3,3)=+S*DATAN(XD*YD/(ZD*R))
C
      OMEGA(1,1)=XD*LAMDA(1,1)
      OMEGA(1,2)=YD*LAMDA(1,2)
      OMEGA(1,3)=ZD*LAMDA(1,3)
      OMEGA(2,1)=XD*LAMDA(2,1)
      OMEGA(2,2)=YD*LAMDA(2,2)
      OMEGA(2,3)=ZD*LAMDA(2,3)
      OMEGA(3,1)=XD*LAMDA(3,1)
      OMEGA(3,2)=YD*LAMDA(3,2)
      OMEGA(3,3)=ZD*LAMDA(3,3)
C
      DLAMD(1,1,2)=-(S/R)*(XD/(R+ZD))
      DLAMD(1,1,3)=-(S/R)*(XD/(R+YD))
      DLAMD(1,2,1)=DLAMD(1,1,2)
      DLAMD(1,2,2)=-(S/R)*(YD/(R+ZD))
      DLAMD(1,2,3)=-(S/R)
      DLAMD(1,3,1)=DLAMD(1,1,3)
      DLAMD(1,3,2)=DLAMD(1,2,3)
      DLAMD(1,3,3)=-(S/R)*(ZD/(R+YD))
      DLAMD(2,1,1)=DLAMD(1,1,2)
      DLAMD(2,1,2)=DLAMD(1,2,2)
      DLAMD(2,1,3)=DLAMD(1,2,3)
      DLAMD(2,2,1)=DLAMD(1,2,2)
      DLAMD(2,2,3)=-(S/R)*(YD/(R+XD))
      DLAMD(2,3,1)=DLAMD(1,2,3)
      DLAMD(2,3,2)=DLAMD(2,2,3)
      DLAMD(2,3,3)=-(S/R)*(ZD/(R+XD))
      DLAMD(3,1,1)=DLAMD(1,1,3)
      DLAMD(3,1,2)=DLAMD(1,2,3)
      DLAMD(3,1,3)=DLAMD(1,3,3)
      DLAMD(3,2,1)=DLAMD(1,2,3)
      DLAMD(3,2,2)=DLAMD(2,2,3)
      DLAMD(3,2,3)=DLAMD(2,3,3)
      DLAMD(3,3,1)=DLAMD(1,3,3)
      DLAMD(3,3,2)=DLAMD(2,3,3)
      DLAMD(1,1,1)=-DLAMD(1,3,3)-DLAMD(1,2,2)
      DLAMD(2,2,2)=-DLAMD(2,3,3)-DLAMD(1,1,2)
```

```
      DLAMD(3,3,3)=-DLAMD(2,2,3)-DLAMD(1,1,3)
C
      VP=VP-((OMEGA(1,1)+OMEGA(1,2)+OMEGA(1,3))*MX
     *      +(OMEGA(2,1)+OMEGA(2,2)+OMEGA(2,3))*MY
     *      +(OMEGA(3,1)+OMEGA(3,2)+OMEGA(3,3))*MZ)
C
      BXP=BXP+LAMDA(1,1)*MX+LAMDA(1,2)*MY+LAMDA(1,3)*MZ
      BYP=BYP+LAMDA(2,1)*MX+LAMDA(2,2)*MY+LAMDA(2,3)*MZ
      BZP=BZP+LAMDA(3,1)*MX+LAMDA(3,2)*MY+LAMDA(3,3)*MZ
C
      GBP(1,1)=GBP(1,1)+DLAMD(1,1,1)*MX+DLAMD(1,2,1)*MY+DLAMD(1,3,1)*MZ
      GBP(1,2)=GBP(1,2)+DLAMD(1,1,2)*MX+DLAMD(1,2,2)*MY+DLAMD(1,3,2)*MZ
      GBP(1,3)=GBP(1,3)+DLAMD(1,1,3)*MX+DLAMD(1,2,3)*MY+DLAMD(1,3,3)*MZ
      GBP(2,2)=GBP(2,2)+DLAMD(2,1,2)*MX+DLAMD(2,2,2)*MY+DLAMD(2,3,2)*MZ
      GBP(2,3)=GBP(2,3)+DLAMD(2,1,3)*MX+DLAMD(2,2,3)*MY+DLAMD(2,3,3)*MZ
      GBP(3,3)=GBP(3,3)+DLAMD(3,1,3)*MX+DLAMD(3,2,3)*MY+DLAMD(3,3,3)*MZ
C
   10 CONTINUE
   20 CONTINUE
   30 CONTINUE
C
      GBP(2,1)=GBP(1,2)
      GBP(3,1)=GBP(1,3)
      GBP(3,2)=GBP(2,3)
C
C        ROTATE MAGNETIC FIELD COMPONENTS FROM PRISM FIXED TO
C        INERTIAL COORDINATES
C
      V=VP
C
      BX=ROTI(1,1)*BXP+ROTI(1,2)*BYP+ROTI(1,3)*BZP
      BY=ROTI(2,1)*BXP+ROTI(2,2)*BYP+ROTI(2,3)*BZP
      BZ=ROTI(3,1)*BXP+ROTI(3,2)*BYP+ROTI(3,3)*BZP
C
      GB(1,1)=ROTI(1,1)*GBP(1,1)+ROTI(1,2)*GBP(2,1)+ROTI(1,3)*GBP(3,1)
      GB(1,2)=ROTI(1,1)*GBP(1,2)+ROTI(1,2)*GBP(2,2)+ROTI(1,3)*GBP(3,2)
      GB(1,3)=ROTI(1,1)*GBP(1,3)+ROTI(1,2)*GBP(2,3)+ROTI(1,3)*GBP(3,3)
      GB(2,1)=ROTI(2,1)*GBP(1,1)+ROTI(2,2)*GBP(2,1)+ROTI(2,3)*GBP(3,1)
      GB(2,2)=ROTI(2,1)*GBP(1,2)+ROTI(2,2)*GBP(2,2)+ROTI(2,3)*GBP(3,2)
      GB(2,3)=ROTI(2,1)*GBP(1,3)+ROTI(2,2)*GBP(2,3)+ROTI(2,3)*GBP(3,3)
      GB(3,1)=ROTI(3,1)*GBP(1,1)+ROTI(3,2)*GBP(2,1)+ROTI(3,3)*GBP(3,1)
      GB(3,2)=ROTI(3,1)*GBP(1,2)+ROTI(3,2)*GBP(2,2)+ROTI(3,3)*GBP(3,2)
      GB(3,3)=ROTI(3,1)*GBP(1,3)+ROTI(3,2)*GBP(2,3)+ROTI(3,3)*GBP(3,3)
C
      RETURN
      END
```

APPENDIX F

THE GRVREP FORTRAN ALGORITHM

```
C*********************************************************************
C
C
C     SUBROUTINE GRVREP (GRAVITY FIELD DUE TO A RECTANGULAR PRISM)
C
C
C*********************************************************************
C
C
C     PROGRAMMED BY:  JOHN M. QUINN  AND  DONALD L. SHIEL   8/8/86
C                     NAVAL OCEANOGRAPHIC OFFICE
C                     STENNIS SPACE CENTER, MS  39522-5001
C
C
C*************************************************************     ****
C
C
C     PURPOSE:  THIS ROUTINE COMPUTES THE GRAVITY FIELD COMPONENTS DUE
C               TO A RECTANGULAR PRISM LOCATED AT (XB,YB,ZB) RELATIVE TO
C               SOME ORIGIN LOCATED AT THE OCEAN SURFACE AT THE LOWER
C               LEFT-HAND CORNER OF THE SURVEY AREA.  THE PRISM HAS
C               DIMENSIONS (LAMX,LAMY,LAMZ).  ITS ORIENTATION IS
C               DESCRIBED BY EULER ANGLES (ALPHA,BETA,GAMA)
C               CORRESPONDING TO YAW, PITCH, AND ROLL ACCORDING TO THE
C               3-2-1 CONVENTION, RELATIVE TO THE USUAL GEODETIC
C               COORDINATES FOR WHICH X=NORTH, Y=EAST, AND Z=DOWN.  THE
C               PRISM HAS UNIFORM DENSITY RHO.
C
C
C*********************************************************************
C
C
C     REFERENCE:  A UNIFIED APPROACH TO GEOPOTENTIAL FIELD MODELING;
C                 BY: JOHN M. QUINN AND DONALD L. SHIEL;  NAVAL
C                 OCEANOGRAPHIC OFFICE TECHNICAL REPORT # 309 (1993)
C
C
C*********************************************************************
C
C
C     PARAMETER DESCRIPTIONS:
C
C       X      - INERTIAL X (NORTH) COORDINATE OF OBSERVATION POINT (KM)
C       Y      - INERTIAL Y (EAST) COORDINATE OF OBSERVATION POINT (KM)
C       Z      - INERTIAL Z (DOWN) COORDINATE OF OBSERVATION POINT (KM)
C       XB     - INERTIAL X (NORTH) COORDINATE OF CENTER OF PRISM (KM)
C       YB     - INERTIAL Y (EAST) COORDINATE OF CENTER OF PRISM (KM)
C       ZB     - INERTIAL Z (DOWN) COORDINATE OF CENTER OF PRISM (KM)
C       XP     - PRISM FIXED X-AXIS COORD. OF OBSERVATION POINT (KM)
C       YP     - PRISM FIXED Y-AXIS COORD. OF OBSERVATION POINT (KM)
C       ZP     - PRISM FIXED Z-AXIS COORD. OF OBSERVATION POINT (KM)
C       LAMX   - DIMENSION OF PRISM ALONG X-AXIS (KM)
C       LAMY   - DIMENSION OF PRISM ALONG Y-AXIS (KM)
C       LAMZ   - DIMENSION OF PRISM ALONG Z-AXIS (KM)
C       ALPHA  - YAW ROTATION ANGLE ABOUT Z-XIS OF PRISM (DEG.)
C       BETA   - PITCH ROTATION ANGLE ABOUT Y-AXIS OF PRISM (DEG.)
C       GAMA   - ROLL ROTATION ANGLE ABOUT X-AXIS OF PRISM (DEG.)
C       G      - NEWTON'S GRAVITATIONAL CONSTANT (KM**3/GM-SEC**2)
C       RHO    - DENSITY OF PRISM (GM/KM**3)
C       ROT    - ROTATION MATRIX FROM INERTIAL TO PRISM FIXED COORDS.
```

```
C       ROTI    - INVERSE ROT. MATRIX -- PRISM-FIXED TO INERTIAL COORDS.
C       V       - GRAVITATY POTENTIAL IN INERTIAL COORDINATES (KM**2/SEC**2)
C       GX      - INERTIAL X-COMPONENT OF OBSERVED MAGNETIC FIELD ((KM/SEC**2)
C       GY      - INERTIAL Y-COMPONENT OF OBSERVED MAGNETIC FIELD (KM/SEC**2)
C       GZ      - INERTIAL Z-COMPONENT OF OBSERVED MAGNETIC FIELD (KM/SEC**2)
C       GG      - INERTIAL GRAVITY FIELD GRADIENT MATRIX (SEC**(-2))
C                 GG(1,1)=DGX/DX
C                 GG(1,2)=DGX/DY
C                 GG(1,3)=DGX/DZ
C                 GG(2,1)=DGY/DX
C                 GG(2,2)=DGY/DY
C                 GG(2,3)=DGY/DZ
C                 GG(3,1)=DGZ/DX
C                 GG(3,2)=DGZ/DY
C                 GG(3,3)=DGZ/DZ
C       GAMMA   - GRAVITY POTENTIAL TRANSFORMATION MATRIX (KM**2)
C       OMEGA   - GRAVITY FIELD TRANSFORMATION MATRIX (KM)
C       LAMDA   - GRAVITY GRADIENT TRANSFORMATION MATRIX (DIMENSIONLESS)
C
C
C*********************************************************************
C
C
C     NOTE:  THE PRISM IS ROTATED THROUGH EULER ANGLES ALPHA,
C            BETA AND GAMA.  THESE ANGLES DEFINE A NET
C            ROTATION R(GAMA,BETA,ALPHA).  THESE ROTATION ANGLES
C            ARE DEFINED IN ACCORDANCE WITH THE 3-2-1 CONVENTION
C            THAT IS IN GENERAL USE BY BRITISH AND AMERICAN
C            AERODYNAMICISTS.  IN THIS CONVENTION THE ANGLE ALPHA
C            CORRESPONDS TO A COUNTERCLOCKWISE ROTATION ABOUT THE
C            POSITIVE Z-AXIS, THE ANGLE BETA CORRESPONDS TO A
C            CLOCKWISE ROTATION ABOUT THE NEW Y-AXIS, AND THE ANGLE
C            GAMMA CORRESPONDS TO A COUNTERCLOCKWISE ROTATION ABOUT THE
C            FINAL X AXIS.  THE CONSECUTIVE ROTATIONS MUST BE PERFORMED
C            IN THE ABOVE ORDER.  THE INVERSE ROTATION MUST BE
C            PERFORMED IN THE REVERSE ORDER.
C
C            THE INERTIAL COORDINATE SYSTEM IS REFERENCED TO AN
C            ORIGIN AT THE LOWER LEFT-HAND CORNER OF THE SURVEY AREA.
C
C            THE PRISM-FIXED COORDINATE SYSTEM IS REFERENCED TO AN
C            ORIGIN THAT IS AT THE CENTER OF THE PRISM.  THE PRISM
C            FIXED COORDINATES ROTATE WITH THE PRISM RELATIVE TO
C            THE INERTIAL COORDINATES.
C
C*********************************************************************
C
C
      SUBROUTINE GRVREP(X,Y,Z,V,GX,GY,GZ,GG)
C
C
      IMPLICIT DOUBLE PRECISION (A-H,O-Z)
      DOUBLE PRECISION RHO,LAMX,LAMY,LAMZ,LAMDA(3,3)
      DIMENSION OMEGA(3,3),GAMMA(3,3),GG(3,3),GGP(3,3)
      DIMENSION ROT(3,3),ROTI(3,3)
      COMMON /GRVBLK/ RHO,LAMX,LAMY,LAMZ,XB,YB,ZB,ALPHA,BETA,GAMA
C
C
      PI=3.141593D0
      ALPH=ALPHA*PI/180.D0
```

```
      BET=BETA*PI/180.D0
      GAM=GAMA*PI/180.D0
      G=6.6720D-23
C
C        COMPUTE FORWARD AND INVERSE ROTATION MATRICES
C
      ROT(1,1)=+DCOS(ALPH)*DCOS(BET)
      ROT(1,2)=+DSIN(ALPH)*DCOS(BET)
      ROT(1,3)=-DSIN(BET)
      ROT(2,1)=-DSIN(ALPH)*DCOS(GAM)+DCOS(ALPH)*DSIN(BET)*DSIN(GAM)
      ROT(2,2)=+DCOS(ALPH)*DCOS(GAM)+DSIN(ALPH)*DSIN(BET)*DSIN(GAM)
      ROT(2,3)=+DCOS(BET)*DSIN(GAM)
      ROT(3,1)=+DSIN(ALPH)*DSIN(GAM)+DCOS(ALPH)*DSIN(BET)*DCOS(GAM)
      ROT(3,2)=-DCOS(ALPH)*DSIN(GAM)+DSIN(ALPH)*DSIN(BET)*DCOS(GAM)
      ROT(3,3)=+DCOS(BET)*DCOS(GAM)
C
      ROTI(1,1)=+DCOS(ALPHA)*DCOS(BET)
      ROTI(1,2)=+DCOS(ALPH)*DSIN(BET)*DSIN(GAM)-DSIN(ALPH)*DCOS(GAM)
      ROTI(1,3)=+DCOS(ALPH)*DSIN(BET)*DCOS(GAM)+DSIN(ALPH)*DSIN(GAM)
      ROTI(2,1)=+DSIN(ALPH)*DCOS(BET)
      ROTI(2,2)=+DSIN(ALPH)*DSIN(BET)*DSIN(GAM)+DCOS(ALPH)*DCOS(GAM)
      ROTI(2,3)=+DSIN(ALPH)*DSIN(BET)*DCOS(GAM)-DCOS(ALPH)*DSIN(GAM)
      ROTI(3,1)=-DSIN(BET)
      ROTI(3,2)=+DCOS(BET)*DSIN(GAM)
      ROTI(3,3)=+DCOS(BET)*DCOS(GAM)
C
C        ROTATE FROM INERTIAL TO PRISM-FIXED COORDINATES
C
      XP=ROT(1,1)*(X-XB)+ROT(1,2)*(Y-YB)+ROT(1,3)*(Z-ZB)
      YP=ROT(2,1)*(X-XB)+ROT(2,2)*(Y-YB)+ROT(2,3)*(Z-ZB)
      ZP=ROT(3,1)*(X-XB)+ROT(3,2)*(Y-YB)+ROT(3,3)*(Z-ZB)
C
C        COMPUTE THE GRAVITY POTENTIAL, THE VECTOR FIELD AND THE
C        GRADIENT TENSOR FIELD IN THE PRISM FIXED COORDIANTES
C
      VP=0.0D0
      GXP=0.0D0
      GYP=0.0D0
      GZP=0.0D0
      GGP(1,1)=0.0D0
      GGP(1,2)=0.0D0
      GGP(1,3)=0.0D0
      GGP(2,1)=0.0D0
      GGP(2,2)=0.0D0
      GGP(2,3)=0.0D0
      GGP(3,1)=0.0D0
      GGP(3,2)=0.0D0
      GGP(3,3)=0.0D0
      DO 30 JB=1,2
      IF (JB .EQ. 1) XL=+LAMX/2.0D0
      IF (JB .EQ. 2) XL=-LAMX/2.0D0
      IF (JB .EQ. 1) SX=+1.0D0
      IF (JB .EQ. 2) SX=-1.0D0
      XD=XP-XL
      DO 20 KB=1,2
      IF (KB .EQ. 1) YL=+LAMY/2.0D0
      IF (KB .EQ. 2) YL=-LAMY/2.0D0
      IF (KB .EQ. 1) SY=+1.0D0
      IF (KB .EQ. 2) SY=-1.0D0
      YD=YP-YL
```

```
      DO 10 LB=1,2
      IF (LB .EQ. 1) ZL=+LAMZ/2.0D0
      IF (LB .EQ. 2) ZL=-LAMZ/2.0D0
      IF (LB .EQ. 1) SZ=+1.0D0
      IF (LB .EQ. 2) SZ=-1.0D0
      ZD=ZP-ZL
      S=SX*SY*SZ
      R2=XD**2+YD**2+ZD**2
      R=DSQRT(R2)
      IF (R+ZD .EQ. 0.0D0) PRINT *, ' A'
      IF ((R-YD)/(R+YD) .EQ. 0.0D0) PRINT *, ' B'
      IF ((R-XD)/(R+XD) .EQ. 0.0D0) PRINT *, ' C'
      IF (R+XD .EQ. 0.0D0) PRINT *, ' D'
      LAMDA(1,1)=+S*DATAN(YD*ZD/(XD*R))
      LAMDA(1,2)=-S*DLOG(ABS(R+ZD))
      LAMDA(1,3)=-S*DLOG(ABS(R+YD))
      LAMDA(2,1)=LAMDA(1,2)
      LAMDA(2,2)=+DATAN(XD*ZD/(YD*R))
      LAMDA(2,3)=-S*DLOG(ABS(R+XD))
      LAMDA(3,1)=LAMDA(1,3)
      LAMDA(3,2)=LAMDA(2,3)
      LAMDA(3,3)=+S*DATAN(XD*YD/(ZD*R))
C
      OMEGA(1,1)=XD*LAMDA(1,1)
      OMEGA(1,2)=YD*LAMDA(1,2)
      OMEGA(1,3)=ZD*LAMDA(1,3)
      OMEGA(2,1)=XD*LAMDA(2,1)
      OMEGA(2,2)=YD*LAMDA(2,2)
      OMEGA(2,3)=ZD*LAMDA(2,3)
      OMEGA(3,1)=XD*LAMDA(3,1)
      OMEGA(3,2)=YD*LAMDA(3,2)
      OMEGA(3,3)=ZD*LAMDA(3,3)
C
      GAMMA(1,1)=XD*OMEGA(1,1)
      GAMMA(1,2)=YD*OMEGA(1,2)
      GAMMA(1,3)=ZD*OMEGA(1,3)
      GAMMA(2,1)=XD*OMEGA(2,1)
      GAMMA(2,2)=YD*OMEGA(2,2)
      GAMMA(2,3)=ZD*OMEGA(2,3)
      GAMMA(3,1)=XD*OMEGA(3,1)
      GAMMA(3,2)=YD*OMEGA(3,2)
      GAMMA(3,3)=ZD*OMEGA(3,3)
C
      VP=VP-G*RHO*((GAMMA(1,1)+GAMMA(1,2)+GAMMA(1,3))
     *       +(GAMMA(2,1)+GAMMA(2,2)+GAMMA(2,3))
     *       +(GAMMA(3,1)+GAMMA(3,2)+GAMMA(3,3)))
C
      GXP=GXP+G*RHO*(OMEGA(1,1)+OMEGA(1,2)+OMEGA(1,3))
      GYP=GYP+G*RHO*(OMEGA(2,1)+OMEGA(2,2)+OMEGA(2,3))
      GZP=GZP+G*RHO*(OMEGA(3,1)+OMEGA(3,2)+OMEGA(3,3))
C
      GGP(1,1)=GGP(1,1)+G*RHO*LAMDA(1,1)
      GGP(1,2)=GGP(1,2)+G*RHO*LAMDA(1,2)
      GGP(1,3)=GGP(1,3)+G*RHO*LAMDA(1,3)
      GGP(2,2)=GGP(2,2)+G*RHO*LAMDA(2,2)
      GGP(2,3)=GGP(2,3)+G*RHO*LAMDA(2,3)
      GGP(3,3)=GGP(3,3)+G*RHO*LAMDA(3,3)
C
   10 CONTINUE
   20 CONTINUE
```

```
   30 CONTINUE
C
      GGP(2,1)=GGP(1,2)
      GGP(3,1)=GGP(1,3)
      GGP(3,2)=GGP(2,3)
C
C        ROTATE GRAVITY FIELD COMPONENTS FROM PRISM FIXED TO
C        INERTIAL COORDINATES
C
      V=VP
C
      GX=ROTI(1,1)*GXP+ROTI(1,2)*GYP+ROTI(1,3)*GZP
      GY=ROTI(2,1)*GXP+ROTI(2,2)*GYP+ROTI(2,3)*GZP
      GZ=ROTI(3,1)*GXP+ROTI(3,2)*GYP+ROTI(3,3)*GZP
C
      GG(1,1)=ROTI(1,1)*GGP(1,1)+ROTI(1,2)*GGP(2,1)+ROTI(1,3)*GGP(3,1)
      GG(1,2)=ROTI(1,1)*GGP(1,2)+ROTI(1,2)*GGP(2,2)+ROTI(1,3)*GGP(3,2)
      GG(1,3)=ROTI(1,1)*GGP(1,3)+ROTI(1,2)*GGP(2,3)+ROTI(1,3)*GGP(3,3)
      GG(2,1)=ROTI(2,1)*GGP(1,1)+ROTI(2,2)*GGP(2,1)+ROTI(2,3)*GGP(3,1)
      GG(2,2)=ROTI(2,1)*GGP(1,2)+ROTI(2,2)*GGP(2,2)+ROTI(2,3)*GGP(3,2)
      GG(2,3)=ROTI(2,1)*GGP(1,3)+ROTI(2,2)*GGP(2,3)+ROTI(2,3)*GGP(3,3)
      GG(3,1)=ROTI(3,1)*GGP(1,1)+ROTI(3,2)*GGP(2,1)+ROTI(3,3)*GGP(3,1)
      GG(3,2)=ROTI(3,1)*GGP(1,2)+ROTI(3,2)*GGP(2,2)+ROTI(3,3)*GGP(3,2)
      GG(3,3)=ROTI(3,1)*GGP(1,3)+ROTI(3,2)*GGP(2,3)+ROTI(3,3)*GGP(3,3)
C
      RETURN
      END
```

DISTRIBUTION LIST

NAVY	
Chief of Naval Operations	5
Chief of Naval Research	2
David Taylor Naval Ship Research and Development Center	2
Dept. of the Navy, Submarine Combat and Weapons Systems	1
Mine Countermeasure Group Two	1
Mine Warfare Command	1
Marine Corps Research, Development and Acquisitions Command	1
Naval Air Systems Command	1
Naval Air Test Center	2
Naval Air Warfare Center	4
Naval Avionics Center	1
Naval Coastal Systems Center	2
Naval Command Control and Ocean Surveillance Center	2
Naval Oceanographic Office N342, N4312	150
Naval Oceanographic Office N2, N25CL, N25CP, N5	4
Naval Oceanography Command	3
Naval Oceanography Command Detachments (All)	50
Naval Ocean Systems Center	3
Naval Postgraduate School	3
Naval Research Laboratory, Washington DC	6
Naval Research Laboratory Detachment SSC	6
Naval Sea Systems Command	3
Naval Surface Warfare Center, White Oak	4
Naval Surface Weapons Center, Dahlgren	3
Naval Surface Weapons Laboratory Detachment, White Oak	3
Naval Technical Intelligence Center	1
Naval Undersea Warfare Center Detachment, San Diego	1
Naval Underwater Systems Center Detachment, New London Laboratory	1
Naval Underwater Systems Center Detachment, Newport Laboratory	1
Naval Underwater Warfare Center	3
Naval Weapons Center	1
Office of Advanced Technology	2
Office of Naval Research, Washington DC	3
Office of Naval Research Detachment SSC	2
Office of Naval Technology	1
Space and Naval Warfare Systems Command PMW-182, PMW-185	2
USMC 3rd. R.P.V. Experimental Brigade	2
U. S. Naval Academy (Nimitz Library)	1
AIR FORCE	
Air Force Institute of Technology	1
Air Force Office of Scientific Research	1

Pacific Missile Test Center	3
Rome Research Laboratory	2
U. S. Air Force Academy (Technical Library)	1
USAF Air Warfare Center	1
USAF Hq., Electronics Systems Division	1
USAF Phillips Laboratory, AFGL	2
USAF Phillips Laboratory, Kirkland AFB	1
USAF Weapons and Tactics Center	1
ARMY	
Harry Diamond Laboratory (Technical Library)	1
U. S. Army Combat Systems Test Activity	2
U. S. Army Research Laboratory	3
U. S. Military Academy (Technical Library)	1
DOD	
DARPA, Submarine Technology Program	1
DARPA, Nuclear Monitoring Program	1
Defense Mapping Agency, Aerospace Center	4
Defense Mapping Agency, GPS-NAVSTAR JPO	1
Defense Mapping Agency Headquarters	4
Defense Mapping Agency, Hydrographic and Topographic Center	3
Defense Mapping Agency, Systems Center	3
Defense Mapping School	2
Defense Technical Information Center	2
Los Alamos National Laboratory	2
National Security Agency	1
Sandia National Laboratory (Technical Library)	1
NON-DOD	
Australian Geological Survey	1
British Geological Survey	2
Bedford Institute of Oceanography (Technical Library)	1
Canadian Defence Research Establishment Pacific	2
Colorado School of Mines, Center for Potential Field Studies	2
Geological Survey of Canada, Geophysics Division	3
Geological Survey of Canada, Atlantic Geoscience Centre	3
Geological Survey of Canada, Pacific Geoscience Centre	3
Geothe Universitat, Institute Fur Meteorologie und Geophysik	3
Hatfield Marine Science Center	3
Istituto Nazionale Di Geofisica	1
IZMIRAN	2
Institut de Physique du Globe de Paris	2
Johns Hopkins University, Applied Physics Laboratory	1
Lawrence Livermore Laboratory (Technical Library)	1
McGill University, Dept. of Earth and Planetary Sciences	1

NASA, Geodynamics Branch	5
NOAA, NGDC	3
NOAA, Pacific Marine Environment Laboratory	2
Oregon State University, College of Oceanography	1
Purdue University, Dept. of Earth and Atmospheric Sciences	1
Raytheon Corporation	2
Royal Australian Navy, Maritime Hq.	2
SACLANT ASW Research Centre	2
Scripps Institution of Oceanography	2
Stanford University, Dept. of Geological Sciences	1
Tracor, Incorporated	3
U. S. Geological Survey, Denver	5
U. S. Geological Survey, Menlo Park	2
University of Cantebury, Dept. of Geology	1
University of Michigan, Dept. of Geophysics	1
University of Rhode Island, Graduate School of Oceanography	1
University of Sydney, School of Mathematics and Statistics	1
University of Toronto, Dept. of Physics, Geophysics Laboratory	1
University of Washington, School of Oceanography	2
Woods Hole Oceanographic Institution	2